J. HYM. RES.
Vol. 16(1), 2007, pp. 51–146

Diversity, Classification and Higher Relationships of Mymarommatoidea (Hymenoptera)

Gary A. P. Gibson[1], Jennifer Read and John T. Huber

(GAP) Agriculture and Agri-Food Canada, Biodiversity and Integrated Pest Management, K. W. Neatby Bldg., 960 Carling Avenue, Ottawa, Ontario, Canada, K1A 0C6; email: gibsong@agr.gc.ca
(JR) Agriculture and Agri-Food Canada, Biodiversity and Integrated Pest Management, K. W. Neatby Bldg., 960 Carling Avenue, Ottawa, Ontario, Canada, K1A 0C6; email: readj@agr.gc.ca
(JTH) Canadian Forestry Service, Natural Resources Canada, c/o ECORC, K. W. Neatby Bldg., 960 Carling Avenue, Ottawa, Ontario, Canada, K1A 0C6; email: huberjh@agr.gc.ca

Abstract.—The supraspecific, extinct and extant fauna of Mymarommatoidea (Hymenoptera) is revised. Ten extinct and ten extant described species are classified in six genera and two families, Mymarommatidae and Gallorommatidae **n. fam.** A key to the families and genera is provided. Classified in Gallorommatidae is the extinct Cretaceous genus, *Galloromma* Schlüter, including the type species, *G. bezonnaisensis* Schlüter, and *G. agapa* (Kozlov and Rasnitsyn) **n. comb.** (from *Palaeomymar*). Classified in Mymarommatidae is one extinct Cretaceous genus, *Archaeromma* Yoshimoto, one extinct Tertiary genus, *Palaeomymar* Meunier, and three extant genera, *Mymaromma* Girault, *Mymaromella* Girault, and *Zealaromma* **n. gen.** *Mymaromma* and *Mymaromella* **rev. stat.** are resurrected from prior synonymy under *Palaeomymar* and a neotype male is designated for *Palaeomymar succini* Meunier. *Protooctonus* Yoshimoto is transferred from Mymaridae to Mymarommatidae and is newly synonymised under *Archaeromma*. Newly classified in *Archaeromma* are the Cretaceous species *A. masneri* (Yoshimoto) **n. comb.** (from *Protooctonus*), and *A. mandibulatum* (Kozlov and Rasnitsyn) **n. comb.**, *A. senonicum* (Kozlov and Rasnitsyn) **n. comb.** and *A. japonicum* (Fursov, Shirota, Nomiya and Yamagishi) **n. comb.** (all from *Palaeomymar*). Classified in *Mymaromma* are *M. anomalum* (Blood and Kryger) **rev. comb.**, *M. buyckxi* Mathot **rev. comb.**, *M. goethei* Girault **rev. comb.**, *M. mirissimum* (Girault) **n. comb.** and *M. ypt* (Triapitsyn and Berezovskiy) **n. comb.** (all from *Palaeomymar*). Classified in *Mymaromella* is the extinct Tertiary species, *M. duerrenfeldi* (Schlüter and Kohring) **n. comb.**, and the extant species *M. chaoi* (Lin) **n. comb.**, *M. cyclopterus* (Fidalgo and De Santis) **n. comb.** and *M. mira* Girault **rev. comb.** (all from *Palaeomymar*). Classified in *Zealaromma* are the newly designated type species of the genus, *Z. insulare* (Valentine) **n. comb.** (from *Palaeomymar*) and *Z. valentinei* **n. sp.** Description of the structural diversity of extant and extinct mymarommatids is based on the 20 described species plus 15 undescribed extant morphospecies and several fossils from Tertiary Baltic amber and Burmese, Canadian and New Jersey Cretaceous amber. Evidence for monophyly of the genera is presented and the following phylogenetic relationships are hypothesized: *Galloromma* + (*Archaeromma* + (*Zealaromma* + (*Mymaromella* + (*Palaeomymar* + *Mymaromma*)))). Absence of mesotibial and metatibial spurs are newly proposed synapomorphies for Mymarommatoidea. New information is given on the structure of Serphitidae (Serphitoidea) based on study of several Taimyr and Canadian Cretaceous fossils, and structural features that are shared among Serphitoidea, Mymarommatoidea, Chalcidoidea and Platygastroidea are discussed relative to establishing their relationships. Several features, including gastral laterotergites, a mesopectal region similar to a netrion, and a forewing venation that could be ancestral to that of Platygastroidea suggest Serphitoidea is closely related to Platygastroidea. No new evidence was found to support a Serphitoidea + Mymarommatoidea sister-group relationship. Independent parameres in the groundplan of the male genitalia of Mymarommatoidea and Serphitoidea is a likely symplesiomorphy that differentiates them from Chalcidoidea and Platygastroidea. Two different types of specialized claval sensilla could support

[1] Corresponding author (e-mail: gibsong@agr.gc.ca)

monophyly of Mymarommatoidea + Chalcidoidea, but further study throughout parasitic Hymenoptera is necessary to substantiate character-state distribution and homology.

The superfamily Mymarommatoidea (Hymenoptera) has been referred to as "arguably the most enigmatic wasp taxon" (Vilhelmsen and Krogmann 2006, p. 290). Individuals are among the smallest of microhymenoptera, only about 0.3–0.8 mm in body length, but Mymarommatidae is one of the easiest families of Hymenoptera to recognize because of several highly distinctive features. Most conspicuously, the head has a hyperoccipital band of pleated membrane that enables the occipital region to expand and contract in a bellows-like manner, the forewing membrane has a mesh-like pattern, the hind wing is reduced to an apically bifurcate haltere-like structure, and the petiole is composed of two tubular segments (Gibson 1986, Gibson et al. 1999, Vilhelmsen and Krogmann 2006). Partly because of their minute size, mymarommatids are rarely collected and are poorly represented in most collections, but they have been captured on several subantarctic and Pacific islands (Valentine 1971, Beardsley et al. 2000) and on all continents north into Canada (Clouâtre et al. 1989), Scandinavia (Hansen 1997) and far eastern Russia (Triapitsyn and Berezovskiy 2006). Specimens are also known in Dominican, Sicilian, Baltic, Canadian, Japanese, Taimyr, New Jersey, Burmese, French, Spanish and Lebanese amber, indicating the group has been present for at least 120 million years (Grimaldi and Engel 2005) and has long had a world distribution. Despite their long and apparently ubiquitous presence, almost nothing is known of their biology. Yoshimoto (1984) suggested that they are egg parasitoids, but the life stage they attack and their hosts remain to be discovered. A single individual was reared from a bracket fungus (Gibson 1993) and Huber (1987) noted that most specimens captured in the Northern Hemisphere had been collected in shady and relative moist areas such as deciduous forests. Clouâtre et al. (1989) did extract specimens from forest litter in eastern Canada, but they were also extracted from vegetation litter samples on three subantarctic islands (Valentine 1971). Based on sweep samples, Kryger (cited in Bakkendorf 1948, p. 216) suggested that mymarommatids are associated with low vegetation and remarked on their "very slow-moving gait — as an old man tired to death".

Partly because of the lack of comprehensive comparative studies, Mymarommatidae has a complex nomenclatural history and uncertain phylogenetic relationships within Apocrita. Gibson (1986) and Vilhelmsen and Krogmann (2006) postulated several autapomorphies to support monophyly of the group, but these hypotheses and other character-state knowledge are based primarily on a single European species whose morphology has been studied in detail (Debauche 1948, Vilhelmsen and Krogmann 2006). Knowledge of other mymarommatid species and genera is limited largely to original descriptions. All 9 previously described extant species and 6 of the 10 extinct species are currently classified in *Palaeomymar* Meunier, 1901, which was established for a species in Baltic amber. Kozlov and Rasnitsyn (1979) stated that the diversity of the fossils they knew from the Cretaceous extended beyond the limits of a single genus, but that it did not seem possible to introduce any clear generic classification without an analysis of all accumulated material. Gibson et al. (1999) also suggested that the extant species could be classified in two genera based on differences in foretibial spur and forewing structure.

The primary purpose of our study is to describe and illustrate the range of mor-

phological variability encompassed by the extant and extinct mymarommatoid fauna. This is necessary to classify the described species in higher taxa within a phylogenetic perspective and to determine what features are of specific or generic value so that these are included in future descriptions. Our study is also intended to provide the accurate morphological data for Mymarommatoidea necessary for reliable phylogenetic analyses of Hymenoptera. We do not attempt to resolve the higher relationships of Mymarommatoidea within Apocrita because our study of other groups is insufficient for reliable hypotheses of character state homology and distribution. However, we did examine other parasitic Hymenoptera, particularly those groups that have been postulated as closely related to mymarommatids, to investigate shared features. We discuss our observations so that the features can be examined more comprehensively for these and other Hymenoptera prior to comprehensive phylogenetic analyses.

HISTORICAL REVIEW

Taxonomy.—Three genera have been established in Mymarommatidae for extant species: *Mymaromma* Girault (1920), *Petiolaria* Blood and Kryger (1922), and *Mymaromella* Girault (1931). These authors were unaware that Meunier (1901) had established *Palaeomymar* for a mymarommatid in Baltic amber that Duisburg (1868) illustrated and discussed but did not name. Although Duisburg did not formally name the species, he gave reasons why he believed it probably belonged to *Mymar* Curtis (Mymaridae). Prior to Meunier, Stein (1877) had discovered a female in Baltic amber that he thought was the same species as the female illustrated by Duisburg and named it *Mymar duisburgi*. Meunier (1901) subsequently examined Duisburg's original amber material and realized that Stein's interpretation of Duisburg's species was incorrect. He reassigned *M. duisburgi* to *Eustochus* Haliday (Mymaridae) and established the new genus and species, *Palaeomymar succini* Meunier, based on five males of Duisburg's material. Unaware of either Stein (1877) or Meunier (1901), Bakkendorf (1948) rediscovered Duisburg (1868) and concluded that the illustration seemed to be identical with what Blood and Kryger (1936) had illustrated as the female of *Petiolaria anomala*. Doutt (1973) later synonymised *Mymaromma*, *Mymaromella* and *Petiolaria* under *Palaeomymar*, though he incorrectly cited *M. duisburgi* as the type species of *Palaeomymar*. *Petiolaria* had previously been synonymised under *Mymaromma* by Girault (1930) and *Mymaromella* under *Mymaromma* by Annecke and Doutt (1961). Ever since Doutt (1973), *Mymaromma*, *Mymaromella* and *Petiolaria* have all been considered as synonyms of *Palaeomymar*. Based on our study, we recognize *Palaeomymar* only for *P. succini* and classify all the extant species in *Mymaromma*, *Mymaromella*, and *Zealaromma* **n. gen.** This classification and our newly proposed nomenclatural acts are summarized in Table 1.

In addition to *P. succini* and the extant species, the following extinct species have been classified in *Palaeomymar*: *P. duerrenfeldi* Schlüter and Kohring (1990), *P. japonicum* Fursov et al. (2002), and *P. agapa*, *P. mandibulatus* and *P. senonicus* Kozlov and Rasnitsyn (1979). These species were described from Tertiary and Cretaceous amber deposits spanning about 5–100 mya (Table 1). The other four described extinct species are in three different genera. Yoshimoto (1975) established *Archaeromma* for *Ooctonus minutissimus* Brues, 1937, and his new species, *A. nearcticum*, from Canadian Cretaceous amber. He also described *Protooctonus masneri* from the same material and assigned this taxon to Mymaridae (Chalcidoidea), but we consider that it is a mymarommatid (see below). Finally, *Galloromma bezonnaisensis* Schlüter (1978) was established for a specimen from French Cretaceous amber. Based on our study, we classify all the Cretaceous

Table 1. Proposed classification of Mymarommatoidea including temporal and spatial distribution of type material. Abbreviations: E = extant, K = Cretaceous, T = Tertiary; ages based on Grimaldi and Engel (2005).

Classification proposed	Original genus	Temporal and spatial distribution
† Gallorommatidae **n. fam.**		
Gallorommа Schlüter, 1978		
agapa (Kozlov & Rasnitsyn, 1979) **n. comb.**	*Palaeomymar*	K: Taimyr [Cenomanian (95 mya)]
bezonnaisensis Schlüter, 1978	*Gallorommа*	K: French [Cenomanian (100 mya)]
Mymarommatidae		
† *Archaeromma* Yoshimoto, 1975		
japonicum (Fursov, Shirota, Nomiya & Yamagishi, 2002) **n. comb.**	*Palaeomymar*	K: Japanese [Santonian (85 mya)]
mandibulatum (Kozlov & Rasnitsyn, 1979) **n. comb.**	*Palaeomymar*	K: Taimyr [Santonian (85 mya)]
masneri (Yoshimoto, 1975) **n. comb.**	*Protooctonus* Yoshimoto, 1975	K: Canadian [Campanian (75 mya)]
minutissimum (Brues, 1937)	*Ooctonus* Haliday, 1833	K: Canadian [Campanian (75 mya)]
nearcticum Yoshimoto, 1975	*Archaeromma*	K: Canadian [Campanian (75 mya)]
senonicum (Kozlov & Rasnitsyn, 1979) **n. comb.**	*Palaeomymar*	K: Taimyr [Santonian (85 mya)]
† *Palaeomymar* Meunier, 1901		
succini Meunier, 1901	*Palaeomymar*	T: Baltic [Eocene (44 mya)]
Mymaromma Girault, 1920 **rev. stat.**		
anomalum (Blood & Kryger, 1922) **rev. comb.**	*Petiolaria* Blood & Kryger, 1922	E: Britain
buyckxi Mathot, 1966 **rev. comb.**	*Mymaromma*	E: Congo
goethei Girault, 1920 **rev. comb.**	*Mymaromma*	E: Australia
mirissimum (Girault, 1935) **n. comb.**	*Mymaromella*	E: Australia
ypt (Triapitsyn & Berezovskiy, 2006) **n. comb.**	*Palaeomymar*	E: Far East Russia
Mymaromella Girault, 1931 **rev. stat.**		
chaoi (Lin, 1994) **n. comb.**	*Palaeomymar*	E: China
cyclopterus (Fidalgo & De Santis, 1882) **n. comb.**	*Palaeomymar*	E: Argentina
† *duerrenfeldi* (Schlüter & Kohring, 1990) **n. comb.**	*Palaeomymar*	T: Sicilian [Pliocene (5 mya)]
mira Girault, 1931 **rev. comb.**	*Mymaromella*	E: Australia
Zealaromma Gibson, Read & Huber **n. gen.**		
insulare (Valentine, 1971) **n. comb.**	*Mymaromma*	E: New Zealand
valentinei Gibson, Read & Huber **n. sp.**	*Zealaromma*	E: New Zealand

species in *Archaeromma* and *Gallorommа*, and the Tertiary species either in *Palaeomymar* or extant genera (Table 1).

Classification and relationships.—Mymarommatids were included in Mymaridae prior to Debauche (1948), who established the family Mymarommidae (*sic*) after a comprehensive morphological comparison of *M. anomalum* with several mymarid genera. Annecke and Doutt (1961) rejected Debauche's classification and regarded *Mymaromma* as merely an extremely aberrant mymarid, placing it in the subfamily Mymarinae, tribe Ooctonini. Subsequently, some authors included mymarommatids in Mymaridae (e.g. Valentine 1971, Doutt 1973), sometimes as their own subfamily (Yoshimoto 1975), whereas others treated them as a separate family in Chalcidoidea (e.g. Mathot 1966, Königsmann 1978, Yoshimoto 1984). Without explanation, Nikol'skaya (1978) classified *Palaeomymar*

in the otherwise extinct Cretaceous family Serphitidae (Serphitoidea). Kozlov and Rasnitsyn (1979) subsequently provided rationale for this placement based on a single feature shared by the two taxa — a two-segmented petiole. They noted that Yoshimoto (1975) had also described the extinct Canadian Cretaceous genus *Distylopus* (Chalcidoidea: Tetracampidae) as having a two-segmented petiole, but they considered the original description was not sufficiently detailed to establish its systematic position. Gibson (1986) later found that only a single segment formed the petiole of the unique specimen of the type species, *D. bisegmentus* Yoshimoto. He studied petiolar structure as one of 23 adult and larval characters throughout parasitic Hymenoptera and proposed that mymarommatids constituted a monophyletic taxon based on four autapomorphies — head consisting of two plates connected by pleated membrane, hind wing stalk-like with hamuli forming a distal bifurcation, forewing with reticulate pattern, and mesotergal-mesotrochanteral muscle with axillar portion absent. He also proposed that Chalcidoidea, including Mymaridae, was monophyletic based on three autapomorphies and that Chalcidoidea and Mymarommatidae were sister-groups based on three synapomorphies — unique presence of axillar phragmata as sites of origin for all or part of the mesotrochanteral depressor muscles, mesotrochanteral depressor muscle without a mesofurcal or mesoscutal portion, and the male genitalia without an independent basal ring. The last similarity likely is homoplastic because Chiappini and Mazzoni (2000) showed that the male genitalia of some Mymaridae have a distinct basal ring. Regardless, the proposed synapomorphies for Chalcidoidea + Mymarommatoidea are all internal and likely never will be informative for testing relationships with Serphitidae because these are known only as amber fossils.

Kozlov and Rasnitsyn (1979) suggested that their new genus *Microserphites* (Serphitidae) was intermediate between Mymarommatidae and Serphitidae because the pronotum did not appear to extend to the base of the forewing, unlike in other serphitids. However, the single specimen constituting *Microserphites* is damaged (top of head and mesonotum not preserved), and the pronotum was described as extending to the tegula in one of their three Cretaceous mymarommatid species. Gibson (1986) suggested that the single unique feature shared between mymarommatids and serphitids, a 2-segmented petiole, likely was derived independently because otherwise members of the two taxa are so dissimilar. Rasnitsyn (1988) subsequently considered the ancestry of mymarommatids as uncertain, being questionably most closely related to either Chalcidoidea or Serphitidae. When Ronquist et al. (1999) reanalyzed Rasnitsyn's data using cladistic methods they recovered Mymarommatidae as the sister group of Chalcidoidea and Serphitidae as either the sister group of Platygastroidea or within a clade that contained Platygastroidea. Rasnitsyn (2002) later included Mymarommatidae and Serphitidae as separate families in Platygastroidea, and these two families as the sister group of Chalcidoidea (Rasnitsyn 2002, fig. 331). This classification more closely reflects the views of Ronquist et al. (1999), but renders Platygastroidea *sensu* Rasnitsyn (2002) paraphyletic. More recently, Rasnitsyn et al. (2004) included Mymarommatidae as one of two families of Serphitoidea, whereas Grimaldi and Engel (2005) treated the families as separate superfamilies. To date, mymarommatids have not been included in published molecular analyses of hymenopteran (Dowton and Austin 2001, Castro and Dowton 2006) or chalcid (Campbell et al. 2000) relationships. Regardless, molecular techniques cannot resolve the question of whether mymarommatids are more closely related to serphitids than to chalcids because serphitids are extinct.

When Gibson (1986) proposed Mymarommatidae as the sister group of Chalcidoidea he left them unplaced to superfamily. He did this because he considered that mymarommatid relationships were ambiguous and because if mymarommatids and chalcids were sister groups then mymarommatids could be included or excluded from "Chalcidoidea" depending on whether internal or external features were used to define that taxon. Noyes and Valentine (1989) first treated mymarommatids as the superfamily Mymarommatoidea, as reviewed by Gibson et al. (1999). The latter authors proposed two additional autapomorphies for the group — mesopleuron, metapleuron and propodeum fused ventral to propodeal spiracle, and propleura and prosternum fused into carapace below pronotum. Most recently, Vilhelmsen and Krogmann (2006) proposed four additional autapomorphies for Mymarommatoidea — absence of a mesothoracic spiracle, fusion of the propleural arm with the profurcal arm, presence of a pair of rods on the anterior surface of the prophragma, and absence of a metafurca.

MATERIALS AND METHODS

Sources of material.—This study was based on specimens obtained from the collections listed below. An asterisk indicates the collection included amber material. The names of individuals who facilitated loans of specimens are given in parentheses.

ANIC	Australian National Insect Collection, Canberra, ACT, Australia (John LaSalle, Nicole Fisher).
AMNH*	Division of Invertebrate Zoology, American Museum of Natural History, New York, NY, USA (David Grimaldi).
BMNH	The Natural History Museum, London, England (John Noyes).
BPBM	Bernice P. Bishop Museum, Department of Entomology, Honolulu, HI, USA (John Beardsley).
CIRAD	Centre de coopération internationale en recherche agronomique pour le développement (CIRAD), Montpellier, France (Gerard Delvare).
CNC*	Canadian National Collection of Insects, Ottawa, ON, Canada.
FAUF	Biological Control Research Institute, Fujian Agricultural University, Fuzhou, Fujian Province, China (Naiquan Lin).
GPPC*	George Poinar Personal Collection, maintained at Oregon State University, Corvallis, OR, USA (George Poinar).
GZG*	Geowissenschaftliches Zentrum der Universität Göttingen, Museum, Göttingen, Germany (Mike Reich).
ISNB	Institut Royal des Sciences Naturelles de Belgique, Brussels, Belgium (Paul Dessart).
MCZ*	Museum of Comparative Zoology, Cambridge, MA, USA (Philip Perkins).
MLPA	Museo de la Plata, Facultad de Ciencias Naturales y Museo, Universidad Nacional de La Plata, La Plata, Argentina (Marta Loiácono).
NHRS*	Naturhistoriska riksmuseet, Stockholm, Sweden (Dave Karlsson).
NZAC	New Zealand Arthropod Collection, Entomology Division, DSIR, Auckland, New Zealand (Jo Berry).
PIN*	Palaeontological Institute, Russian Academy of Sciences, Laboratory of Arthropods, Moscow, Russia (Alex Rasnitsyn).
QMBA	Queensland Museum, Queensland Cultural Centre, Brisbane, QLD, Australia (Chris Burwell).
ROMT*	Department of Natural History, Royal Ontario Museum, Toronto, ON, Canada (Janet Waddington).
UCRC	UCR Entomological Teaching and Research Collection, University of California, Riverside, CA, USA (Johan Liljeblad, Jeremiah George, Serguei Triapitsyn, John Heraty).
USNM	United States National Museum of Natural History, Smithsonian Institution, Washington, DC, USA (Michael Gates).

ZMB* Institute of Systematic Zoology, Museum für Naturkunde der Humboldt-Universität zu Berlin, Berlin, Germany (Michael Ohl, Thomas Schlüter).

ZMUC* Zoological Museum, University of Copenhagen, Copenhagen, Denmark (Lars Vilhelmsen).

Techniques.—The minute size of mymarommatids, the comparatively poor state of preservation of many amber fossils, and the inability to examine body parts of a specimen from all angles in any single amber inclusion prevented us from determining the exact structure and morphological variation encompassed by Tertiary and Cretaceous representatives to the same extent as for extant taxa. For this reason, less complete and comparable descriptions are provided for the extinct genera and a comprehensive description and comparative and functional analysis of extant mymarommatid structure is given prior to discussing the extinct fauna. Character states observed in the fossil taxa are sometimes discussed in the comparative and functional analysis for the purpose of justifying character polarity hypotheses.

The terminology of Basibuyuk and Quicke (1995) is used for the components of the foreleg antenna cleaner, whereas other terms for structure follow Gibson (1997) and Vilhelmsen and Krogmann (2006). The abbreviations used to designate structures in the illustrations are listed in Appendix I. In the text, figure numbers that precede an abbreviation designate figures that have the abbreviation for the relevant structure illustrated, whereas figure numbers following the abbreviation illustrate the structure but do not have these specifically indicated. Our description of the mesosoma is intended to supplement the comprehensive study of the internal and external anatomy of *M. anomalum* by Vilhelmsen and Krogmann (2006) and does not repeat many, normally concealed, anatomical features they described.

We did not locate specimens of the apterous species that Valentine (1971) said he had from mainland New Zealand, which would be important for assessing the effect of wing reduction on mesosomal morphology. Among the material examined, we distinguished 15 morphospecies in addition to the described species (Appendix II). Our study was intended to evaluate morphological diversity rather than formally name species. We therefore describe only one species that is important for phylogenetic inference and for which sufficient specimens are available to interpret structure confidently. Appendix II is given as an aid to locate the specimens we examined and the morphospecies we differentiated for future species descriptions. Many of the specimens are mounted such that features are not visible or directly comparable because of the state of preservation (air *vs.* critical-point dried), method of mounting (card *vs.* point) and/or one body part concealing another. Consequently, an accurate appraisal of the distribution of some character states was not possible and we did not attempt to fully resolve the species limits of *Mymaromma*. Based on variation in intensity of the reticulate pattern of the first petiolar segment, what we interpret as *Mymaromma* sp. 7 may constitute a species complex. Specimens from Taiwan have quite a strongly reticulate first petiolar segment and therefore are very similar to *M. anomalum* and *M. ypt*. The specimens from Taiwan assigned to *M.* sp. 7 were one of three samples of *Mymaromma* for which we had numerous ethanol-preserved individuals; the other two were *M. anomalum* from Sweden and *M.* sp. 6 from Taiwan. Specimens of these three taxa were critical-point dried, dissected, and gold coated for more detailed anatomical study using a Philips XL30 environmental scanning electron microscope (SEM). A single female of *Z. valentinei* was also gold coated for observation, but specimens of the other species were left uncoated as originally mounted on card

points or rectangles. In some instances, the electron beam caused the setae of uncoated specimens to bend (e.g., Figs 55, 71, 144c) so that some images do not accurately reflect setation.

Amber inclusions were examined after the upper surface was covered with a thin film of glycerine and a cover slip. This was done in order to improve visibility through scratches and other minor surface irregularities. In order to obtain an optimal viewing angle, amber blocks were often positioned in a V-like glass well or inserted into a piece of plasticine at the desired angle before glycerine and a cover slip were added. The amber piece was washed subsequently in water to remove the glycerine. After one re-examination of the male paratype of *P. agapa*, the tiny amber shard containing the specimen was lost while it was being transferred to its storage vial by the senior author. The inclusions were examined with a Nikon SMZ1500 binocular microscope using 15x oculars and a 1.6x HR Plan APO objective for a maximum magnification of 270x. When possible, they were examined also with a Nikon Optiphot compound microscope, usually at a magnification of 200x. The binocular microscope had a light base with a mirror for transmitted light, and a halogen spot light and a hand-held fibre optic ring light were used to obtain optimal lighting. Inclusions were photographed with a Leica DC500 digital camera attached to a Leica Z16 APO macroscope or a Nikon E800 compound microscope. The serial images obtained were combined with AutoMontage™ and these and the scanning electron microphotographs were digitally retouched using Adobe Photoshop™ to enhance clarity.

In the original publications, the holotypes of *Galloromma bezonnaisensis* Schlüter (1978) and *Palaeomymar duerrenfeldi* Schlüter and Kohring (1990) were stated as deposited in the "Institute für Paläontologie, Freie Universitätat, Berlin". These types are now in ZMB.

EXTANT FAUNA

Description.—Body less than 1 mm in length. Body yellow to partly brown without metallic luster, often with a dark brown triangular region or band on mesopleuron below base of forewing (Fig. 82: sa), and tarsal segments often with extreme apices brown; forewing disc sometimes more or less infuscate within basal half (Figs 166, 168).

Head capsule: Head capsule composed of three parts, a strongly convex anterior or "frontal" plate (Figs 14: frp; 13, 30, 53), a flat, semicircular, posterior or "occipital plate" (Figs 14, 23: ocp; 41, 50), and a ventral "postgenal" plate (Figs 23: pgp; 41, 50). Frontal plate separated dorsally and laterally from occipital plate by pleated membrane originating from above base of each mandible (Figs 13, 14, 53). Occipital plate articulating with postgenal plate along transverse margin above occipital foramen (Figs 23, 41, 50) and capable of rotating anteriorly into head capsule (Fig. 15) or posteriorly beyond vertex in a bellows-like manner (Figs 13, 42). Frontovertex transversely reticulate-scabrous to strigose and sparsely setose (Figs 25, 30, 32, 33, 36, 46, 53). Face usually quite smooth, only very finely striate to strigose (Figs 25, 31, 33, 47, 48), though sometimes with conspicuous mesh-like sculpture (Figs 49, 52, 54); with two "subtorular" setae on midline immediately below toruli (insert, Figs 33, 52) plus 6–12 "interorbital" setae in region between eyes and oral margin (Figs 31, 33, 47–49, 52, 54); oral margin slightly reflexed medially (Figs 25, 33, 56), but clypeus undifferentiated by sutures or evident anterior tentorial pits. Ocelli present (Figs 32, 36, 45, 53) or absent (Figs 25, 30, 33, 46). Toruli subcontiguous and slightly protuberant, at or above level of dorsal margin of eyes (Figs 25, 30, 33, 36). Gena bare except for long seta overlapping base of mandible (Figs 19, 29, 48); malar space variable in length, sometimes long (Figs 47, 52), particularly if eye with few

ommatidia (Fig. 47), but usually short to sublinear (Figs 25, 29, 31, 36, 49) and only rarely with distinct malar sulcus (Fig. 30). Eye variable in size, composed of about 5–55 comparatively large ommatidia (*cf.* Figs 33, 47). Occipital plate with sculpture mesh-like (Fig. 41) to more or less wrinkled-rugulose (Fig. 14); bare except for long seta at extreme ventrolateral corner (Figs 16, 45, 46, 51) and sometimes with a pair of setae paramedially near center (Figs 45, 46: ms); rarely with a ventromedial pit above occipital foramen (Figs 45, 46: opp). Postgenal plate bare except for two long setae laterally in line with ventrolateral seta of occipital plate (Fig. 41), with region between occipital foramen and labiomaxillary complex sclerotized and smooth, the postgenae comparatively widely separated medially (Figs 23, 41, 50). Occipital foramen near dorsal margin of postgenal plate, the orifice surrounded laterally and ventrally by U-shaped region divided by oblique lateral suture (Fig. 24), with single setiform sensillum dorsolaterally, three setiform sensilla ventrolaterally, and with posterior tentorial pits (Fig. 19: ptp) usually visible immediately below ventrolateral sensilla.

Mouthparts: Mandible bidentate or tridentate, exodont, their apices not meeting medially when closed (Figs 23, 25, 31, 33, 49, 52), and with 3–5 setae on outer surface, including dorsal seta usually associated with a campaniform sensillum (Figs 27, 34: cs); bidentate mandible with more or less straight dorsal margin ending as acute dorsoapical angulation and with shorter, acute tooth near middle of ventral margin (Figs 34: vt; 47–49, 52, 54); tridentate mandible both with small ventral tooth (Figs 26, 27: vt) and variably distinct dorsal tooth (Fig. 27) or angulation (Fig. 26) extending at least slightly above oral margin (Figs 29, 30: dt). Labrum (Figs 20–22: lbr) thin, flaplike, often convoluted apically, the exposed surfaces smooth (Figs 19–22) but with papillae directed ventrally from inner, ventral surface. Labiomaxillary complex in ventral view a more or less oval to triangular, flat plate having medial labium (Fig. 20: lab) separated from lateral maxillae (Fig. 20: max) over apical third to two-thirds (Figs 20, 41, 50, 55), and with medial, apparently socketed, papilliform process projecting (Figs 21, 22: pap) externally between labrum and labium. Externally visible part of labium undifferentiated, without palpi, but with pair of setae paramedially near its base (Figs 19–21, 41, 41, 55). Externally visible part of maxilla with long seta laterally near presumptive base; distally differentiated into small subapical lobe (Fig. 41: mxs) bearing terminal spine (Fig. 41: mxp) and longer lateral lobe (Fig. 41: mxg), or with apically narrowed ventral lobe (Figs 21, 57: mxs) bearing spine (Figs 21, 22, 57: mxp) and with dorsal flap (Fig. 21: mxg) or lobe (Fig. 57: mxg) having short, distally projecting papillae (Figs 21, 57) and pustulate surface apically (Figs 20, 21, 22, 57: mxg).

Antenna: Antenna geniculate; flagellum without multiporous plate sensilla; first flagellar segment often shorter than second segment but not anelliform (Figs 171–178). Female antenna 9–11-segmented, distinctly clavate; funicle with 7 (Figs 173: fu; 178) or 6 (Figs 174, 175) segments, the segments progressively more setose toward clava and with unmodified trichoid (hairlike) setae; clava composed of 1 (Figs 173: cl; 174, 175, 178) or 2 (Figs 71, 172: cl) segments, and with at least four different types of sensilla, including trichoid setae on inner and outer surfaces similar to setae of funicle (Figs 58, 72: s1), a few much longer and thicker, usually basally bent sensilla on dorsal or sometimes outer surface (Figs 63, 64, 70: s2), one or more rows of comparatively short and more or less sinuate sensilla on ventral surface (Figs 64, 72: s3), two or three basally bent and slightly lanceolate sensilla, each arising from distinct depression, on outer surface near midline or more dorsally (Figs 62, 63, 70, 71: s4), and often a straight, spine-like sensillum projecting from apex

of clava (Figs 64: as; 65, 67, 69). Male antenna rarely 12-segmented (Fig. 176), usually more (Fig. 171) or less (Fig. 177) distinctly 13-segmented; filiform, but apical 2–4 segments usually somewhat more closely associated or partly fused to form inconspicuously differentiated clava (Figs 60, 61, 66, 68, 73); flagellum relatively sparsely setose, most segments usually with a whorl of long trichoid sensilla medially to subapically (Fig. 171), fl_9 and fl_{10} or fl_8–fl_{10} each with a basally bent, slightly lanceolate sensillum arising from distinct depression distally (Figs 60, 66, 68: s4; 61, 73), and apical segment with spine-like sensillum projecting from apex.

Mesosoma: Pronotum in dorsal view not visible (Figs 78, 79), very short and vertical medially (Fig. 111). Pronotum in lateral view triangular with acute posterodorsal angle extending almost to base of forewing (Figs 80, 103), with single seta posteriorly near dorsal margin (Fig. 80); dorsal and posterior margins often appressed to lateral margin of mesoscutum and anterior margin of mesopleuron, respectively (Figs 80, 95, 96, 101, 108), but not rigidly connected by tongue and groove interlocking system so that posterior margin often displaced from anterior margin of mesopleuron over dorsal third to half (Figs 13: am; 53, 82, 97, 99); posterior margin sometimes with distinct notch (Figs 16, 82: pn; 99, 101) near dorsal quarter, but without evident spiracle. Pronotum in ventral view not continuous between sides (i.e., not annular) (Fig. 86). Propleura forming entire lateral and ventral surfaces of propectus (Fig. 86), divided mediolongitudinally (Figs 43, 112) or more or less extensively and indistinguishably fused medially (Figs 18, 44, 86). Prosternum reflexed internally at about 90 degrees to posterior margin of propleura, comprising a transverse, vertical surface largely concealed between propleura and base of procoxae (Vilhelmsen and Krogmann 2006, fig. 8). Prepectus not visible externally. Tegula absent, but base of forewing with bare, oval, humeral plate (Figs 82, 101: hp) resembling a tegula. Mesoscutum (Figs 45, 78, 79, 91, 93) scabrous, without evident notauli or parapsidal lines, and bare except for four long setae posteriorly in a transverse line; transscutellar articulation straight-transverse. Scutellum (Figs 45, 78, 79, 91, 93, 109) in dorsal view without differentiated axillae, consisting of convex, more or less hourglass-shaped (i.e., lateral margins incurved) anterior scutellum and transverse, concave posterior scutellum (frenum) (Figs 78, 79, 91, 93). Anterior scutellum in dorsal view scabrous to longitudinally scabrous-strigose, but bare except for seta on either side within anterior half (Figs 79, 108, 109); in lateral view, the almost vertical side finely sculptured (Figs 91, 93, 97, 109). Posterior scutellum more or less distinctly, longitudinally strigose (Figs 78, 79, 91, 93, 109). Mesopleuron high-rectangular with anterior margin reflexed as slender rim (Figs 13: am; 82, 97) normally concealed by posterior margin of pronotum; dorsal margin with three setiform "subalar" sensilla below base of forewing (Fig. 98: sas); without differentiated mesepisternum and mesepimeron, and distinct subalar area (acropleuron) not differentiated except often by colour difference described above. Metanotum dorsomedially slender and more or less concealed under posterior margin of scutellum (Figs 78, 84: no_3; 79, 91, 93, 97, 99, 101); laterally separate from metapleuron and propodeum (Fig. 105: no_3, pl_3, pro) or fused with metapleuron (Fig. 84: no_3, pl_3), propodeum (Figs 102: "no_3", pro; 97, 98, 100), or both metapleuron and propodeum (Figs 109, 110: "no_3"). Meso- and metapleuron completely fused (Figs 80, 83, 103, 108) except for short suture below base of wings (Fig. 80: mms) or partly (Fig. 87: mms) to completely separated by oblique suture (Figs 82: mms; 95–97, 99, 101); bare, variable in sculpture. Meso/metapleural complex, when separated by suture, often with suture slightly widened or posterior mar-

gin of mesopleuron with tiny notch (Figs 97, 98: mn) dorsally at same level as notch on posterior margin of pronotum. Meso/metapleural complex, when fused, usually with variably distinct, curved groove (paracoxal sulcus *sensu* Vilhelmsen and Krogmann 2006, fig. 1) extending from intersegmental pit (Fig. 80: isp) to metapleural pit (Figs 80–82, 87: pl_3p) or propodeal spiracle (Figs 103, 108), and rarely with very tiny pit (Fig. 87: pl_2p) at height similar to metapleural pit (Fig. 87: pl_3p). Metapleuron indistinguishably fused with propodeum except usually above propodeal spiracle (Figs 80, 82–84, 97–102); without (Figs 95, 96, 99, 103, 108) or with variably distinct metapleural pit (Figs 80–82, 87, 97, 101: pl_3p); dorsal margin with a single setiform sensillum near base of hind wing (Figs 85, 98, 105, 110: dms); anteroventral corner often projecting slightly anteriorly to abut reflexed rim of slightly projecting mesocoxal foramen (Figs 86, 87) (in lateral view the two protrusions usually form a pit (Figs 80, 86: isp) between them). Metathoracic-propodeal complex with single setiform or digitiform "postalar sensillum" (Figs 84, 85, 98, 100, 102, 105, 110, 127: pas), almost always with two setiform "prespiracular sensilla" (Figs 84, 85, 98, 110, 127: pss; 100, 105), and usually with one, or rarely two, "suprapleural" setiform sensilla (Figs 85, 98: sps) anterior to postalar sensillum between dorsal margin of metapleuron and ventral margin of scutellar-axillar complex. Propodeum with sculpture variable, more or less reticulate to transverse-strigose at least dorsally (Figs 78, 79, 91, 93, 107); with single seta near posterior margin of spiracle (Figs 84: prs; 80–83, 95–102, 105, 109); posteriorly reflexed into variably distinct and high flange (Figs 92, 94, 104: pf) on either side of short foraminal tube (Figs 90–97, 99, 101, 103, 104, 107) or into continuous ∩-like flange encircling petiolar insertion dorsally and laterally (Figs 81, 87: pf) (in either instance the flange and dorsal rim of metacoxal foramen abut to form pincer-like structure surrounding deep pit (Figs 80, 86: isp; 104, 108)). Propodeal spiracle (Figs 84, 100, 105, 109: sp) below level of propodeal surface, surrounded by spiracular aperture (Figs 84, 100, 105, 109: spa); spiracular aperture usually circular to oval (Figs 80, 84, 100, 105, 109: spa), rarely slit-like (Fig. 82: spa), and usually continuous to anterolateral margin of propodeum as deep slit (spiracular peritreme) (Figs 80, 82, 84, 100: spp), with the peritreme and dorsal margin of metapleuron either forming acute angle (Figs 82–84) or more uniformly convex margin (Figs 97–102).

Wings: Forewing pedunculate (Figs 163–166, 168) with more or less lanceolate to broadly spatulate disc (Figs 113, 124: dsc) and slender basal stalk (Fig. 124: stk). Forewing disc sometimes almost flat (Fig. 166), but usually more or less distinctly convoluted by series of longitudinal folds (Figs 163, 164); without venation but with raised lineations on both upper and lower surfaces of membrane forming a double layered mesh-like pattern interior to level of insertion of marginal setae (Figs 123, 163–165); discal setae varying from short and spine-like (Fig. 166) to long and hair-like (Figs 163, 164), sometimes appearing dense when very long (Fig. 116), but aligned in row along folds when disc convoluted (Figs 163, 164); marginal setae, when long, arising distinctly from within periphery of apical portion of disc (Figs 163, 165, 168). Forewing stalk (Fig. 124: stk) more or less distinctly subdivided into "proximal" and "distal" portions, the distal part consisting of strongly narrowed base of disc (Fig. 124: std). In dorsal view, proximal part of stalk (Fig. 124: stp) differentiated into convex, anterior and posterior longitudinal bands separated by furrow over most of length except basally (Figs 127, 134); posterior band bare but anterior band with sparse, short spicules at least anteriorly and with a campaniform sensillum distally (Figs 125, 126, 128: cs) near base of long

seta (Figs 125–128: mc). In ventral view, proximal part of stalk with at least basal half of anterior margin folded under wing as basally widened region of membrane (Figs 129, 132: cc), the membrane with scattered spicules (Figs 129, 132) or these sometimes in row (Figs 95, 130) and, at least sometimes, with a campaniform sensillum basally to medially (Figs 132, 135: cs), and with non-folded portion differentiated into anterior band having short spicules and concave trough along posterior margin (Figs 130, 132: ret). Hind wing with bulbous base (Fig. 136) and slender stalk terminated by pincer-like structure; stalk with two or rarely three subbasal setae and one medial to subapical seta on anterior margin (Fig. 136), and sometimes with a slender band of membrane posteriorly (Figs 135, 136: mb), the membrane sometimes also with single short seta (Fig. 135); apical pincer formed by socketed hamulus (Fig. 135: ham) and slender projection opposite to hamulus (Figs 134, 135: op), the projection and sometimes also the hamulus apically bifurcate (Figs 134–136).

Legs: Meso- and metacoxae with basicoxite reduced to a small lobe (Figs 81, 104, 107: bc) inserted into widely separated foramina (Fig. 86). Femora with differentiated trochantellus; posterior surface of femora sometimes with small bumps (Fig. 146). Tibial spur formula 1:0:0. Protibia without row of modified setae (secondary fine comb) along anterior margin apically; calcar curved and apically bifurcate (Figs 137, 138, 139a, 140: ca) or straight and simple (Figs 142, 144a, 145a: ca); mesotibia ventroapically with two strong, apically divergent, socketed setae projecting distally from tube-like elevations of cuticle (Figs 139b, 141b, 144b: ps); metatibia with strong setae originating from cuticular protrusions ventroapically (Figs 139c, 141c, 144c: ps) and anteroapically (Figs 139c, 144c). Tarsi 5-segmented; protarsus with fine comb of basitarsus (Figs 137: fc; 140, 143, 145a) aligned longitudinally, the lanceolate setae slightly flattened and differentiated in length so apices form a concave arc.

Metasoma: Metasoma 8-segmented, the basal two segments tubular, hence with 2-segmented petiole (Figs 83, 104: pt_1, pt_2; 88, 92, 94). First petiolar segment almost smooth (Figs 81, 83, 104, 107), transversely strigose (Figs 90, 92–94) or reticulate (Fig. 88), and often with single seta on either side in anterior half (Figs 92, 94, 104, 107). Second petiolar segment finely sculptured dorsally and often with tiny spicules (Fig. 83, insert) or transversely strigose (Figs 92, 94). Post-petiolar segments (= gaster) of air-dried specimens usually flattened-oval in cross-section, but terga broadly overlapping sterna laterally (i.e., without differentiated laterotergites), and smooth and shiny (Fig. 147); without spiracles except usually on Mt_7 (Figs 149: sp; 150–152, 158, 159). Gaster (Fig. 147) in dorsal view with posterodorsal margin of Mt_3 broadly and deeply incurved and Mt_4 the largest tergite; Mt_3 with two to several setae dorsolaterally near anterior margin; Mt_7 with single seta near spiracle (Figs 149–152) or usually paralaterally when spiracle absent (Fig. 154); syntergum (Mt_{8+9}) with 2–4 setae in row near posterior margin (Figs 150, 152, 153, 155) and usually with cerci (Figs 150, 152: cer; 149, 151, 158), the cercus usually flat or low convex, subcircular, differentiated from tergite by distinct groove, and bearing 1–4 long setae (Figs 150, 151, 158), but sometimes partly fused with tergite or apparent only as subcircular depression (Fig. 152). Hypopygium of female (Fig. 148: hyp) with several setae apically (Figs 148, 149, 153), the sclerite extending almost to apex of metasoma and concealing ovipositor when appressed to syntergum (Fig. 148: syn), but apex capable of separating widely from syntergum (Figs 149: syn; 147, 153) for ventral rotation of ovipositor (Figs 152, 153: ov; 147, 149). Hypopygium of male bare, but with a campaniform sensillum laterally near base (Fig. 160: cs). Male

genitalia without basal ring or phallobase, consisting of large medial aedeagus (Figs 154, 155, 158, 160: aed), ventrolateral volsellae with digiti (Figs 160, 162: vol, dig), and sometimes with externally protruding parameres (Figs 154, 156: par; 155). Aedeagus in dorsal view (Fig. 158) divided apically and distinctly bilobed basally, with basal lobes much smaller and more slender than posteriorly broadened apical lobes and each basal lobe with small pit near its anterior margin; in ventral view gonopore positioned apically (Fig. 160: gp); internally with paired apodemes extending anteriorly (Figs 169, 170: aea). Volsella (Figs 160, 162:vol) extending anteriorly into body as slender apodeme (Figs 169, 170: voa) and posteriorly broadened into a digitus (Figs 161, 162: dig) having one or two short spines (Figs 161, 162: dis), the two volsellae together forming a posteriorly directed, Y-shaped structure. Paramere, when present, projecting externally from between syntergum and hypopygium lateral to aedeagal-volsellar complex as elongate-digitiform process with a long terminal seta (Figs 154, 156: par), and extending internally as rod-like structure (Fig. 169: paa) articulating with genital complex basal to volsellar apodemes.

Comparative and functional morphology.— **Head capsule**: Certainly the most bizarre structural modification of extant mymarommatids is their unique "bellows-like" head (Figs 13, 42). The functional significance of this remains uncertain, but Cretaceous fossils suggest that origin of a hyperoccipital band of pleated membrane and a moveable occipital plate likely evolved concurrently with exodont mandibles. If mymarommatids are egg parasitoids it is possible that the adult emerges from the host egg by opening its exodont mandibles and rupturing rather than chewing the chorion. Expansion of the occipital region to enlarge the head (*cf.* Figs 13, 14) may serve to fill the enclosing space so that the mandibles are appressed firmly against the chorion. By doing so, the mandibles are more likely to break the membrane rather than simply pushing the head away from it when they are opened outwards. Such an hypothesis does not explain why the occipital plate can also rotate deeply within the head capsule (Fig. 15), unless this is merely an artifact of drying made possible by the bellows-like structure.

The seemingly ventral position of the occipital foramen on the head (Figs 14, 15, 45, 53) is a consequence of the modified head structure. The occipital foramen actually is near the center of the head, as in other hymenopterans, but it appears to be more ventral because the posterior surface of the head is abruptly angled along a transverse axis near the dorsal margin of the occipital foramen (Figs 23, 41, 50). This angulation serves as the hinge that allows the occipital plate to rotate anteriorly (Fig. 15) and posteriorly (Fig. 13) relative to the frontal plate. The structure of the occipital foramen and the region between the foramen and labiomaxillary complex appears to be quite consistent across the family (Figs 23, 24, 41, 50), though we examined this in detail for very few species.

Many species have the frontal plate more coarsely sculptured ventrolaterally near where the hyperoccipital band of pleated membrane originates than immediately posterior to the eye (Figs 29, 30, 54). The sculpture is developed as short vertical ridges in some species and specimens of *M. anomalum* from Sweden have a small series of ridges or denticles ventrolaterally on both the frontal and occipital plates (Figs 16, 17). The denticles interdigitate when the occipital plate is vertical relative to the frontal plate (Fig. 17) and together they may serve as a weak locking mechanism to align the occipital and frontal plates and to inhibit rotation of the occipital plate. The exact distribution of such interlocking denticles is not known, but most species apparently lack them (Figs 42, 45, 51, 53). All examined species have a single seta ventrolaterally on the

occipital plate that typically projects somewhat over the hyperoccipital band of pleated membrane (Figs 15, 16, 41, 51). This seta likely serves to sense whether the occipital plate is rotated within the head capsule. A long seta on the gena and the ventral-most seta of the postgenal plate also overlap the base of the mandible (Figs 19, 35). These setae likely serve to sense when the mandible is opened.

The only head capsule feature of extant mymarommatids that appears to be of generic value is the presence or absence of paramedial setae on the occipital plate. Species of *Mymaromella* have a pair of setae (Figs 45, 46: ms), whereas those of *Mymaromma* and *Zealaromma* do not. All examined mymarommatids have two subtorular setae (Figs 33, 52, insert), but they differ in the number and pattern of interorbital facial setae (*cf.* Figs 25, 31, 33, 47–49). Both species of *Zealaromma* have four interorbital setae above the oral margin (Fig. 56). There are only two interorbital seta above the oral margin in *Mymaromma* (Figs 18, 20), but species of *Mymaromella* either have two or four such setae. Both species of *Zealaromma* share a distinctive facial sculpture (Figs 52, 54), but a few species of *Mymaromella* also have distinct facial sculpture (Fig. 49). Other features such as the presence or absence of ocelli and relative size of the eyes and number of ommatidia are even more variable among species.

Mouthparts: The exodont mandibles of *Zealaromma* (Figs 52, 54) and *Mymaromella* (Figs 47–49) are bidentate and comparatively gracile except in *Mymaromella* sp. 23. The single known female of this species uniquely has large, robust mandibles within a conspicuously large oral orifice (Figs 36, 37, 39). Because the left mandible is open its inner surface is visible (Figs 36, 37: i). The inner surface is smooth with one dorsoapical and one dorsomesal seta and two campaniform sensilla, one below the dorsomesal seta and one ventromesally (Fig. 37: cs). The relative position of the two mandibles show that a mandible is rotated as it is opened so that the "dorsal" surface of a closed mandible projects laterally when open (Figs 36, 37: d) and the "outer" surface becomes "ventral" (Fig. 37: o). The "dorsal" surface (Fig. 40: d) is slightly concave, has two small, outcurved teeth apically, and two setae basally, one adjacent to a campaniform sensillum (Fig. 40: cs). The outer surface (Fig. 37: o) is flat, has three setae, and its apical margin is quite long, almost vertical, with a knife-like edge (Fig. 37: c). We infer that the dorsal surface of the mandible in its closed position in *M.* sp. 23 is homologous with the external surface of the mandible of other mymarommatids because it is concave with two teeth and has a seta associated with a campaniform sensillum. We did not observe a campaniform sensillum associated with a dorsal seta on the outer mandibular surface in all mymarommatids examined, but based on wide distribution of the sensillum we suspect that this was because the mandible was not clean enough for it to be observed rather than it being absent. In species of *Mymaromella*, the campaniform sensillum usually is within the depression from which the dorsal seta arises and therefore can be observed only under some angles (*cf.* Figs 34, 35: cs). Similarly, we are not certain whether a second, more mesal campaniform sensillum evident on the outer mandibular surface in some species (Fig. 35) is characteristic of all species and genera, or whether campaniform sensilla are characteristic of the internal surface of all mymarommatid mandibles.

The mandibles of most species of *Mymaromma* differ from those of *Mymaromella* and *Zealaromma* because each has an additional dorsal angle (Figs 25, 26) or tooth (Figs 19, 27, 28) that projects above the oral margin, at least slightly (Figs 29, 30: dt). The only known exception is *Mymaromma* sp. 9, which has bidentate mandibles (Fig. 31). The mandibles of some species of *Mymaromella*, if viewed slightly from below, sometimes appear to

have a very tiny dorsal tooth (Fig. 44), but this is the base of the socketed seta at the dorsal margin of the mandible and it does not project above the oral margin when viewed anteriorly (Fig. 48).

The labiomaxillary complex of mymarommatids is strongly reduced, which makes definitive homology of its components with those of other parasitic Hymenoptera uncertain. Extant mymarommatids have a ventral labiomaxillary plate composed of a medial labium (Fig. 20: lab) and lateral maxillae (Fig. 20: max) that are fused together over at least their posterior third. The externally visible part of the labium we interpret as the prementum (Fig. 21: lpm). A medial papilliform process (Figs 21, 22: pap) also projects externally from between the labrum and labium. Except for *Mymaromma* sp. 9 (Fig. 31, insert), the labium is much wider in species of *Mymaromma* (Figs 18–21, 23, 28) than in *Mymaromella* (Figs 41, 41, 44, 48, 49) and *Zealaromma* (Figs 50, 52, 55, 56). Because of the condition of available specimens we could not determine the exact structure of the maxilla in *M.* sp. 9. In other species of *Mymaromma* and in *Zealaromma* the maxilla often appears to be composed of a single lobe terminated by a spine (in *Zealaromma* the lobe projects slightly on either side of the base of the spine, Figs 56, 57), but there is also a second fleshy lobe above the ventral lobe of the maxilla. This dorsal maxillar lobe appears flat when the labiomaxillary complex is appressed to the head capsule (Fig. 21: mxg) and more tubular when the complex is distended (Fig. 57: mxg). When the dorsal maxillar lobe is expanded, oblique rows of distally projecting papillae are visible in lateral view (Fig. 57), which appear as dorsally projecting papillae when the lobe is flattened (Fig. 21). Furthermore, the dorsal lobe is differentiated apically as a pustulate lobe (Figs 20–22, 56, 57) that projects slightly beyond the terminal spine of the ventral maxillar lobe. Species of *Mymaromella* have a slightly different maxillar structure because the spine-like process (Fig. 41: mxp) originates from a small lobe (Fig. 41: mxs) on the inner side of a longer fleshy lobe (Fig. 41: mxg), which in at least some species has distally projecting papillae on its upper/outer surfaces (*cf.* Fig. 57). We consider that the small subapical lobe bearing the spine is a remnant of the maxillary palpus (Fig. 41: mxp), the inner surface from which it arises as likely a remnant of the stipes (Fig. 41: mxs), and the longer outer lobe as likely a remnant of the galea (Fig. 41: mxg). We also consider the thin, apically pustulate lobe above the stipes in *Mymaromma* and *Zealaromma* as a more internalized galea (Figs 21, 22, 57: mxg), i.e., homologous with the outer lobe of the maxilla in *Mymaromella*. The structural homology of the papilliform process that projects externally between the labrum and labium (Figs 21, 22: pap) is uncertain, though it might be the hypopharynx or a part of the maxilla (possibly the ligula).

Our interpretation of the labiomaxillary complex differs from that of Debauche (1948, fig. 16a), who considered that the maxillary stipes were fused medially so that they completely covered what we interpret as the prementum of the labium (Fig. 21: lpm). He also considered the long posterolateral setae of the labiomaxillary complex as the maxillary palpi. The two very similar paramedial setae he considered simply as sensory hairs. The maxillary regions in *Mymaromma* that we consider as the stipes he interpreted as the galea.

The structure of the labiomaxillary complex was not visible in most fossil mymarommatids we examined, but a paratype of *Palaeomymar senonicus* clearly has the labium only about as wide as the maxillae and these apparently separated for most if not all of their length (Fig. 203). We could not determine the presence of maxillary or labial palpi.

Antenna: For this study we included what Beardsley et al. (2000) identified as an unnamed species from Hawaii near *Mymaromma goethei* in *M. goethei* (Appen-

dix II). Females we include in *M. goethei* have six (Figs 174, 175) rather than seven funicular segments. We also saw one female of *Mymaromella* sp. 6 that has seven funicular segments in one antenna and six segments in the other. Males we identify as *M. goethei* from Australia and Hawaii have 12-segmented antennae (Fig. 176). The males of other species have 13-segmented antennae (Figs 171, 177), though the apical two segments sometimes are only indistinctly separated (Fig. 177). We suggest that the 12-segmented antenna of male *M. goethei* and what is either the same or a very similar species in Hawaii results from the loss of a funicular segment, as for females, rather than the loss of the apical claval segment.

Male mymarommatids lack the s2-type and s3-type sensilla present on the clava of females, but both sexes have s4-type sensilla. The latter sensilla are more or less lanceolate in shape, are directed apically because they are strongly bent basally, and each originates from a distinct circular depression (Figs 58, 60, 62, 64, 66, 68, 70, 71: s4). Females of *Mymaromma* and *Zealaromma* have two s4-type sensilla and females of *Mymaromella* two or three such sensilla on the outer surface of the clava. Both sensilla are on the apical claval segment in *Zealaromma* (Fig. 71). The sensilla are near the dorsal margin of the clava in *Mymaromma* (Figs 58, 59) and *Zealaromma* (Fig. 71), but near the midline or even more ventrally in *Mymaromella* (Figs 62, 63, 65, 67, 69). Males lack s4-type sensilla from the apical flagellar segment, but the preceding two or three segments have a single s4-type sensillum distally depending on whether the female of the species has two or three such sensilla on the clava (*cf.* Figs 65 and 66, 67 and 68, 71 and 73). We observed strong, basally curved sensilla projecting from the outer or dorsal surfaces of the clava of some Cretaceous females, but are uncertain whether they are s2-type or unusually long s4-type sensilla.

Mesosoma: The internal and external mesosomal structure of *Mymaromma anomalum* was studied comprehensively by Vilhelmsen and Krogmann (2006). They noted that in *M. anomalum* the propleura and prosternum are fused, except for a short distance anteriorly, so that there is a continual ventral "carapace" (Vilhelmsen and Krogmann 2006, fig. 6; *cf.* Figs 18, 86). Because of the fusion they were uncertain as to their original structure. Our survey demonstrated that both species of *Zealaromma* (Fig. 112) and at least some fossil mymarommatids have medially abutting propleura (not visible in all inclusions). We could not observe this feature in all examined species of *Mymaromella* and *Mymaromma*, but species of *Mymaromella* appear to have medially abutting propleura or at least a sulcus or differentiated line of sculpture along the ventral midline (Figs 43, 44), whereas species of *Mymaromma* have an undifferentiated carapace similar to *M. anomalum*.

Vilhelmsen and Krogmann (2006) showed that the mesothoracic spiracle and an externally evident prepectus were missing from *M. anomalum*, but stated that it would be desirable to establish position of a spiracle relative to the prepectus for inferring possible sister-group relationships of mymarommatids. They also noted that the pronotum had a notch in its posterior margin at about one third of its height from the dorsal margin (Vilhelmsen and Krogmann 2006, fig. 1), but did not comment that this position is similar to that of the mesothoracic spiracle in most parasitic Hymenoptera other than the Chalcidoidea. Our survey shows that all mymarommatoids lack a mesothoracic spiracle and an external prepectus, but that there is a pronotal notch in many *Mymaromma* (Figs 16, 82: pn) and *Mymaromella* (Figs 97, 99, 101). We did not observe a pronotal notch in *Zealaromma* (Figs 103, 108) or any Cretaceous representative, though the lateral structure of the pronotum was not clearly visible in many amber inclusions.

Vilhelmsen and Krogmann (2006) further stated that the pronotum is rigidly associated with the mesopleuron in *M. anomalum*. Our survey showed that the pronotum extends to the mesopleuron ventrally in mymarommatids and does not appear to be moveable relative to the mesothorax, but in many species and specimens the posterior margin is separated from the mesopleuron over its dorsal third to half (Figs 13, 82, 97, 99). Vilhelmsen and Krogmann (2006) also described and illustrated an internal structure near the posterior margin of the pronotum that they postulated was the prepectus fused to the pronotum. Our study did not include internal features, but we concur with their interpretation that the structure parallel to the posterolateral margin of the pronotum (Vilhelmsen and Krogmann 2006, fig. 4) likely is the prepectus. They concluded that the structure is fused with the pronotum. If so, it is not homologous with a posterolateral pronotal inflection *sensu* Gibson (1985). Remnants of membrane on the dorsal and posterior margins of the putative prepectus (Vilhelmsen and Krogmann 2006, figs 4, 5) suggest that this is where membrane from the mesoscutum and anterior margin of the mesopleuron attach, respectively, providing the pronotum with the flexibility to be separated from the mesopleuron dorsally (Figs 13, 53, 82, 97, 99) but at the same time retaining structural continuity between the pronotum and mesothorax. Even if separation of the pronotum from the mesopleuron dorsally is only an artifact of drying, their separation shows their margins are not rigidly interlocked by a tongue and groove mechanism as in taxa with a posterolateral pronotal inflection.

Vilhelmsen and Krogmann (2006) noted that the mesopleuron and metapleuron are fused together in *M. anomalum*, which was hypothesized as an autapomorphy of Mymarommatidae by Gibson et al. (1999). Our survey shows that the meso- and metapleura are separate sclerites in *Mymaromella* (Figs 95–99, 101) and in those fossil taxa where the feature is visible. Except for a very short distance immediately below the hind wing (Fig. 80: mms), the sclerites are fused in *Zealaromma* (Figs 103, 108) and in most *Mymaromma*. *Mymaromma* sp. 9 has the meso- and metapleura completely separated (Fig. 82: mms) and they are separated over about their ventral half in *Mymaromma* sp. 7 (Fig. 87: mms). In *Mymaromella*, there is often a tiny notch in the posterior margin of the mesopleuron (Figs 97, 98: mn) or a slight widening of the suture between the meso- and metapleuron at a similar height as the notch on the pronotum. Based on this positional similarity, the notch on the posterior margin of the mesopleuron could be a remnant of the metapleural spiracle.

The dorsal surface of the mesosoma of mymarommatids we examined is very similar to that described for *M. anomalum* by Vilhelmsen and Krogmann (2006) except for species-specific sculptural differences. However, structure of the metathoracic-propodeal complex differs conspicuously among *Mymaromma*, *Mymaromella* and *Zealaromma*. As described by Vilhelmsen and Krogmann (2006), the aperture of the propodeal spiracle continues as a slender peritreme dorsally to the anterior margin of the propodeum in *M. anomalum* (*cf.* Fig. 84: spp). The spiracular aperture (Figs 80, 82, 84, 100, 105: spa) is the more or less enlarged ventral portion of the spiracular peritreme that overlies the actual opening of the propodeal spiracle (Figs 84, 100, 105, 109: sp). They interpreted the spiracular peritreme as the antecostal suture, which separates the metanotum from the propodeum. A slit-like spiracular peritreme is characteristic of both *Mymaromma* and *Mymaromella*, but its direction differs in the two genera and this determines whether the postalar sensillum and prespiracular sensilla appear to be located on the metathorax (Fig. 84: pas, pss) or on what appears to be the anterolateral angle of the propodeum (Fig. 98:

pas, pss). In *Mymaromella*, the spiracular peritreme is directed anterodorsally and the metanotum and propodeum are fused mesal to the spiracular peritreme, though sometimes a carina is present that may represent the line of fusion (Figs 98, 102: c). Consequently, a slit separates the dorsal margin of the metapleuron from the lateral margin of the metanotum/propodeum and in lateral view the peritreme and dorsal margin of the metapleuron together form a relatively evenly convex arc (Figs 97–102). The prespiracular sensilla (Figs 98: pss; 100, 102) are on the metanotum/propodeum above the spiracle and the postalar sensillum is anterior to these, often also obviously on the metanotum/propodeum (Fig. 98: pas). However, this position for the postalar sensillum is not so obvious in species that have the anterolateral angle of the metanotum/propodeum narrowly attenuated (*cf.* Figs 99, 100), and in *M.* sp. 17 the sensillum appears to be disassociated from the metanotum/propodeum (Fig. 102: pas). *Mymaromella* sp. 17 is the only mymarommatid we observed having a single prespiracular sensillum (Fig. 102), though this observation is based on only a single clean specimen. Additional individuals are required to determine whether the number of prespiracular sensilla are variable in *M.* sp. 17 or the loss of one sensillum is correlated with what appears to be a more highly reduced "metanotum" in this species (Fig. 102: "no_3"). In *Mymaromma*, the spiracular peritreme is directed dorsally, apparently continuous with the antecostal suture, and the metanotum and metapleuron are fused together to form a single ∩-like sclerite anterior to the peritreme (Fig. 84). In lateral view, the peritreme and dorsal margin of the metapleuron converge dorsally to form an acute angle (Figs 82–84), and the prespiracular sensilla are on the metathorax near the presumed line of fusion between the lateral margin of the metanotum and dorsal margin of the metapleuron (Fig. 84: pss). The postalar sensillum (Fig. 84: pas) appears to originate from the dorsal margin of the metapleuron anterior to the prespiracular sensilla. In very clean specimens (Fig. 85: no_3?; Vilhelmsen and Krogmann 2006, fig. 11), the sensillum is seen to originate from a small, more or less triangular region that is differentiated above the dorsal margin of the metapleuron. The posterior edge of the differentiated region projects slightly so that the postalar sensillum sometimes appears bilobed (Vilhelmsen and Krogmann 2006, fig. 11).

The different locations of the postalar and prespiracular sensilla in *Mymaromma* and *Mymaromella* show that their different metathoracic-propodeal structures are not a result of a simple shift in direction of the spiracular peritreme, and that one propodeal structure was not derived directly from the other. If the peritreme simply shifted direction this should not affect position of the sensilla on the body relative to the different sclerites.

The metanotum or the anterodorsal angle of the metanotum/propodeum appear to be separated quite widely from the base of the hind wing in *Mymaromma* (Figs 83, 84: hwb) and often in *Mymaromella* (Figs 95, 101, 102), though sometimes in *Mymaromella* there actually is a slender, inconspicuous intervening region (Fig. 100). The metanotum in other Hymenoptera, including Mymaridae, is more or less truncate laterally (Fig. 11: no_3). Typically, the metanotum extends to the inner margin of the base of the hind wing and the anterodorsal margin of the propodeum extends to the posterior margin of the hind wing (Fig. 11: no_3, hwb, pro). In Mymaridae, there are setiform sensilla at the extreme anterolateral angle of the propodeum below the base of the hind wing (Fig. 11). Furthermore, the mymarid metanotum (Figs 11, 12) typically has a single seta near its anterior margin sublaterally and three more lateral setae, one of the setae being somewhat more medial than two setae at the extreme lateral margin of the metanotum. In some mymarids, such

as *Mymar*, the somewhat more medial seta originates from the inner surface of the metanotum (Fig. 12). Mymarommatids do not have a sensillum in the position of the sublateral metanotal seta of mymarids, but at least some have one, and apparently sometimes two, setiform suprapleural sensilla (Figs 85, 98: sps) between the metapleuron and scutellar-axillar complex anterior to the postalar sensillum. We postulate that the prespiracular sensilla (Figs 84, 85, 98, 101, 102: pss) in mymarommatids are of metanotal origin based on their positional homology with similar sensilla in mymarids (Figs 11, 12). We also postulate that the postalar sensillum is of metanotal origin because of its position in most *Mymaromella* (Figs 98, 100: pas). Although the postalar sensillum appears to originate from the dorsal margin of the metapleuron in *Mymaromma* (Fig. 84: pas), we suggest that the thickened region from which it originates (Fig. 85: no_3?) actually is lateral remnant of the metanotum that remains near the base of the hind wing (Fig. 84: hwb) and that became disassociated from the dorsal part of the metanotum (Fig. 84: no_3) when the metapleuron and metanotum (Fig. 84: pl_3, no_3) fused together. We are less certain of the origin of the suprapleural sensillum (Figs 85, 98: sps), but it too likely is metanotal.

In *Zealaromma*, the propodeal spiracle is posterior to the anterior margin of the propodeum (Figs 105, 109: sp) and in *Z. valentinei* the dorsal margin of the metapleuron forms a more or less evenly convex arc (Fig. 105: pl_3). These features are more similar to the structure of *Mymaromella* (Figs 98, 100, 102) than *Mymaromma* (Figs 82, 84). Otherwise, the two species of *Zealaromma* have structures of the metathoracic-propodeal complex that differ from each other and from the other two genera. *Zealaromma insulare* has the metanotum (Fig. 109: no_3) fused laterally with both the metapleuron and propodeum so that smooth cuticle completely separates the spiracular aperture from the anterior margin of the composite structure (Fig. 109), whereas sutures separate the metanotum from both the metapleuron and propodeum in *Z. valentinei* (Figs 105: no_3, pl_3, pro; 106). In *Z. valentinei*, the posterior margin of the metapleuron is carinate dorsal to the propodeal spiracle and it overlies a smooth band that extends from the spiracular aperture to the intersection of the metapleuron, metanotum and propodeum (Fig. 105). The linear smooth region is similar to the spiracular peritreme in *Mymaromma* and *Mymaromella* except that the region is sclerotized. Although the metathoracic-propodeal structures appear to be quite different in *Z. insulare* (Figs 105, 106) and *Z. valentinei* (Figs 109, 110), in both species the postalar sensillum is widely separated from the prespiracular sensilla (*cf.* Figs 105, 110: pas, pss). This shared feature suggests that the metathoracic-propodeal structure of *Z. insulare* evolved from a *Z. valentinei*-like structure through fusion of the metanotum, metapleuron and propodeum. It also suggests that what appears as a laterally truncate, independent metanotum in *Z. valentinei* (Fig. 105: no_3) is not structurally homologous with the laterally truncate, independent metanotum of other Hymenoptera (*cf.* Figs 11, 12 with Fig. 105). This conclusion is based on our hypothesis that the postalar sensillum is of metanotal origin and our observation that the sensillum sometimes appears to be disassociated from the metanotum/propodeum in *Mymaromella* because of elongation and narrowing of the anterolateral corner of the metanotum/propodeum. This transformation series is illustrated by Figs 98 → 100 → 102, and we suggest that the anterior position of the postalar sensillum in *Zealaromma* evolved through a similar transformation series. If so, the superficially laterally truncate margins of the metanotum of *Z. valentinei* are not the "true" margins of the metanotum. Dissections of *Z. valentinei* are necessary to determine whether the postalar sensillum is actually

separated from the "metanotum" or whether the apparently laterally truncate metanotum (Figs 105, 106) extends anteriorly as a slender band beneath the dorsal margin of the metapleuron and bears the postalar sensillum at its apex.

Although the structure of the metathoracic-propodeal complex of *Z. valentinei* may not be directly ancestral to the structures that characterize *Mymaromma* or *Mymaromella*, both of the latter structures likely evolved from a mymarommatid that had an independent metanotum. The structures characteristic of *Mymaromma* and *Mymaromella* could both be derived from such a hypothetical structure. Fusion of the lateral margin of an independent metanotum with the dorsal margin of the metapleuron in one lineage would result in the structure characteristic of *Mymaromma* (*cf.* Figs 105, 84), whereas fusion of the posterolateral margin of an independent metapleuron with the propodeum in another lineage would result in the structure characteristic of *Mymaromella* (*cf.* Figs 105, 98). As noted below, at least some Cretaceous representatives appear to have a propodeal spiracle in the same approximate position as in *Mymaromella* and a line extending dorsally from the spiracle (Fig. 187: sp), but it is uncertain whether this line represents a peritreme or only a smooth band. Furthermore, the presence or absence of an independent metanotum could not be determined from the amber inclusions. Both *Mymaromma* and *Mymaromella* possess a slit-like spiracular peritreme (Figs 80, 82, 84, 97–102), which is not present in *Zealaromma* (Figs 105, 109). This suggests that the common ancestor of extant mymarommatids had both an independent metanotum and a slit-like spiracular peritreme, but that the peritreme was lost in the common ancestor of *Z. valentinei* + *Z. insulare*.

We only observed a single seta dorsally between the meso-/metapleuron and scutellar-axillar complex anterior to the postalar sensillum in *Z. insulare* and *Z. valentinei* (Figs 105, 110: dms?). Because this seta is very close to the base of the hind wing and is quite obvious we tentatively consider it as homologous with the seta on the dorsal margin of the metapleuron rather than with the suprapleural sensillum of *Mymaromma* and *Mymaromella*. However, dirt or position of wings prevented observation of the presence or absence of the different sensilla in many specimens and further study is necessary to document their distribution accurately in all species of *Mymaromma* and *Mymaromella*.

Another feature of the metathoracic-propodeal complex that differs among mymarommatids is the presence or absence a metapleural pit, and its position when present. We did not observe a metapleural pit in species of *Zealaromma* (Figs 103, 108), whereas species of *Mymaromma* have quite a distinct pit that is comparatively close to the propodeal spiracle (Figs 80–83: pl_3p). Species of *Mymaromella* are variable in presence or absence of a metapleural pit (*cf.* Figs 95–97, 99, 101) and it is so small that often it is visible only with SEM (Figs 97, 101). Therefore, the apparent absence of a metapleural pit in some species of *Mymaromella* may be because of the angle of view or dirt concealing the minute hole. When visible, the pit is at least midway between the propodeal spiracle and the ventral margin of the metapleuron (Figs 97, 101). We are uncertain of the presence or absence and relative position of a metapleural pit in fossil mymarommatids because of the difficulty in observing such a tiny feature. However, *P. agapa* appears to have an unusually large and distinct metapleural pit that is quite close to the propodeal spiracle (Fig. 187: pl_3p, sp). A few species of *Mymaromma* also have a tiny pit on the mesopleuron (Fig. 87: pl_2p) at a similar height as the larger metapleural pit (Fig. 87: pl_3p), but this requires clean specimens and SEM for observation.

The final variable feature of the propodeum is its structure posteriorly. In *My-*

maromma, the posterior margin extends as a ∩-like flange over (Figs 78, 79) and on either side of the petiolar insertion (Figs 81, 83). The flange normally conceals the propodeal foramen in dorsal (Figs 78, 79) or lateral (Fig. 80) view. If the metasoma is dissected from the mesosoma (Figs 86, 87) the propodeal foramen is seen to project slightly as a circular ring (sometimes also visible if mesosoma observed from posterolateral view, Fig. 81). The ventral edge of each side of the propodeal flange abuts the posterodorsal margin of the slightly protruding metacoxal foramen so that the two form a rigid pincer-like structure around a deep pit (Figs 80, 86: isp; 81, 83, 87). Although the posterior propodeal structures of *Mymaromella* and *Zealaromma* are superficially quite different from that of *Mymaromma*, they differ only by lacking the propodeal flange dorsally above the petiolar insertion. Consequently, the protuberant, somewhat tubular propodeal foramen is more readily visible (Figs 90–97, 99, 101, 103, 104, 107). We could not determine the exact structure of the propodeum in fossils, but they appear to have structures (Figs 184, 191) similar to those *Mymaromella* that lack a distinct vertical flange on either side of the foramen (*cf.* Fig. 94). In *Mymaromella* and *Zealaromma*, the rim of the metacoxal foramen and the flange on either side of the propodeal foramen form the same pincer-like structure as in *Mymaromma* (*cf.* Figs 92, 94, 104 with Figs 81, 87: pf). Although usually less noticeable, a similar pincer-like structure is formed between the dorsal margin of the mesocoxal foramen and the anteroventral angle of the metapleuron, and sometimes between the anteroventral margin of the mesopleuron and posterolateral margin of the pronotum (Figs 80, 86: isp). The adaptive function of the pincer-like structures is unknown. In most individuals, the anteroventral projection of the metapleuron and the ventral margin of the propodeal flange appear to extend only to the outer edge of the rim of the meso- and metacoxal foramina, respectively, mesal to an oblique trough in the rim of the coxae dorsolaterally (Fig. 87: ct). The trough likely cradles the dorsal, constricted part of the coxa (basicoxite) that inserts into its respective foramen (Figs 81, 104, 107: bc). In *Zealaromma*, the propodeal flange projects ventrally as quite a strong digitiform process (Figs 104, 107). If the metacoxa is raised, the propodeal process would articulate within a basal groove of the metacoxa on the inner side of the basicoxite (Figs 104, 107). The lateral margin of the posteriorly protruded metacoxal foramen would likewise articulate within a basal groove on the outer side of the basicoxite (Fig. 107). Consequently, the ventrally projecting propodeal process and posteriorly projecting metapleural process may help stabilise or help control movement of the metacoxa, at least in *Zealaromma*.

Extant mymarommatids have only a single seta on the propodeum near the spiracle (Figs 84: prs; 80–83, 95–103, 109). Mymaridae usually also have only a single propodeal seta (Fig. 11: prs), though there is virtually no information concerning the distribution of propodeal setae in Hymenoptera and quite likely the number of setae is at least partly correlated with body size.

Wings: What we described as the distal part of the forewing stalk in mymarommatids has its anterior and posterior margins curved dorsally. In Cretaceous mymarommatids (Figs 185, 194, 195, 205) and in many extant species the recurved margins form only quite a short, ∪-shaped gutter basal to the widened disc surface (Fig. 125). Some extant species have the margins abutting along a longer distance to form more of a complete tube (Figs 124, 131). A slightly thicker basal part of the stalk (Figs 124: stp; 167) forms a "proximal" portion that in dorsal view has a single campaniform sensillum and seta distally (Figs 125–128: cs, mc). We consider the proximal part of the forewing stalk to be composed of remnants of the wing base

and venation similar to those of Chalcidoidea (see discussion of suprafamilial relationships). We interpret the part of the anterior convex band that folds under the wing as the costal cell (Figs 127, 129: cc; 130, 132), the region between the putative costal cell and the distal seta and campaniform sensillum as the marginal vein (Figs 95, 127, 129, 185: mv; 130, 132), and the distal part of the putative marginal vein that appears bulbous or curves slightly away from the wing margin in slide preparations or in fossils as the remnant of the stigmal vein (Figs 185: stv; 194). The retinaculum is the posterior band that in ventral view is concave (Figs 127, 132: ret). A slender band that extends toward the base of the wing from the base of the putative marginal vein, which separates the costal cell from the retinaculum, we interpret as the submarginal vein (Figs 95, 127, 132, 185: smv). In slide preparations, the regions described above as the marginal and stigmal veins often appear to be filled with air (Fig. 167), which supports the hypothesis that these represent vein remnants. The length of the putative marginal vein is variable (*cf.* Figs 95, 127, 130, 132), but our survey was insufficient to determine whether length is a generic or only a specific feature. A line of "dots" are visible near the anterior margin of what we interpret as the costal cell in some slide preparations (Fig. 167). These dots are in the same position as a line of spicules on the costal cell of some species when studied with SEM (Figs 95, 130). Other species have scattered spicules on the costal cell (Figs 129, 132). A distinct line of dots on the forewing basal to the marginal vein in some Cretaceous fossils (Figs 185, 201) suggests that a straight line is the groundplan state, but our survey of extant species was insufficient to determine whether the arrangement of spicules could be informative for differentiating supraspecifc taxa.

The anterior and posterior margins of the forewing are curved into a U-shaped gutter in *Mymaromma* sp. 10 (Fig. 125). A cross-section of the forewing immediately distal to the long seta reveals a more or less S-shaped folding pattern (Fig. 126). In cross-section, the posterior band is thin and forms a deeply concave fold that comprises the retinaculum (Fig. 126: ret), whereas the anterior band is tubular and folds dorsally upon itself so as to abut the posterior band. The tubular portion appears to be subdivided into two parts by a thin septum and the larger portion is filled with some substance. If this substance is dried haemolymph and if the smaller portion that appears empty is a trachea (Fig. 126: tra?), then this further supports the contention that the anterior tubular portion is a remnant of a vein.

Members of *Mymar* have even more conspicuously pedunculate forewings (Fig. 2) than mymarommatids. The anterior margin of the forewing (Figs 4, 5: am) is curved dorsally and is folded over to its posterior margin so as to form a longitudinally divided tube distal to where the hind wing attaches to the retinaculum. The margin is folded over immediately beyond a single long seta (Figs 3, 4: mc) and there are several campaniform sensilla (Fig. 4: cs) distal to the seta, unlike the single, more basal sensillum of mymarommatids. In *Mymar*, the long seta is homologous to the distal macrochaeta of other mymarids and the campaniform sensilla likely are all that remain of a reduced stigmal vein. Consequently, the forewing of *Mymar* is quite similar to that of mymarommatids except for position of the campaniform sensilla relative to the long seta. The sensilla are positionally correct in *Mymar*, but not in mymarommatids, if they are stigmal in origin and the long seta delimits the apex of the marginal vein. The forewings of *Mymar* are additionally similar to most mymarommatids in having long marginal setae that arise from within the wing periphery (Fig. 7). In mymarommatids, the setae are inserted conspicuously within the wing periphery only in those

species with long marginal setae (Figs 113–119, 121, 163, 165, 168). The deep insertion of the marginal setae is not apparent when these are short (Figs 120, 122, 164). The functional significance of a deep insertion for the setae likely is to minimize their flexion at the wing margin when the wing is moved through the air so as to help keep the setae in the same plane as the wing surface. This would result in the disc and projecting setae together forming a larger wing "surface". The forewings of mymarommatids are unique in having a mesh-like pattern on the disc (Figs 163–165, 195, 211) that is formed by lines of raised membrane on both the upper and lower surfaces (Fig. 123). Although the pattern is not distinct in some amber fossils (Figs 183, 205), this appears to be an artifact of preservation. The pattern likely is less distinct in amber fossils because the resin fills the depressions between the lines of raised membrane similar to using glycerine to fill small surface irregularities in amber. The mesh-like reticulations may serve to provide strength to the relatively large wing disc so that it is not deformed as it is pushed through the air. Similarly, the longitudinal folds of the disc membrane that result in a more or less corrugated forewing in many mymarommatids (Figs 113–115) may help wing rigidity. The longitudinal folding affects wing shape to some extent because the forewings usually appear more elongate-lanceolate in species with deeper folds than in species with less distinct folding (*cf.* Figs 113–115, 163 with Figs 116, 118, 166). Consequently, shape and relative dimensions of the forewings can be affected by method of specimen preservation, such as slide versus dry mounting.

The length and thickness of both the marginal and discal setae are quite variable among mymarommatids (*cf.* Figs 113–122). Species of *Mymaromella* tend to have short, spine-like discal setae (Figs 166, 168), whereas those of *Mymaromma* (Fig. 163) and *Zealaromma* (Figs 164, 165) have longer, more hair-like setae, but there is considerable variation. The forewings of all but one species of *Mymaromma* are characterized by the presence of a conspicuously long posterobasal marginal seta that is separated by several short setae from long marginal setae apically (Figs 113–115, 163). All the posterobasal marginal setae are quite long in *Mymaromma* sp. 10, but this may be correlated with its very long and conspicuous discal setae (Fig. 116). Many species of *Mymaromella* have the posterobasal setae all short (Figs 117, 120, 166), though some have quite a long posterobasal seta (Figs 118, 119) similar to species of *Mymaromma*. The forewing marginal setal pattern of *Z. insulare* (Figs 122, 164) is modified similar to *Mymaromella* sp. 20 (Fig. 121), whereas *Z. valentinei* has a forewing marginal setal pattern that is unique among extant mymarommatids. The forewing of *Z. valentinei* has three or four quite long basolateral setae basally on the posterior margin (Fig. 165), which is similar to some Cretaceous mymarommatids (Figs 188, 194). Other Cretaceous species (Fig. 195) and some Tertiary (Fig. 211) fossils have a single conspicuously long posterobasal seta, and one Tertiary species has uniformly short posterobasal setae (Figs 207–209) (see further below).

The stalk-like hind wing of mymarommatids (Figs 135, 136) terminates in a C-like structure formed from a single, curved, socketed hamulus (Fig. 135: ham) and an opposing process that appears to be a projection of the wing (Figs 134, 135: op). Consequently, the opposing process is a functional analogue, but probably not homologous with what Basibuyuk and Quicke (1997) called "modified-erect setae". Between them, the hamulus and opposing process grasp the hind margin of the forewing. The apex of the hamulus inserts into the retinaculum (Figs 130: ret; 129, 133) and the apex of the opposing process is appressed against the dorsal surface of the wing (Figs 134: op; 133). This

functional complex is quite similar to that of *Mymar*, in which the stalk (Fig. 2) has two socketed hamuli and additional distal projections that grasp the forewing (Fig. 5) (in some species the wing continues as filament beyond the hamuli). The hind wing stalk of mymarommatids is composed of a tubular vein along the anterior margin and sometimes a slender band of membrane posteriorly (Figs 135, 136: mb), though distinct membrane usually is not evident. The stalk has long setae along its leading margin and these setae project within the retinaculum when the wings are joined (Figs 129, 130), perhaps serving to sense position of the hind wing and/or to further position the hind wing relative to the forewing. The process of the hind wing is bifurcate in most if not all species (Figs 134–136). At least some species have longitudinal striations on the dorsal surface of the posterior band of the proximal part of the forewing. The striations likely act as "tracks" along which the bifurcation of the hind wing process slides (Figs 133, 134). Furthermore, at least some species have short, distally projecting denticles on the posterior margin of the retinaculum (Fig. 132: ret) below much of the region we interpret as the marginal vein. These denticles may function as a ratchet, enabling the hamulus and hind wing to slide distally in the retinaculum when the forewing is moved downward, but impeding movement of the hamulus if it is slid along the posterior margin of the retinaculum when the forewing is moved upward. Such a ratchet structure could be used to help maintain the fore- and hind wing complex at a specific angle relative to the body for extended periods of time. It is unknown whether the forewings can be rotated for the correct movements necessary to produce lift during upward and downward arcs of the wing. It may be that mymarommatids actually do not fly, but simply use their comparatively large forewing surfaces as "kites" and are blown passively in wind currents. If the latter, the rod-like hind wings, apparently strong coupling system between the fore- and hind wings, ratchet slide mechanism, and other modifications of the forewing discussed above may all serve to reinforce the forewing to prevent its deformation and hold it at the necessary angle so that the individual can balloon.

Legs: As first mentioned by Gibson (1993), extant mymarommatids have two different structures of the protibial spur or calcar *sensu* Basibuyuk and Quicke (1995). Species of *Mymaromella* (Figs 137, 139a: ca) and *Zealaromma* (Fig. 140: ca) have a comparatively long and curved, apically bifurcate calcar, whereas those of *Mymaromma* (Figs 142, 144a, 145a: ca) have a short, simple or needle-like calcar. The protibia also has a strong, socketed seta ventroapically on either side of the calcar that originates from a tube-like elevation of the cuticle (Figs 138, 140, 141a, 144a, 145a, b: ps). Because of their position and structure, under some angles of view one of these socketed setae can be mistaken for the calcar in *Mymaromma* (*cf.* Figs 142, 143, 144a: ca, ps); however, the calcar originates from a concave region that is continuous to the apex of the protibia (Figs 144a, 145b). There is also a much smaller second projection within the concave region of some species of *Mymaromma* (Fig. 145b). Extant mymarommatids lack meso- and metatibial spurs, but there are two strong, socketed setae that originate from tube-like elevations of the cuticle ventroapically on the mesotibia (Figs 139b, 141b, 144b: ps) and metatibia (Figs 139c, 141c, 144c: ps) similar to the protibia. The two ventroapical setae project beyond the apex of the respective tibiae and usually diverge distally. We refer to the two ventroapical setae on the tibiae as "pseudospurs" because they resemble the articulated spurs of parasitic Hymenoptera with true tibial spurs. Because of their size, we were unable to determine whether spur-like projections visible on the meso- and metatibiae of some fossil mymarommatids are

true spurs or pseudospurs. We suspect they are pseudospurs because there are more than two spines on the metatibiae of some fossils similar to extant mymarommatids (Figs 139c, 144c).

The only other leg feature we found to differ among mymarommatids was the presence of small "bumps" on the posterior surfaces of the femora (Figs 143–145), particularly the mesofemur (Fig. 144) of both species of *Zealaromma*. The function of the bumps and whether or not they are campaniform sensilla is unknown.

Basibuyuk et al. (2000) examined the sensilla of the orbicula of the tarsal claws of an unidentified mymarommatid species in their review of that structure in Hymenoptera. We did not attempt to extend their survey to determine whether the character states they documented for the species vary in Mymarommatidae.

Metasoma: Individuals of *Zealaromma* lack cerci and have four setae in a row near the posterior margin of the syntergum (Figs 153, 155). *Mymaromma* and *Mymaromella* have cerci and these usually are almost flat, subcircular and with four long setae (Figs 150: cer; 158). The number of cercal setae is reduced (Fig. 151) in some species of both genera and rarely the cercus is almost indistinguishably integrated with the tergal surface except for being somewhat concave (Fig. 152: cer). However, there is always at least one seta that is more or less obviously associated with the cercal depression on either side of two paramedial syntergal setae. In such instances, the syntergum appears to have four setae in a row (Fig. 152) rather than the two paramedial setae (Figs 150, 151, 158) that are otherwise characteristic of *Mymaromma* and *Mymaromella*. This suggests that the cerci were lost in *Zealaromma* through their fusion with the tergal surface and that the two outer syntergal setae of *Zealaromma* are homologous with cercal setae in *Mymaromma* and *Mymaromella*. Individuals of *Zealaromma* also lack metasomal spiracles (Figs 153–155), though males of *Z. insulare* retain a seta on Mt_7 (Fig. 154) that in *Mymaromma* and *Mymaromella* is associated with the spiracle (Figs 149–152).

Lin (1994, fig. 3) illustrated the male genitalia of a species identified as *M. anomalum*. Triapitsyn and Berezovskiy (2006) stated that this was a misidentification of their new species, *M. ypt*, and gave another illustration of the genitalia (fig. 9) based on their specimens. Both illustrations show a posteriorly directed Y-shaped structure over a larger medial structure. The medial structure tapers posteriorly and is divided apically; anteriorly it has lateral rods that extend for a distance greater the medial rod of the Y-shaped structure. The two drawings appear quite different from our SEM microphotographs of the male genitalia of *Mymaromma* sp. 7 (Figs 158–160), but the differences likely are mostly because of the different methods used to prepare and study the genitalia (slide mounting *vs.* SEM) rather than species differences. Microscope slide preparations of the male genitalia of *M.* sp. 7 and of a specimen of *M. anomalum* from Japan also show a medial Y-shaped structure (Fig. 170: voa) and two longer and stronger paramedial processes (Fig. 170: aea) similar to those in the drawings of Lin (1994) and Triapitsyn and Berezovskiy (2006). Additionally, there are a pair of very slender, obliquely angled, somewhat sinuate structures (Fig. 170: paa?) exterior to the paramedial processes, which extend to the same level as the medial rod of the Y-shaped structure (Fig. 170). A photograph of the apex of the male metasoma of a male of *M. ypt* sent to us by Serguei Triapitsyn (UCRC) shows that it also has the slender oblique structures. The oblique structures extend anteriorly to the same level as in Fig. 170, but posteriorly they appear to articulate with the anteriorly directed arms associated with the sclerotized ∩-shaped structure (Fig. 170: syn?).

Zealaromma males differ conspicuously from those of *Mymaromma* and *Mymaro-*

mella because they have elongate-digitiform processes that project laterally from between the syntergum and hypopygium (Figs 154, 156: par). Each process has a long terminal seta and the processes point in different directions in some specimens (*cf.* inserts in Figs 155, 156), which indicates they are articulated or membranous basally. The processes resemble the exserted cerci of some Chalcidoidea (e.g. Torymidae), but there are several setae on the cerci of chalcids whether these are exserted or plate-like, similar to mymarommatids (Figs 150, 158) and some other parasitic Hymenoptera (Fig. 157). We consider the elongate processes of the male genitalia of *Zealaromma* to be parameres. The genitalic structure of *Zealaromma* is similar to that of male Maamingidae, which was described and illustrated by Early et al. (2001, figs 12, 13). The genital complex of *Maaminga rangi* Early et al. (2001) apparently lacks a phallobase, but has a medial, apically divided aedeagus (Fig. 157: aed), a volsella with a spined digitus (Fig. 157: vol, dig) ventrolaterally on either side of the aedeagus, and a digitiform paramere with two terminal setae (Fig. 157: par). The digitiform parameres of *M. rangi* widen anteriorly and articulate with the aedeagal-volsellar complex basally (Fig. 157). In microscope-slide preparations of the male genitalia of *Z. valentinei*, the bases of the externally visible parameres (Fig. 169: par) appear be continuous with slender rods (Fig. 169: paa) that extend anteriorly lateral to the much stronger paramedial rods (Fig. 169: aea). The slender rods curve toward the aedeagal-volsellar complex at a level near the end of the medial Y-shaped structure (Fig. 169: voa), where they possibly articulate with the complex. Except for the externally projecting parameres, structure of the genitalia observed in the slide preparation of *Z. valentinei* is quite similar to that of *Mymaromma* sp. 7 (*cf.* Figs 169, 170).

The aedeagus of male chalcids has paired aedeagal apodemes (Gibson 1997, fig. 7). We therefore interpret the longer paramedial rods visible in slide preparations of the male genitalia of *Zealaromma* and *Mymaromma* as the apodemes of the aedeagus (Figs 169, 170: aea). A pit in each smaller anterior lobe of the aedeagus (visible with SEM) may represent the base of the respective apodeme. The medial rod of the Y-shaped process in males of both genera (Figs 169, 170: voa) appears to be continuous with the two ventrolateral volsellae/digitae (Figs 161, 162, 169: dig). In the slide of *Z. valentinei*, the medial rod appears to consist of two appressed apodemes rather than just a single apodeme (Fig. 169) (also suggested in Lin 1994, fig. 3). Based on positional similarity, we suggest that the internal, obliquely angled, slender rods of male *Mymaromma* (Fig. 170: paa?) may be homologous with the internal rod-like portions of the parameres of male *Zealaromma* (Fig. 169: paa). We are uncertain as to the structural homologues of the two darker, c-shaped regions in Fig. 170. The smaller, apical c-shaped region (Fig. 170: anp?) may be a sclerotized anal plate, which separates the anus from the genital complex (Fig. 159: an, anp). The lateral longitudinal processes associated with the larger c-shaped structure appear to be lateral, anteriorly extended portions of the syntergum (Fig. 170: syn?). The larger c-shaped structure consists of lateral, slightly convex bands and a straight, transverse ventral band (Fig. 170). The former may simply be the edges of one of the tergites and the latter the edge of a sternite, but further study is necessary to resolve this.

EXTINCT FAUNA

Tertiary taxa.—The only mymarommatid genus described from Tertiary amber is *Palaeomymar* Meunier. The type species, *P. succini* Meunier (1901), was based on 5 of the original 13 males and 3 females that Duisburg (1868) discussed and illustrated. We did not locate any amber inclusion we consider as part of their material (see

"Neotype designation" under *Palaeomymar*) and therefore base our interpretation of *P. succini* on their descriptions and illustrations.

Although Duisburg (1868) did not describe his specimens in detail he stated why he thought they probably belonged to *Mymar* Curtis. The diagnosis he gave for *Mymar* included 13-segmented antennae for males, 9-segmented antennae for females, and 4-segmented tarsi. He said that the fossils differed from *Mymar* primarily in wing features and stated specifically that the long marginal setae began near the apical half of the forewing, as he illustrated (Duisburg 1868, fig. II). The forewing of *P. succini* illustrated by Meunier (1901, fig. 12) also shows the marginal setae along the posterior margin gradually increasing in length apically, i.e., without a conspicuously long basal seta. Meunier (1901) described five rather than four tarsal segments for *P. succini*, but this discrepancy is not surprising because Duisburg (1868, fig. II) illustrated, and thus likely examined, a female at only 85x magnification. All known mymarommatids have five tarsal segments. Meunier (1901, fig. 13) only described and illustrated the 13-segmented antenna of a male and provided no information to confirm or contradict Duisburg's comparison of the female antenna with that of *Mymar*. The habitus line drawing of Duisburg (1868, fig. II) appears to show only five funicular segments, but known female mymarommatids have either six or seven segments. Based on the stated similarity of the antenna to *Mymar*, the flagellum likely consisted of six funicular segments and an unsegmented clava.

We examined 10 Baltic amber mymarommatid inclusions, 8 from ZMUC, 1 from GZG, and 1 from NHRS. The inclusions from ZMUC contained five males and three females that likely constitute three species. The first species, represented by a male (ZMUC: 17-5/1963) and a female (ZMUC: 1-5/1967), is characterized by a long, curved protibial calcar (Fig. 212) and a forewing that has the posterobasal marginal seta obviously longer than several setae distal to it (Fig. 211). The female also has seven funicular segments and an unsegmented clava. Based only on these features it is likely that the species, if extant, would be assigned to *Mymaromella*. Two pieces of amber, both labelled as ZMUC: 16-1/961, each has a single male. One is insufficiently preserved to determine its relevant features, but the other male has a long posterobasal marginal seta and lacks a long calcar. If extant, this male probably would be assigned to *Mymaromma*. Another two males (ZMUC: 8-19/1954, 1890-108) and two females (ZMUC: 28-3/1958, 16-1/1961) are characterized by the absence of a long protibial calcar, uniformly short setae along the posterior margin of the forewing basally (Figs 207–209), and a 6-segmented funicle in the females (Fig. 179). Because of these features we believe that this third species is the one that Duisburg (1868) illustrated and Meunier (1901) named as *P. succini*. Although Duisburg (1868) and Meunier (1901) described and Meunier (1901, fig. 13) illustrated a 13-segmented male antenna for *P. succini*, males may only have 12 antennal segments. The left antenna of the male in ZMUC: 8-19/1954 is clearly visible in ventral view. The apical four segments are all about the same length and form a differentiated clava because they are slightly thicker and more broadly attached than 6 more slender funicular segments (*cf.* Fig. 177). The apical flagellar segment illustrated by Meunier (1901, fig. 13) is very short and it may only be a subsection of the apical segment that is differentiated by a whorl of projecting setae. The ZMUC: 8-19/1954 male in ventral view also appears to have the propleura fused into a carapace, the mandibles lack any distinct dorsal tooth or angle, and although the labiomaxillary complex is quite broad the labium appears to be only about as wide as the maxilla. The genitalia project ventrally from the metasoma and

lateral digitiform processes (parameres) are not evident. If our observations are correct, the ZMUC amber inclusions indicate that Tertiary mymarommatids had more diverse combinations of features than the extant fauna. No extant mymarommatid has a short calcar (characteristic of *Mymaromma*) and all the setae along the posterior margin of the forewing short basally (characteristic of many *Mymaromella* but not *Mymaromma*).

The GZG specimen is a male positioned dorsal side up in a thin piece of amber glued to a microscope slide. It has a long, curved protibial calcar and the left forewing, viewed with the compound microscope, appears to have a very long posterobasal seta. Also visible are the dorsolongitudinal and dorsoventral flight muscles plus the mesotergal-trochanteral muscles. Using a compound microscope, the mesotergal-trochanteral muscle of one side clearly attaches to the apex of an obliquely projecting, rod-like axillar phragma (*cf.* Vilhelmsen and Krogmann 2006, fig. 13). The NHRS specimen, also a male in an amber block glued to a microscope slide, is positioned in a somewhat dorsolateral view. It also appears to have a long, curved calcar, but the forewing marginal setal pattern is not clear because the forewings are crossed over basally.

The only other described Tertiary mymarommatid, *P. duerrenfeldi*, is based on a single male from Sicilian amber. Sicilian amber is dated at about 5 mya compared to Baltic amber at about 44 mya (Grimaldi and Engel 2005). The lateral habitus drawing of *P. duerrenfeldi* provided by Schlüter and Kohring (1990, fig. 1) illustrated a comparatively long and straight (needle-like) protibial calcar and a broad forewing that is evenly rounded apically. Our study of the holotype confirmed that the calcar is long but that it is also curved distally. The forewings are most similar to those of extant *Mymaromella* because of their shape and the presence of short, spine-like discal setae (represented by dots in fig. 1 of Schlüter and Kohring, 1990). The left wing, examined with a compound microscope, appears to have a posterobasal marginal seta that is obviously longer than several more distal short setae, though it is shorter than the posterobasal seta in Fig. 118 (the right wing also has a "line" apparently projecting from its posterobasal margin that superficially appears as a seta, but it is longer than that of the left wing and may be an artifact). The mandibles definitely are bidentate, similar to those of extant *Mymaromella* and *Zealaromma* (*cf.* Figs 47, 54), and the vertex appears to have ocelli under some angles of light when examined with a dissecting microscope. The body cuticle is translucent in lateral view so that presence or absence of a suture between the meso- and metapleuron is not evident. The exact structure of the propodeum cannot be determined, but it apparently does not have a strong propodeal flange because the basal constriction of the first petiolar segment is visible in lateral view (*cf.* Fig. 99). Schlüter and Kohring (1990, figs 1, 2) described and illustrated a 12-segmented antenna for *P. duerrenfeldi*, including seven funicular and three claval segments. The terminal claval segment of the right antenna was drawn with its basal half bulbous and its apical half more narrowly digitiform. The clava is more distinctly 4-segmented when examined with a compound microscope because a transverse line (suture) divides the two subsections of the terminal segment (*cf.* Fig. 177). Because the flagellum has seven distinct funicular segments we believe the antennae to be 13-segmented with a 4-segmented clava. Consequently, the female of *P. duerrenfeldi* probably has 7 funicular segments and a 1-segmented clava.

Cretaceous taxa.—We examined type material of all the described Cretaceous species except for *P. japonicum* Fursov et al. (2002). The unique female of *P. agapa* differs from females of other described mymarommatid species in several respects. Most conspicuously, it lacks the

highly derived head structure that characterizes other mymarommatids. The vertex, genae and temples appear to be uniformly sclerotized and finely, transversely strigose (Fig. 186). The sculpture is similar to that of the cheeks of some extant members (Figs 13, 16, 30). The vertex lacks a hyperoccipital band of pleated membrane and the convex vertex merges smoothly into the posterior surface of the head (Figs 183, 186), which is medially concave and with the occipital foramen near its center (Fig. 186). The head structure of *Galloromma bezonnaisensis* is uncertain (see below), but our study of type material and/or published illustrations indicate that all other described Cretaceous species had the same derived head structure as extant mymarommatids (Fig. 198; Kozlov and Rasnitsyn 1979, figs 8, 9; Fursov et al. 2002, fig. 1).

As noted by Kozlov and Rasnitsyn (1979), the female of *P. agapa* also has a different mandibular structure than other mymarommatids. Although closed in the holotype, in lateral view the mandibles are comparatively thin and the outer surface is convex. The apex of the right mandible broadly overlaps the left mandible almost to its base and each mandible appears to be tapered to a point. Because they are closed, any internal dentition is not visible. There is a distinct transverse region between the dorsal surface of the mandibles and the oral margin, but we could not determine whether there is a labrum within this apparent "cavity". Extant mymarommatids are characterized by exodont mandibles. Each has a comparatively broad outer surface with the apex outcurved and with two or three externally visible, asymmetrical teeth. Furthermore, when closed, the apices of the mandibles do not overlap and their dorsal margins abut or even overlap the oral margin of the head capsule (Figs 18, 19, 25–31, 33–39, 47–49, 52, 54). The mandibles are not clearly visible in most fossils, but they are fully open and obviously exodont in the holotype of *P. mandibulatus* (Figs 197, 198). The left mandible is completely exposed and has a blunt subapical ventral tooth and a much smaller subbasal tooth (Fig. 198: sbt). Except for the tiny subbasal tooth, the exposed mandible of *P. mandibulatus* is quite similar to that described for *Mymaromella* and *Zealaromma*. The holotype (PIN: 3311/450) and a paratype (PIN: 3311/448) of *P. senonicus* that we examined have the mandibles closed, but their apices are widely separated and we agree with the description of Kozlov and Rasnitsyn (1979) that the apex of the mandibles are bent outwards slightly. Both specimens appear to have the labium separate from the maxillae (Fig. 203), but we were unable to distinguish palpi. Bidentate mandibles that are widely separated from each other and that do not meet in the middle was also given as a generic feature of *Archaeromma* by Yoshimoto (1975), which we confirm for *A. minutissimum* and *A. nearcticum*. The mandibles of *P. japonicum* were described as having two sharp teeth, which almost certainly are exodont based on Fursov et al. (2002, fig. 1). The exact structure of the mandibles of *G. bezonnaisensis* is unknown.

The female of *P. agapa* and extant mymarommatids also appear to differ in relative position of the toruli. In *P. agapa*, when the head is viewed in profile the toruli are near the center of the head and its large eyes (Kozlov and Rasnitsyn 1979, fig. 10). In extant mymarommatids the toruli are near the dorsal margin of the eyes, regardless of whether these are reduced in size (Fig. 47) or are as large (Figs 25, 33) as those of *P. agapa* (Fig. 186). The holotypes of *P. mandibulatus* and *P. senonicus* are similar to that of *P. agapa* because they have large eyes (Figs 198, 203) and the toruli appear to originate at about mid height when the head is viewed from the left side. However, the apparent placement of the toruli can be affected by the angle of viewing in amber inclusions, as discussed below.

In addition to the cephalic differences, the holotype female of *P. agapa* has a distinctly 13-segmented antenna. When the specimen is viewed from its left side (Fig. 183), the left flagellum is in profile; the right antenna is partly concealed by the head but the apical three claval segments are exposed in dorsal view. The left antenna has seven slender funicular segments and four much wider segments that form a comparatively loosely associated clava (Fig. 180: cl; Kozlov and Rasnitsyn 1979, fig. 10). The exposed claval segments of the right antenna each have a pair of quite long and robust sensilla, one above the other, projecting from the outer surface. Each of the sensilla appear to be strongly bent basally and originate near the middle of the respective segment (Fig. 181a). The claval sensilla on the outer surface of the left antenna are not as distinct because of the angle of view, but at least the penultimate segment has two sensilla that originate near its middle, one almost at the dorsal margin and one midway between the midline and ventral margin (Fig. 181b). Because of their length these sensilla resemble s2-type sensilla of extant mymarommatids, but one or both could be unusually long s4-type sensilla. The claval segments of the left antenna also have several very short sensilla along the ventral margin (Fig. 181b) that are similar to s3-type sensilla of extant mymarommatids (*cf.* Fig. 72).

Females of other described mymarommatids have a clava composed of 1–4 segments, but if the clava is 3- or 4-segmented then the segments are much more compacted than in *P. agapa*. The clava is more tube-like with at least the third and fourth segments separated only by quite an obscure transverse suture (Figs 192, 196, 200, 204). Kozlov and Rasnitsyn (1979) described the female flagellum of *P. senonicus* as having seven funicular and three claval segments, and they illustrated (fig. 8) a paratype in dorsal view with three claval segments. Our study of this paratype in ventral view at 200x magnification revealed two distinct basal claval segments and a terminal segment that is nearly as long as the combined length of the two basal segments (Fig. 204). At 400× magnification the terminal segment also appears to be subdivided by a transverse suture, suggesting four claval segments (one or two very fine transverse lines also appear to subdivide the "fourth" segment). On one side of the clava is a strong, basally bent sensillum that extends from the apex of each of the two basal claval segments and from the "third" segment at the apparent suture line. The apical "fourth" segment has an additional three strong sensilla on the same side. The other side of the clava also appears to have strong sensilla, but they are less distinct and we are uncertain of their number and position. Kozlov and Rasnitsyn (1979, fig. 9) illustrated and described a 4-segmented clava for the holotype female of *P. mandibulatus*. Our study of the holotype in ventral view shows that the right antenna has seven funicular segments and only three distinct, coalesced claval segments (Figs 199, 200), though possibly there is a small and very poorly differentiated terminal segment. Seta-like sensilla are visible projecting from the claval segments (Fig. 200), but not clearly enough to be confident of their number.

Yoshimoto (1975) stated that females of *Archaeromma* have seven funicular and four claval segments. Females identified as either *A. minutissimum* or *A. nearcticum* in the CNC have a distinct clava because it is longer and slightly thicker than any funicular segment, but the claval segments are strongly compacted. Consequently, the sutures and the number of segments comprising the clava are indefinite. At least three claval segments are visible for some females. The female in CNC: CAS-1113 has distinct sutures differentiating two basal claval segments and a terminal part that forms about half the length of the clava. This specimen and the female in CNC: CAS-119 also has other fine,

transverse lines on the terminal claval "segment" that suggest possible additional segmentation. The basal two claval segments of CAS-1113 each have two long, basally bent sensilla on one side; there are other long sensilla on the terminal part but we are uncertain of their exact number. The female in CNC: CAS-343 has six long, basally bent sensilla on one side of its compact clava, whereas other females usually have variably long, basally curved sensilla on one or both sides. Yoshimoto (1975) also described *Protooctonus masneri* as having seven funicular and four claval segments. Our study of the holotype revealed that the compact clava has only three distinct segments (Fig. 196). Although the clava appears to have more or less uniformly long seta-like sensilla in some angles of view (Fig. 196), in other angles the sensilla are longer on one side than the other.

The specimen that Kozlov and Rasnitsyn (1979) described as the male of *P. agapa* differs in several respects from the female. The most significant difference is that the posterior surface of the head is collapsed within the head capsule in a manner similar to extant mymarommatids having the occipital plate rotated anteriorly. The similarity includes a ∩-shaped occipital margin and a comparatively wide, infolded ventral margin that together form an abruptly margined, acute angle laterally. Furthermore, the occipital foramen appears to be at the ventral margin of the head. The mandibles, although slender relative to those of extant mymarommatids, also appear to have the exterior surface slightly outcurved apically, or at least the exterior surface is somewhat concave medially. The two mandibles are angled toward each other such that their apices extend slightly beyond the oral margin and almost meet medially. The left mandible, visible in lateral view, is expanded ventrally and is differentiated into a small, acutely angled submedial tooth and a longer, slender, apical tooth, as was described and illustrated by Kozlov and Rasnitsyn (1979, fig. 11). The antennae are 13-segmented and typical for male mymarommatoids, i.e., filiform with all the flagellar segments having a whorl of long setae medially to subapically. The apical four antennal segments, particularly the apical two, are slightly more strongly coalesced to form an inconspicuously differentiated clava. Kozlov and Rasnitsyn (1979) also noted that the eyes are somewhat larger and the first petiole segment markedly shorter in the male than in the female; furthermore, the ocelli are unusually large. Although described from the same amber deposit, the differences between the unique female and male of *P. agapa* suggest that they could represent the opposite sexes of two different taxa.

Species described in *Archaeromma* and *Protooctonus* are about 75 mya, whereas *Palaeomymar senonicus*, *P. mandibulatus* and *P. japonicum* are about 85 mya and *P. agapa* is about 95 mya. Only *Galloromma bezonnaisensis*, described from amber dated at about 100 mya, is older than *P. agapa* (Table 1). The unique holotype of *G. bezonnaisensis* is in a slender shard of amber that is double embedded in clear epoxy resin. The first resin block was ground to within 0.2 mm of the shard surface (Schlüter 1978) in which the dorsal surface of the specimen and the antennae face up, and then was re-embedded so that the specimen is now encased in a comparatively large block (12 × 12 × 10 mm) of resin. Visibility of the specimen in dorsal view is similar to that shown in the illustrations provided by Schlüter (1978, fig. 50; plate 5, fig. 3; plate 11, fig. 2), though in dorsal view artifacts largely conceal all but the two antennae and the right forewing (Figs 214, 216). In lateral view, a visible boundary line between the two resins is so close to the fossil that it prevents observation of the specimen with the same clarity as photographed by Schlüter (1978, plate 5, fig. 2). The latter photograph is reproduced here as Fig. 215.

The habitus drawings given with the original description of *G. bezonmaisensis* illustrate a comparatively thin mandible that is acutely tapered both in lateral (Schlüter 1978, fig. 49) and dorsal (Schlüter 1978, fig. 50) views. In dorsal view, the presumed left mandible (Fig. 217: mnd) projects anteriorly from near the lateral margin of the head capsule. It is comparatively short and evenly tapered to a point, i.e., neither obviously exodont nor curved mesally. Because of its position and length, the apices of the two mandibles presumably would not meet if they were closed. However, the head is not clearly visible (Fig. 217) and it is possible that only the tip of the mandible is exposed (*cf.* Fig. 193). We cannot confirm the structure of the mandible drawn in lateral view by Schlüter (1978, fig. 50), but in the photograph (Fig. 215) it appears to be similar to the mandible *P. agapa*. The photograph (Fig. 215) and lateral habitus drawing in Schlüter (1978) also show a high-triangular head that dorsally is acutely angled. What appears to be the posterior surface is obliquely angled and almost straight, and therefore could be a flat or collapsed occipital surface that is acutely angled relative to a more obviously convex frontal surface. However, if the "posterior" surface is a flat or collapsed occipital plate then the antennal toruli are almost contiguous with the posterior limit of the vertex (Fig. 215), which is unknown for any other mymarommatid. Such a high placement of the toruli would also suggest the absence of ocelli, which all other Cretaceous mymarommatids apparently have. Based on our study of other amber inclusions (see below) we suspect that the high-triangular head is partly an artifact of preservation and the angle of view, and that both the anterior and apparent "posterior" surfaces comprise the face. If so, the antennal toruli are near the center of the head, similar to *P. agapa* and at least some other Cretaceous mymarommatids. The habitus line illustrations in Schlüter (1978, figs 49, 50) do not help resolve this problem. In lateral view, the antennae appear to be inserted near the middle of the eyes as in *P. agapa*, whereas in dorsal view they appear to be inserted at the dorsal margin of the eyes as in mymarommatids with a differentiated occipital plate. Different interpretations can also be given for the comparatively long ventral surface of the head anterior to the mesosoma (Schlüter 1978, plate 5, fig. 2). If the "posterior" surface of the head is a flat or sunken occipital surface then the position of the mesosoma indicates that the occipital foramen is near the ventral margin of this region, similar to extant mymarommatids. However, based on the lateral habitus photograph in Schlüter (1978), and our own observations, the mesosoma appears to attach to the head from under the "ventral" surface (Fig. 215). If so, this supports an hypothesis that both the apparent anterior and "posterior" surfaces constitute the face, and that the head is not structured as for extant mymarommatids. The sex of the specimen was not stated and is ambiguous based on antennal structure. Schlüter (1978) described the antenna as being 14-segmented with 8 funicular and 4 claval segments. Our study shows that there are four distinct, broadly appressed claval segments that are separated by oblique sutures (Fig. 214), but only seven funicular segments (Figs 214, 216). The claval structure indicates a female antenna. Furthermore, male mymarommatids usually have most of the flagellar segments of similar length and/or these widened medially because of the characteristic medial whorl of setae (*cf.* Figs 171, 172 and Figs 176, 175), whereas at least the basal four segments of the left flagellum of the holotype of *G. bezonmaisensis* are comparatively short and uniformly widened distally (Figs 214, 216). However, the terminal segment of the flagellum appears to be smaller than the penultimate segment (Schlüter 1978, fig. 50) and, as noted by Schlüter (1978), the flagellar segments have quite long and conspicuous setae

(Fig. 216: fs). These last two features are more characteristic of a typical male flagellum than that of a female, though some Cretaceous amber fossil females have quite distinct setae (Figs 196, 204). The illustrations of the antennae in lateral view given in Schlüter (1978, fig. 49; plate 5, fig. 2; plate 11, fig. 1) show a much more distinctly filiform flagellum (Fig. 215), which is also characteristic of a male antenna. However, the flagellum likely appears filiform in lateral view (Fig. 215) because the claval segments are compressed rather than cylindrical in cross-section. Consequently, their perceived width depends on the angle of view (Fig. 214; *cf.* Figs 181a, 181b). A short, dark region projecting posteriorly from the gaster could be the apex of ovipositor sheaths (Fig. 215: ovs?), but because of the condition of the specimen this cannot be confirmed. Furthermore, the gaster appears to be oval in cross-section (Fig. 215). Although gastral shape is not diagnostic, males usually have the gaster flattened whereas females more commonly have it oval in cross-section. The first petiolar segment is only slightly longer than the second segment in lateral view (Fig. 215) and therefore is very similar to the structure of *P. agapa* (Fig. 184), though petiolar structure does not seem to be sexually dimorphic or a generic feature (see further below). Finally, the setae along the posterobasal margin of the forewing are all quite long and of a similar length (Fig. 216).

In addition to the described taxa discussed above, we studied undescribed mymarommatoids from GPPC and AMNH Burmese amber. Burmese amber is dated at about 95–105 mya (Grimaldi and Engel 2005) and therefore the fossils are at least as old as *P. agapa* and *G. bezonmaisensis*. The GPPC material consisted of four inclusions containing three females and one male. The best preserved female (GPPC: HY17A) is in a clear piece of amber and is visible in both dorsal and ventral view, though in dorsal view a vertical crack cuts through the left antenna at the base of the sixth funicular segment and the left half of the head and mesosoma are partly obscured. This female is similar to that of *P. agapa* because in dorsal view the vertex is transversely strigose and uniformly convex, the posterior margin of the head lacks an abrupt margin and is shallowly concave, and the temples are comparatively long (Fig. 213). In ventral view, the lower posterior surface of the head is distinctly concave between the mouthparts and occipital foramen. Although the exact structure of the labiomaxillary complex is not visible, the mandibles are open so that their apices project anteriorly, distinctly beyond the head capsule (Fig. 193). They are conspicuously curved and, based on length and the distance between their bases, it is obvious that if closed one mandible would cross over the other. Each mandible is thicker basally and strongly tapered to a slender point. Although the base of the right mandible is obscured by what appears to be head tissue, a small subbasal tooth is clearly visible on the left mandible (Fig. 193: sbt). This female also resembles *P. agapa* because it has a 13-segmented antenna with four distinct claval segments. Both antennae project obliquely in the amber block so that the segments are foreshortened in dorsal or ventral view (Fig. 182), but because of the view it is definite that the claval segments are articulated. In ventral view, the middle two segments of the clava each have one, and the apical claval segment two, long, robust, basally bent sensilla on either side (Fig. 182, black arrows). Because of the oblique view of the antenna it is difficult to be certain where on each segment the sensilla arise, though the ventral sensilla of the middle two claval segments appear to originate from the apical margin of the respective segment (Fig. 182). The basal claval segment and the apical funicular segment also have what appear to be straight sensilla projecting from the respective segments (Fig. 182, white arrows).

These may be a different type or the same type as the other sensilla, but differ in appearance because of the angle of view. The protibial calcars are curved distally and have a short inner tine subapically, and because of their length resemble the long calcars of *P. agapa* (Fig. 183, insert). The relative position of the toruli is unknown because the head cannot be observed in lateral view. We are also uncertain of the marginal setal pattern because the forewings are partly twisted over the body, but there appear to be about 15 subequally long setae along the posterior margin basal to the longer distal marginal setae. If accurate, this setal pattern differentiates the species from *P. agapa*, which has three or four (the two wings differ) comparatively long basal setae followed by several shorter setae basal to the longer distal marginal setae (Fig. 188). The forewings of *P. mandibulatus* (Fig. 202), *P. senonicus* (Fig. 205) and *P. japonicum* (Fursov et al. 2002, fig. 1) all have a single, long, posterobasal seta followed by several shorter setae. Because of preservation, the forewing marginal setal pattern was not visible for all examined Canadian Cretaceous amber specimens. Most specimens appear to have a variable number of short setae distal to a single long posterobasal seta. The holotype of *A. nearcticum* (CNC: CAS-76) has about five short setae distal to the long seta, a pattern also possessed by one female (CNC: CAS-845) and one male (CNC: CAS-748) identified as *A. minutissimum*. Another female identified as *A. minutissimum* (CNC: CAS-1160a) clearly has nine short setae distal to the long posterobasal seta. However, one female paratype of *A. nearcticum* (CNC: CAS-598) has three quite long and three shorter setae basal to the much longer distal marginal setae (Fig. 194), which is similar to the setal pattern of the *P. agapa* female (Fig. 188). Consequently, the forewing marginal setal pattern either is quite variable in Canadian Cretaceous species or the fossils represent several species. Regardless, the presence or absence of a single long posterobasal seta likely is species-specific rather than correlated with fossil age or lineage.

A second Burmese female (GPPC: HY17B) is also in clear amber but is not visible in dorsal view because of the dimensions of the amber block and a crack above the specimen. In ventral view, the antenna has seven funicular segments and at least three claval segments that form a compact tube. The apical "segment" constitutes nearly half the length of the clava, but it might be subdivided. Projecting from along one side of the clava are four very long and thin, suberect, seta-like sensilla (one each on basal two claval segments and two on apical half of clava). At least the apical two funicular segments have similar long setae. Robust, curved sensilla are not clearly visible, but shorter, more prone setae project from the other side of the clava. The protibial calcars are curved and an inner tine is not visible. Because of this the calcar resembles one of the curved setae of the fine comb of the basal tarsal segment of extant taxa (*cf.* Fig. 137: fc). The apparent absence of an inner tine might be because of the angle of view, though a tine is not visible on either calcar using either a binocular or compound microscope. This specimen demonstrates that the angle of view can make a big difference for interpreting structure within amber inclusions. In ventral view, the head is obliquely angled with the mandibles toward the viewer. In this view, the frontal surface of the head is comparatively long and thin and the toruli appear to be very high on the head, slightly above the dorsal margin of the eyes. However, in lateral view the head is lenticular and the toruli are near the center of the face (the eyes are not evident so the position of the toruli relative to these is not known). The head is observed slightly from the posterior in lateral view. The center of the head appears to be collapsed and the dorsal and lateral posterior margins ∩-like margined. What appear to be two, apically tapered, thin

mandibles project anteriorly, though we could not determine their structure. The posterior margin of the forewing has seven comparatively short marginal setae that gradually increase in length distally. The third female (GPPC: HY17C) is clouded by sphericles within the amber block and is not clearly visible, but in dorsal view the posterior surface of the head resembles an occipital plate because it appears to be semicircular and slightly concave. The male (GPPC: HY17D) is in clear amber, but only partly visible in lateral view. In this view, the head is similar to that of the GPPC: HY17B female except that it is more highly convex and the toruli apparently are near the center of its large eyes and face. The head resembles that of *G. bezonnaisensis* (Fig. 215) because the antennae originate at the widest point, though it is not nearly as acutely triangular. Two apically tapered, comparatively thin and curved mandibles project distinctly beyond the head.

We examined seven specimens in five Burmese amber inclusions from the AMNH, of which only one was a female. This female is in a block (AMNH: B-0107) of resin-embedded amber (see Grimaldi et al. 2002) together with a male. The mandibles project anteriorly, distinctly beyond the head, and their apices overlap even though they are only partly open (Fig. 189). The apex of right mandible clearly extends beyond the midline of the head (Fig. 189) and, if closed, would extend to the base of the other. In dorsal view, each mandible is tapered apically and curved toward the other (Fig. 189) and in lateral view is quite thin (Fig. 190). Only the left mandible is completely exposed and its inner margin lacks a distinct subbasal tooth, though it has a subbasal angulation because the base is broader than the tapered apical portion. The antenna is 13-segmented, including a clava composed of four broad, distinctly separated segments (Figs 189, 190). In lateral view, the first three claval segments each have one, and the apical claval segment two, robust, basally curved sensilla along one side. The sensillum of at least the second and third claval segments originates near the middle of the respective segment, whereas the two sensilla of the apical segment are near the basal and apical third. At least the second and third claval segments have a robust sensillum on the other side projecting apically from the respective segment. The head is quite long in frontodorsal view (Fig. 189), but in lateral view it is more or less lenticular with the toruli near its center and that of its large eyes (Fig. 190). A uniformly convex vertex is not as evident as in *P. agapa*, but the vertex is rounded without any indication of an acute angle or pleated membrane. In lateral view, the posterior surface of the head appears to be concave with the occipital foramen near its center (Fig. 190). The forewings have 13 or 14 comparatively short, subequally long marginal setae along the posterior margin basally (*cf.* Fig. 191), similar to the GPPC: HY17A female. The mesosoma, in somewhat dorsolateral view, has a large circle very near the anterior margin of the propodeum that may be the spiracle, and a groove below it that extends to the posterior margin of the propodeum. We are uncertain of the exact structure of the propodeal foramen, but in lateral view the anterior (basal) flange of the first petiolar segment is clearly visible posterior to what appears to be a slightly protruding orifice (Fig. 190). The male in the same amber piece (Fig. 191) and the female of *P. agapa* (Fig. 184) have similar propodeal structures. The male is best observed from the side opposite the female, which presents a dorsolateral view of its body (Fig. 191). The posterior of the head is concave or more or less collapsed. A transverse ridge or angulation extends across the head above the occipital foramen, with the surface ventral to the ridge much more strongly concave or collapsed than the surface dorsal to it. The surface dorsal to the transverse ridge is somewhat similar to

an occipital plate of extant mymarommatids, but it is much more transverse, concave rather than flat, and lacks evident pleating or transverse ribs of sculpture. Furthermore, the front of the head immediately above the toruli is also slightly collapsed so that there is a transverse ridge between the eyes. In Chalcidoidea, a collapsed head, particularly the posterior surface of the head, is common for air-dried, weakly sclerotized specimens. The left mandible of the male is partly visible and it is similar to that of the female except for apparently having an inner tooth subbasally (Fig. 191). The presence or absence of a small inner tooth could be a sexual or taxon-specific feature or it could simply depend on the angle at which the mandible is viewed, particularly if the inner tooth or angulation projects externally, i.e., is somewhat exodont rather than flat and in the same plane as the rest of the mandible. The wings of the male are more clearly visible than for the female and the right forewing has 14 comparatively short setae along its posterior margin basally (Fig. 191). Both the female and male also have the first petiolar segment conspicuously longer than the second petiolar segment (Figs 190, 191). As for other extant and extinct mymarommatids, the male has the anterior margin of the base of the forewing folded under and there is a distinct, short marginal vein with at least one seta projecting from near its apex. The hind wing is reduced, apically bifurcate, and clasped to the forewing as described for extant members. The male also has what appears to be a large propodeal spiracle and a very long, apically bifurcate protibial calcar (Fig. 191, insert).

The forewing setal pattern and petiolar structure shared by the AMNH: B-0107 female and male suggest that they are the opposite sex of the same species and a different species than *P. agapa* and *G. bezonmaisensis*. Another Burmese male (AMNH: Bu-160) likely represents a third specimen of the species based on a very similar forewing marginal setal pattern. Observed from its left side, the propodeum appears to have a long seta posteromesal to a large circular spiracle similar to extant members. Observed from the right side, a short line extends dorsally from the propodeal spiracle, which could be the spiracular peritreme, and forms a convex arc with the dorsal margin of the pleuron similar to the structure of *Mymaromella*. From either side, a complete metapleural suture and distinct metapleural pit are also visible. The head, seen in ventral view, is not collapsed but is distinctly concave similar to that of the *P. agapa* female. In dorsal view, the toruli are near the center of its head and large eyes and its mandibles are as described for the AMNH: B-0107 male. The metasoma also has at least four long setae projecting from its apex, but the exact number of setae and their position is uncertain because they project from somewhere under a large overhanging tergite. A third Burmese male in one of two inclusions labelled as AMNH: Bu-184, seen in dorsolateral view, has the posterior surface of the head deeply collapsed such that the temples appear very long, with parallel horizontal margins facing dorsally. The parallel margins extend anteriorly beyond a small dorsal region that has the ocelli, and extend ventrally as very thin lateral walls relative to a lower, flat, horizontal surface. The head structure is similar to mymarommatids with an occipital plate collapsed into the head except for the differentiated dorsal region bearing the ocelli and the carinate posterior margins of the frontal plate facing dorsally. If it could be viewed in profile, the head likely would have a shape similar to that of *G. bezonmaisensis* (Fig. 215). Because of the angle of view the mandibles are not visible and we are uncertain of the forewing marginal setal pattern. The specimen has a very conspicuous posterior scutellum and a distinct oval region over the base of the forewing next to the concave posterolateral margin of the mesoscutum. This structure

appears to be the same as what we interpret as the humeral plate in extant mymarommatids. Remnants of muscle tissue, including the dorsolongitudinal and dorsoventral flight muscles, are visible. A slender, vertical band of muscle tissue immediately posterior to the dorsoventral flight muscle of the right side almost certainly is the mesotergal-mesotrochanteral depressor. A separate amber block under AMNH: Bu-184 has another more poorly preserved male. This male has the posterior surface of its head conspicuously concave or collapsed and a smaller, slightly collapsed subtriangular vertical region that bears the ocelli. The concave posterior surface is reticulate ventrally, but about its dorsal half is transversely striate. The head is therefore similar to extant members with a collapsed occipital plate, though without a distinct occipital plate. Although the mandibles are not clearly visible in ventral view they do not appear to be exodont. The forewing marginal setae also are not clearly visible. A fifth male (AMNH: Bu-997) has the posterior of the head deeply collapsed behind the ocelli and the toruli apparently near the middle of the head. The forewings have seven setae along the posterior margin basally that are obviously shorter than the more distal marginal setae. These seven setae differ in length, the more basal and apical setae being longer than the medial setae. The left forewing is exceptionally well preserved. Adjacent to the body is a brownish sclerite that is acutely angled distally, which we interpret as the humeral plate. This is separated by a narrow hyaline "break" from a slender brownish band that extends distally along the leading margin of the wing. Along this brown line is a row of "dots" similar to slide preparations of some extant species (Fig. 167). Although not mentioned by Kozlov and Rasnitsyn (1979), the forewings of *P. agapa* (Fig. 185) and *P. mandibulatus* (Fig. 201) also have a row of distinct dots basally along the leading margin. In the AMNH: Bu-997 male, the leading margin of the wing curves posteriorly distal to the row of dots so that the wing appears constricted and there is a distinct, brownish circle from which a seta projects (*cf.* Fig. 185: mc), similar to extant mymarommatids (Figs 127, 128: mc). Kozlov and Rasnitsyn (1979) stated that the tip of the forewing vein (equivalent to the brownish circle in AMNH: Bu-997) was markedly widened backwards in the *P. agapa* female (Fig. 185), and that the vein has one medial and three apical setae, of which two are short. The long distal seta in *P. agapa* (Fig. 185: mc) and the AMNH: Bu-997 male is also visible in the holotype of *P. mandibulatus* (Fig. 201) and several other amber specimens. The AMNH: Bu-997 male, *P. agapa* (Fig. 185) and *P. mandibulatus* (Fig. 201) also have a longitudinal brownish line extending proximally from the seta for nearly one-third the distance to the body, which we interpret as the submarginal vein (*cf.* Figs 95, 185: smv), and faint, almost spectral parallel lines along the posterior margin that we interpret as the retinaculum. The holotype of *P. mandibulatus* very clearly has a slender retinaculum that comprises about the posterior half of its forewing basally, and a stalk-like hind wing with a long seta basally and an apical process inserted into the retinaculum (Fig. 201). The sixth Burmese male (AMNH: Bu-479) is visible from both sides, with the head either in fronto- or posterolateral view. In frontolateral view, the toruli are within the dorsal third of the head, almost at the level of the dorsal margin of the eyes. The dorsal and lateral posterior margins of the head appear to be abrupt, though in posterolateral view the structure and the extent to which the posterior surface of the head is collapsed is not clear. Neither the mandibles nor the forewing marginal setal pattern are visible.

In addition to Burmese amber, we examined three males from New Jersey amber (about 90 mya *vide* Grimaldi and

Engel 2005). All the specimens (AMNH: NJ-179, AMNH: NJ-686a, AMNH: NJ-1005) have the posterior of the head ∩-like carinate, with the posterior surface collapsed similar to extant members with the occipital plate rotated anteriorly (Fig. 15). Two of the specimens (NJ-179, NJ-1005) have the protibial calcars visible. They are slightly curved and obviously shorter than those of the Burmese amber specimens. The left calcar of the NJ-1005 specimen has a fine inner tine originating quite far from its apex (*cf.* Fig. 140). Although the specimens are not well preserved, NJ-179 and NJ-686a appear to have bidentate, exodont mandibles. At least NJ-179 has ocelli, a suture separating the meso- and metapleura, and a structure of the propodeal foramen similar to that described for *P. agapa* and the Burmese amber fossils. The forewings of NJ-686a are not visible, but NJ-179 and NJ-1005 have a conspicuously long posterobasal marginal seta separated by several very short setae from long marginal setae apically (Fig. 195). Consequently, the three New Jersey Cretaceous amber specimens appear to be more similar to *P. japonicum*, *P. mandibulatus*, *P. senonicus* and at least some Canadian Cretaceous amber specimens than to most Burmese amber fossils.

Alonso et al. (2000) stated they had a male from lower Cretaceous Spanish amber (about 115 mya *vide* Grimaldi and Engel 2005) that is intermediate in structure between Mymarommatidae and Mymaridae. The specimen has a 2-segmented petiole but apparently lacks all the other features of Mymarommatidae. Among other features, they described a forewing with a submarginal vein, a small alar membrane and short marginal setae, and an 11-segmented flagellum lacking multiporous plate sensilla. Because of these features they suggested that the specimen might be considered as belonging to the sister-group of Mymaridae + Mymarommatidae. They did not illustrate the specimen and we were unable to obtain it for study.

SYSTEMATICS

The distribution of 28 variable features that are potentially informative for establishing monophyly and relationships of supraspecifc taxa in Mymarommatoidea is given in Table 2. *Mymaromma* sp. 9 is treated separately from other *Mymaromma* because it differs in several features from other examined species of the genus. *Zealaromma insulare* and *Z. valentinei* are also treated separately because these two species differ in several features. The matrix codes and character states are described in Appendix III. State 0 designates the hypothesized plesiomorphic state for 22 of the characters (1–3, 6–11, 14–24, 26–28). Polarity decisions for these characters are based on observed states in *Galloromma* and/or other parasitic Hymenoptera. Characters 4, 5, 12, 13 and 25 represent features of extant mymarommatids that are too small to be observed confidently in fossils and for which other Hymenoptera cannot be used to hypothesize polarity. Our hypotheses of generic relationships and character-state evolution discussed below are illustrated by Fig. 1.

Suprageneric classification.—As far as can be determined, the oldest mymarommatoids that we examined had external structures of the mesosoma and metasoma similar to extant species. They also had the same highly derived forewing and hind wing structures of extant mymarommatids (*cf.* Figs 129, 167 with 185, 194, 201) and likely lacked meso- and metatibial spurs, though we cannot be certain whether tibial spines visible in some fossils are pseudospurs or true tibial spurs. Tubular mesotergal-trochanteral muscles originating from rod-like axillar phragmata are visible in some Tertiary and Cretaceous (Fig. 206) fossils, but our study was insufficient to evaluate other internal features that Vilhelmsen and Krogmann (2006) proposed as autapomorphies of Mymarommatoidea (propleural and profurcal arms fused, prophragma with rods, metafurca absent).

Table 2. Observed character-state distribution in Mymarommatoidea. Symbols: na = non-applicable, ? = unknown state, / = both states present. Characters and states are described in Appendix II.

Taxon/Character	1	2	3	4	5	6	7	8	9	10	11	12	13	14	15	16	17	18	19	20	21	22	23	24	25	26	27	28
Galloromma	0	0	0	?	?	0	?	?	0	0	0	?	?	0	0	?	0	0	0	?	0	0	0	?	?	?	?	?
Archaeromma	1	1	?	?	?	0	0	?	0/1	1	0	?	?	0	0	?	?	?	0	?	0	0/1	0	?	?	?	?	?
Palaeomymar	1	1	0	?	?	0	0	?	3	na	1	?	?	1	0	?	?	?	0	?	0	2	1	?	?	?	?	1
Mymaromella	1	1	0	1	0/1	0/1	0	0	3	na	0	0/1	1	0	0	2	0/1	1	0	0	0	1/2	0	0	0	0	0	1
Zealaromma insulare	1	1	0	0	0	1	0	1	2	1	0	0	0	0	1	3	1	na	0	1	0	2	0	1	0	1	1	0
Z. valentinei	1	1	0	0	0	0	0	1	2	1	0	0	0	0	1	0	1	na	0	1	0	0	0	1	0	1	1	0
Mymaromma	1	1	1	0	1	0/1	1	1	3	na	0/1	0	0	1	1	1	0	0	1	0	0	0/1	1	0	1	0	0	1
Mymaromma sp. 9	1	1	0	0	1	1	0	?	3	na	0	0	0	1	0	1	0	0	1	0	1	1	1	0	0	0	0	1

Contrary to Gibson et al. (1999), fusion of the propleura into a carapace (14: 1) and fusion of the mesopleuron, metapleuron and propodeum below the spiracle (15: 1, 16: 1–3) are not groundplan features. Furthermore, the holotype of *P. agapa* and some Burmese amber fossils lack the bizarre head structure, exodont mandibles, and female claval structures of extant mymarommatids. These Cretaceous fossils indicate that the mymarommatoid groundplan structure included a uniformly sclerotized head capsule (1: 0), non-exodont mandibles (2: 0), and a 13-segmented female antenna with 7 slender funicular segments and 4 wider apical segments that formed a loosely associated clava because the segments were distinctly separated (10: 0; Figs 180, 189, 190). The fossil record indicates a transformation series in which the four claval segments first became closely associated to form a compact tube (10: 1; Figs 71, 192, 196, 200, 204) prior to the apical two segments, and ultimately all the segments, fusing together to form a single claval segment in Tertiary and most extant mymarommatids. Cretaceous females that we classify in *Archaeromma* only have three distinct claval segments (Figs 196, 200, 204), but some species may have had a compact 4-segmented clava.

The cephalic, mandibular, and antennal structures of the holotype of *P. agapa* strongly support classifying this species in a separate genus that constitutes the sister group of all other mymarommatoids. The genus could simply be classified as one more genus in Mymarommatidae or because of its postulated relationships with other mymarommatids be recognized as a higher taxon equivalent to all other mymarommatids. This higher taxon could be a separate subfamily in Mymarommatidae or a family equal to Mymarommatidae. Either of the latter two classifications imply a sister-group relationship and a greater morphological "gap" between it and the other recognized genera, which would not be implicit if the genus was simply

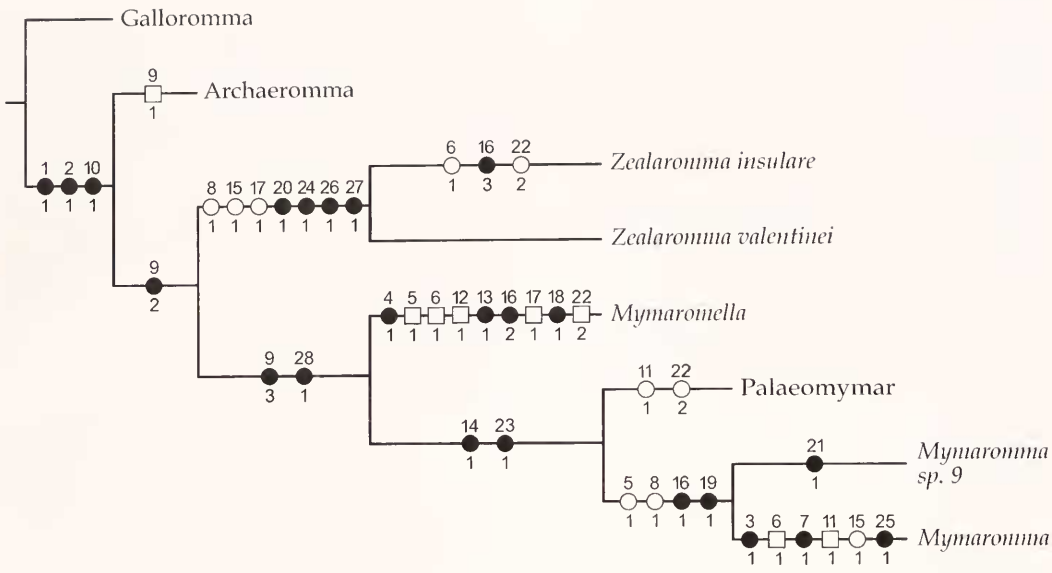

Fig. 1. Hypothesized relationships and character-state evolution among genera of Mymarommatoidea. Extant taxa in italics. Symbols used: ● = synapomorphic feature, ○ = homoplastic feature, □ = feature derived within taxon.

classified as one of several genera within Mymarommatidae. For these reasons, we prefer to classify the genus containing *P. agapa* separately within a higher taxon. Because the bellows-like head of mymarommatids is unique within Hymenoptera, and so bizarre, we prefer not to change the existing morphological family concept of extant Mymarommatidae. We therefore recognize two families in Mymarommatoidea, one of which is extinct. Below, we establish a new family for the genus containing *P. agapa* and, except for *G. bezonmaisensis*, classify all other described Cretaceous, Tertiary and extant mymarommatoids in Mymarommatidae. This family classification will have to be re-evaluated following study of the male from lower Cretaceous Spanish amber that was discussed by Alonso et al. (2000). If they described the features of this male accurately, then it could represent the sister taxon of Gallorommatidae + Mymarommatidae.

A remaining quandary is whether the genus containing *P. agapa* is new or congeneric with *Gallromma*. The head structure of the unique specimen of *G. bezonmaisensis* cannot be determined. Because its head is conspicuously high-triangular (angular) in profile (Fig. 215), it seems unlikely that the vertex and temples are smoothly rounded into the occiput as in *P. agapa* unless the apparent shape is an artifact of preservation and/or the angle of view. Our study of other amber fossils shows that the angle of view can affect apparent head shape. As discussed above, the mesosoma appears to attach to the "ventral" surface of the head (Fig. 215) and, if so, indicates *G. bezonmaisensis* had a uniformly sclerotized head capsule. The structure of the single visible mandible is uncertain, but in lateral view (Fig. 215) it appears to be thin and tapered (*cf.* Fig. 190). Although the sex of the holotype is also uncertain, in dorsal view the flagellum appears to have 4 distinct claval segments (Fig. 214). The premise that the specimen is a female may be supported by the gaster not being flattened and by what might be ovipositor sheaths projecting posteriorly from the gaster (Fig. 215: ovs?). The posterior margin of the forewing

has several comparatively long setae basally (Fig. 216) similar to *P. agapa* (Fig. 188) and some undescribed Burmese amber fossils (Fig. 191) that we consider to belong to the same genus. Finally, the petiolar segments of *G. bezonnaisensis* (Fig. 215) and *P. agapa* (Fig. 184) are of similar length, though this is not a generic feature.

We base our morphological concepts of the taxon containing *P. agapa* mostly on the holotype of *P. agapa*, supplemented by similar specimens in Burmese amber (particularly GPPC: HY17A and AMNH: B-0107). Additional, better preserved specimens from French Bezonnais amber are required to definitively resolve the generic status of *G. bezonnaisensis* relative to *P. agapa*. Because the two taxa could be congeneric, we transfer *P. agapa* to *Galloromma* and classify *Galloromma* and its two currently described species, *G. bezonnaisensis* and *G. agapa* (Kozlov and Rasnitsyn) **n. comb.** in the family Gallorommatidae **n. fam.** We classify other extinct and extant mymarommatoids in Mymarommatidae (Table 1), as justified below.

Classification of Mymarommatidae.—No known autapomorphies support monophyly of *Archaeromma* and our study was insufficient to differentiate males from those of Tertiary and extant mymarommatid genera. We distinguish *Archaeromma* only by females having three or four compact claval segments (9: 0/1). The maxillae and labium may have been completely or almost completed separated in *Archaeromma* (Fig. 203), but this structure undoubtedly is symplesiomorphic. Furthermore, some species of *Mymaromella* have the maxillae and labium differentiated over much of their length (Fig. 44). Of the extant genera, monophyly of *Zealaromma* is well supported by the absence of metasomal spiracles (26: 1) and cerci (27: 1), presence of bumps on the posterior surface of the femora, particularly the mesofemur (24: 1), and likely by sclerotization (secondary) of the spiracular peritreme (20: 1). The 2-segmented female clava (9: 2) of *Zealaromma* is enigmatic. The absence of both s4-type and s3-type sensilla from the basal claval segment (Fig. 71) might indicate that this segment evolved through autapomorphic secondary subdivision of a 1-segmented clava. Alternatively, the female claval structure could indicate *Zealaromma* constitutes a clade that is basal to *Palaeomymar* and other known Tertiary and extant species. Presence of external parameres in male *Zealaromma* (28: 0; Figs 154–156) and their absence from males of *Mymaromma* and *Mymaromella* (28: 1) indicates that *Zealaromma* is at least the sister taxon of these two extant genera. The absence of parameres recorded for *Palaeomymar* (28: 1) is based on only a single fossil and requires verification. The separate metanotum of *Z. valentinei* (16: 0; Figs 105, 106) may represent a third uniquely retained symplesiomorphy among extant mymarommatids. The two different structures of the metathoracic-propodeal complex that characterize *Mymaromma* (16: 1; Figs 82–84) and *Mymaromella* (16: 2; Figs 97–102), and the autapomorphic structure of *Z. insulare* (16: 3; Figs 109, 110), are hypothesized to have evolved through independent fusions of the metanotum with one or both of the metapleuron and propodeum. Among extant species, the posterior margin of the forewing of *Z. valentinei* also uniquely has several quite long setae basally (22: 0; Fig. 165). This setal pattern is similar to that of *Galloromma* (Fig. 188) and some *Archaeromma* (Fig. 194), suggesting a fourth uniquely retained symplesiomorphy among extant mymarommatids. We consider the structures discussed above as strong evidence that *Zealaromma* represents a monophyletic clade basal to *Palaeomymar*, *Mymaromma* and *Mymaromella*. The two known species of *Zealaromma* share a more internalized galea with *Mymaromma* (8: 1) and a completely fused meso- and metapleuron (15: 1) with most *Mymaromma*. They also have four supraclypeal setae (5: 0) and lack a metapleural pit (17: 1) similar

to most *Mymaromella*, but we consider these shared states either as symplesiomorphies or independently derived (see further below).

The best evidence for monophyly of *Mymaromma* is the presence of a ∩-like propodeal flange (19: 1; Figs 81, 87) that surrounds the insertion of the first petiolar segment into the propodeal foramen. Monophyly may also be supported by fusion of the metanotum laterally with the metapleuron (16: 1), which results in the spiracular peritreme forming an abrupt angle with the dorsal margin of the metapleuron (Figs 82–84). Although the holotype of *G. agapa* lacks this structure (Fig. 187), the spiracular peritreme is not clearly visible in *P. succini* or most other fossils. Species of *Mymaromma*, except for *M.* sp. 9, share two other apparently autapomorphic features — tridentate mandibles (3: 1; Figs 25–30) and a broad labium relative to the maxillae (7: 1; Figs 18–21). Individuals of *M.* sp. 9 have bidentate mandibles (Fig. 31) and a comparatively narrow labium (Fig. 31, insert). *Mymaromma* sp. 9 is also the only known species of *Mymaromma* having the meso- and metapleuron completely separated by a suture (15: 0; Fig. 82), but undoubtedly this is symplesiomorphic. A very fine suture also divides the meso- and metapleuron ventrally in *M.* sp. 7 (Fig. 87), which indicates fusion of the meso- and metapleuron in *Mymaromma* evolved independently to similar fusion in *Zealaromma* (Figs 103, 108). Finally, *M.* sp. 9 is the only observed species of *Mymaromma* having lateral setae on the first petiolar segment (state 25: 0; *cf.* Figs 92, 93, 104). However, because of the condition of specimens we were unable to survey this feature comprehensively and are not confident of the character-state distribution given for *Mymaromma* and *Mymaromella*. We did not observe petiolar setae in any fossil mymarommatid, but are uncertain whether this is because the setae are absent or too small to be visible. *Mymaromma* sp. 9 is indicated as the sister species of all other *Mymaromma* based on the features discussed above and is uniquely characterized by an extremely long, slit-like spiracular aperture (21: 1; Fig. 82: spa).

The monophyly of *Mymaromella* is not well established. Fusion of the metanotum posterolaterally to the propodeum (16:2) may support monophyly, but the exact structure of the metanotal-propodeal complex of *P. succini* and other fossils is unknown. The presence of paramedial setae on the occipital plate (4: 1; Figs 45, 46) and a metapleural pit about midway between the ventral margin of the pleuron and propodeal spiracle (18:1; Fig. 97: pl_3p) could also support monophyly, but again these features could not be observed confidently in fossil mymarommatids and polarity is uncertain. Among extant mymarommatids, *Mymaromella* is most variable in the number and position of s4-type sensilla. Females of *Zealaromma* (Fig. 71) and *Mymaromma* (Figs 58, 59) have two s4-type sensilla (12: 0) near the dorsal margin of the outer surface (13: 0), whereas *Mymaromella* females have two or three such sensilla (12: 1; Figs 62, 63, 65, 67, 69) more or less medially (13: 1; Figs 63, 65, 67, 69) or sometimes in the dorsal third (Fig. 62). These character-state distributions suggest that the more ventral position of the sensilla is synapomorphic for *Mymaromella* and that presence of a third sensillum supports a monophyletic subgroup of *Mymaromella*. These hypotheses could be tested by a phylogenetic analysis of the species of *Mymaromella* and by determining the number and position of s4-type sensilla in fossil taxa. At least the apical three claval segments of female *Galloromma* have long, basally curved, robust sensilla (Figs 181, 182). Because of their length, these sensilla most closely resemble s2-type sensilla of extant mymarommatids (Figs 63, 70), but further study is necessary to determine if any of the sensilla originate from circular depressions. If so, they likely are homologous with s4-type sensilla.

The relationships of *Palaeomymar* with *Mymaromma* and *Mymaromella* are also not well substantiated. *Palaeomymar* is recognized as a separate genus because *P. succini* has a short, straight protibial calcar (23: 1; Fig. 210) similar to *Mymaromma* (Figs 142, 144a, 145a), but lacks the ∩-like propodeal flange (19: 0) that supports monophyly of *Mymaromma*. Individuals of *P. succini* also have all the setae along the posterior margin of the forewing short basally (22: 2; Figs 208, 209) similar to some species of *Mymaromella* (Figs 117, 166). A single conspicuously long posterobasal marginal seta (22: 1) is possessed by some species of *Archaeromma* (Figs 195, 202), other Tertiary fossils (Fig. 211), some *Mymaromella* (Figs 118, 119), and known *Mymaromma* (Figs 113, 114, 163) except *M.* sp. 10. Because of this character-state distribution, we consider the lack of a conspicuously long posterobasal marginal seta to be derived in *P. succini* and some *Mymaromella*. If this shared feature results from common ancestry then the reduced foretibial calcar shared by *P. succini* and *Mymaromma* must be independently derived. We consider it more likely that a long posterobasal marginal seta was lost independently from *P. succini* and within *Mymaromella* and that a reduced protibial calcar supports monophyly of *Palaeomymar* + *Mymaromma*. A phylogenetic analysis of the extant species of *Mymaromella* to establish the groundplan state of the marginal setae could test these hypotheses. Monophyly of *Palaeomymar* + *Mymaromma* may also be supported by fusion of the propleura into a carapace (14: 1; Fig. 18), though further study is necessary to verify character-state distribution in *Palaeomymar* as well as *Mymaromma* and *Mymaromella*. A 6-segmented funicle characterizes females and males of *Mymaromma goethei* (11: 1; Figs 174–176) and at least females of *P. succini* (Fig. 179). We consider that this similarity likely results from independent loss of a funicular segment in the two taxa. The phylogenetic position of *P. succini* could be established more confidently by further study to provide missing data, particularly the exact structure of its metathoracic-propodeal complex.

Based on the above analysis, we currently consider the likely generic relationships of Mymarommatidae as *Archaeromma* + (*Zealaromma* + (*Mymaromella* + (*Palaeomymar* + *Mymaromma*))) (Fig. 1).

Mymarommatoidea

Description.—Antennae geniculate, inserted subcontiguously at or above middle of face; flagellum without multiporous plate sensilla. Female antenna with 9–13 segments including a variably structured clava composed of 1–4 segments; clava with short, peg-like sensilla along ventral midline (Figs 72, 181b), long, robust, basally curved sensilla on dorsal and/or outer surface (Figs 58, 63, 181, 182), and at least extant members with 2 or 3 short, basally curved lanceolate sensilla originating from depressions on outer surface (Figs 59, 65, 69, 70). Male antenna 12- or 13-segmented, with the apical 2–4 segments often somewhat coalesced as an indistinct clava, but the flagellum more or less filiform; fl_9 and fl_{10} or fl_8–fl_{10} each with short, basally curved lanceolate sensillum originating from depression distally. Ocelli present or absent. Pronotum with posterodorsal margin not extending to base of forewing and its posterior margin not rigidly interlocked with anterior margin of mesopleuron. Propleura forming exposed lateral and ventral portions of propectus, with ventral margins abutting medially or fused to varying extent. Prosternum vertical, largely concealed between posterior margin of propleura and base of procoxae. Functional mesothoracic spiracle absent. Prepectus not externally visible. Tegula absent. Mesoscutum with distinctive scabrous sculpture, without notauli or median mesoscutal sulcus; scutellum composed of convex anterior scutellum and slightly concave, transverse, longitudinally

strigose posterior scutellum; anterior scutellum without differentiated dorsal axillar regions. Metanotum an independent sclerite or fused with one or both of metapleuron and propodeum. Mesopleuron and metapleuron separated by oblique suture or partly to entirely fused. Forewing humeral plate bare. Forewing pedunculate, stalk-like basally and disc broadly spatulate to lanceolate; disc membrane with mesh-like pattern formed by raised lineations on both surfaces; marginal setae, when long, arising distinctly from within periphery of disc apically; venation strongly reduced within basal quarter of wing, consisting of submarginal, marginal and very short stigmal vein delimited apically by a campaniform sensilla and projecting seta. Hind wing stalk-like, terminated by single hamulus and opposing projection that together form pincer-like structure. Legs with tarsi 5-segmented; protibial calcar straight and simple or curved and bifurcate; meso- and metatibiae of at least extant members without tibial spurs; mesocoxa with basicoxite reduced to small dorsal lobe projecting into mesocoxal foramen, and mesotrochantinal lobe not externally visible. Metasoma 8-segmented with first two segments tubular; post-petiolar segments with terga broadly overlapping sterna without differentiated laterotergites. Female with hypopygium extending to apex of metasoma and therefore often concealing ovipositor, but apex capable of wide separation from syntergum; ovipositor non-telescoping, extended ventrally from gaster by rotation.

KEY TO FAMILIES AND GENERA OF MYMAROMMATOIDEA

1. Cretaceous; female flagellum with 7 funicular segments and 3- or 4-segmented clava (Figs 180, 182, 189, 190, 196, 199, 200, 204) 2
- Tertiary or extant; female flagellum with 6 or 7 funicular segments and 1-segmented clava (Figs 173–175, 178, 179) or 7 funicular segments and 2-segmented clava (Figs 71, 172) . . . . . (Mymarommatidae, part) 3

2(1) Head capsule uniformly sclerotized and with vertex smoothly rounded into concave occiput (Fig. 186); mandibles not exodont (Figs 189, 190, 191, 193), thin, curved mesally and broadly overlapping when closed; clava of female consisting of 4 distinctly separated segments (Figs 180, 182, 189, 190) . . . . . *Galloromma* Schlüter (Gallorommatidae **n. fam.**)
- Head capsule with hyperoccipital band of pleated membrane separating frontal plate from flat occipital plate (*cf.* Figs 13, 14) or frontal plate abruptly angled or hood-like relative to occipital plate if this rotated anteriorly (Fig. 198, *cf.* Fig. 15); mandibles exodont (Figs 197, 198), comparatively broad with concave outer surface and apices not meeting medially when closed (*cf.* Figs 31, 47–49); clava of female consisting of 3 or 4 segments, but these separated by linear sutures and forming compact tube (Figs 192, 196, 199, 200, 204) . . . . . *Archaeromma* Yoshimoto (Mymarommatidae)

3(1) Protibial calcar straight, simple (Figs 142, 144a, 145a); *extant taxa* with posterior margin of propodeum extending as ∩-like flange (Figs 86, 87) and concealing propodeal foramen in dorsal (Figs 78, 79) and lateral (Figs 80, 83) view 4
- Protibial calcar apically curved and bifurcate (Figs 137–139a, 140); *extant taxa* with posterior margin of propodeum extending as variably distinct flange only laterally on either side of short, protruding, tubular foramen (Figs 90–97, 104, 107) 5

4(3) Posterior margin of forewing with several short setae separating conspicuously long basal seta from longer apical setae (Figs 113–115); propodeum with ∩-like flange (Figs 86, 87) concealing foramen in dorsal and lateral view; mesopleuron and metapleuron usually partially (Fig. 87) or completely fused (Fig. 80), only very rarely completely separated by oblique suture (Fig. 82). Extant . . . . . *Mymaromma* Girault

- Posterior margin of forewing with all setae short basally (Figs 207–209); propodeum without distinct ∩-like flange, the foramen projecting as short tube anterior to petiolar insertion (*cf.* Fig. 94); mesopleuron and metapleuron separated by oblique suture (*cf.* Figs 97, 99). Extinct (Baltic amber) ..... *Palaeomymar* Meunier

5(3) Mesopleuron and metapleuron fused together (Figs 103, 108); Mt_7 without spiracles (Fig. 154); mesofemur with row of bumps on posterior surface (Fig. 146b); female clava 2-segmented (Fig. 172) ..... *Zealaromma* **n. gen.**

- Mesopleuron separated from metapleuron by diagonal suture (Figs 95– 97, 99, 101); Mt_7 with spiracles (Figs 149–152, 158); mesofemur without bumps on posterior surface; female clava 1-segmented (Fig. 178) ..... *Mymaromella* Girault

---

Gallorommatidae† n. fam.

Type genus.—*Galloromma* Schlüter, present designation.

Diagnosis.—Distinguished from Mymarommatidae by the following features. Head capsule uniformly sclerotized and sculptured, with convex vertex smoothly rounded into medially concave occiput (Figs 186, 213); occipital foramen originating from middle of occiput. Mandible not exodont (Figs 189, 190, 193); when closed, apices of mandibles broadly overlapping (Fig. 189) and dorsal margin distinctly separated from oral margin of head capsule. Female antenna with 13 distinct segments, including 7 funicular segments and 4 larger apical segments that are distinctly separated to form a loose clava (Figs 180, 182, 189, 190, 214).

Gallorommа† Schlüter

Gallorommа Schlüter, 1978: 74–76. Type species: *Gallorommа bezonmaisensis* Schlüter; original designation.

Description.—In addition to the diagnostic features given above for the family, other features that are not visible in all inclusions but that likely characterize *Gallorommа* are as follows. Head with ocelli (Fig. 186); eye large, with numerous ommatidia (Fig. 186); toruli near level of center of head and eyes (Fig. 183); mandible with subbasal tooth (Figs 191, 193). Protibial calcar conspicuously long, curved, and apically bifurcate (insert, Figs 183, 191). Propleura divided medially. Mesopleuron and metapleuron separated by complete suture; metapleuron with large pit about midway between propodeal spiracle and ventral margin of pleuron (Fig. 187). Propodeum with spiracle near posterior margin of scutellum (Fig. 187) and without distinct ∩-like flange surrounding foramen (Figs 184, 187). Forewing disc spatulate (Fig. 183) with two longitudinal folds, the membrane with comparatively numerous, scattered, short setae; posterior margin with setae all of similar length basally (Figs 191, 216) or with at least three moderately long setae proximal to shorter setae (Figs 188, 194).

Included species. —*Gallorommа agapa* (Kozlov and Rasnitsyn), **n. comb.** *Palaeomymar agapa* Kozlov and Rasnitsyn, 1979: 414–415. Holotype ♀, PIN (examined).

Gallorommа bezonmaisensis Schlüter, 1978: 74–76. Holotype ♀, ZMB (examined).

Mymarommatidae

Type genus.—*Mymarommа* Girault, 1920: 38.

Diagnosis.—Distinguished from Gallorommatidae by the following features. Head capsule with ∩-shaped hyperoccipital band of pleated membrane differentiating flat occipital plate from convex frontal plate (Figs 13, 14, 42); occipital foramen

originating at ventral margin of occipital plate. Mandibles exodont; when closed, their apices not meeting and dorsal margins abutting oral margin of head capsule (Figs 28–31, 47–49). Female antenna with 9–11 distinct segments, including 6 or 7 funicular segments and 1 or 2 claval segments (Figs 172–175, 178, 179) or if with 3 or 4 claval segments then these forming a compact tube with only basal two segments separated by distinct suture (Figs 192, 196, 200, 204).

Remarks.—Huber (2005) discussed the derivation and gender of the generic names.

Archaeromma† Yoshimoto

Archaeromma Yoshimoto, 1975: 503. Type species: *Ooctonus minutissimus* Brues; designated by Yoshimoto (1975: 503).

Protooctonus Yoshimoto, 1975: 511. Type species: *Protooctonus masneri* Yoshimoto; original designation. **n. syn.**

Diagnosis.—Females are distinguished from other Mymarommatidae by their compact clava consisting of at least three, sometimes possibly four, coalesced segments.

Included species.—*Archaeromma japonicum* (Fursov, Shirota, Nomiya and Yamagishi), **n. comb.** *Palaeomymar japonicum* Fursov, Shirota, Nomiya and Yamagishi, 2002: 52–54. Holotype ♂, Y. Shirota collection, Laboratory of Evolutional Ecology, Faculty of Agriculture and Life Sciences, Hirosaki University, Japan.

Archaeromma mandibulatum (Kozlov and Rasnitsyn), **n. comb.** *Palaeomymar mandibulatus* Kozlov and Rasnitsyn, 1979: 413–414. Holotype ♀, PIN (examined).

Archaeromma masneri (Yoshimoto), **n. comb.** *Protooctonus masneri* Yoshimoto, 1975: 511–512. Holotype ♀, CNC (examined).

Archaeromma minutissimum (Brues). *Ooctonus minutissimus* Brues, 1937: 44; combination by Yoshimoto (1975: 503). Holotype ♀, ROMT (examined).

Archaeromma nearcticum Yoshimoto. *Archaeromma nearctica* Yoshimoto, 1975: 506. Holotype ♀, CNC (examined).

Archaeromma senonicum (Kozlov and Rasnitsyn), **n. comb.** *Palaeomymar senonicus* Kozlov and Rasnitsyn, 1979: 412–413. Holotype ♀, PIN (examined).

Remarks.—Our generic placement of *A. japonicum* is tentative because this species is based on a unique male and we distinguish *Archaeromma* from other genera only by the claval structure of females. We classify it in *Archaeromma* because of its age (about 85 mya) and because the illustrations provided with the original description are very similar to specimens from New Jersey amber that we assign to *Archaeromma*.

When Yoshimoto (1975) established *Protooctonus* he stated that the forewing and female antenna "shows great similarity" to that of mymarommatids. He classified the genus in Mymarinae (Mymaridae) because he considered it had a subpetiolate gaster. The female holotype is crushed and the detached head is behind the mesosoma (Fig. 206). The dorsal surface of the mesosoma is clearly visible and structure and sculpture of both the mesoscutum (Fig. 206: msc) and scutellum (Fig. 206: asc + psc) is typical for mymarommatids. There is also a rod-like structure projecting obliquely from the anterolateral margin of the scutellum that almost certainly is an axillar phragma (Fig. 206: axp) and the toruli are subcontiguous and inserted high on the head (Fig. 206). In dorsal view, the posterior surface of the head (Fig. 196: ocp?) appears detached from the vertex and in lateral view the region has concentric lines dorsally (Fig. 206) similar to a hyperoccipital band of pleated membrane. What might be a 2-segmented petiole (Fig. 206: pt_1, pt_2) lies below the detached head anterior to a coxa. For these reasons, we transfer *Protooctonus* from Mymaridae to Mymarommatidae. We also synonymise *Protooctonus* under *Archaeromma* because of the similar antennal structure of the type species (*cf.* Figs 192, 196). The two males designated as paratypes of *P. masneri* by Yoshimoto (1975) are

not conspecific with the holotype female. The males represent an unidentified species of Mymaridae based on the presence of long, raised, multiporous plate sensilla on the flagellum (diagnostic of Chalcidoidea) and widely separated antennal toruli (diagnostic of Mymaridae).

Palaeomymar† Meunier

Palaeomymar Meunier, 1901: 289. Type species: *Palaeomymar succini* Meunier; original designation and monotypy.

Diagnosis.—Distinguished from other Mymarommatidae by the following combination of features. Head with ocelli. Mandible bidentate. Labiomaxillary plate with labium about as wide as maxilla. Female antenna 9-segmented with 6-segmented funicle and 1-segmented clava (Fig. 179); male antenna 12-segmented with 6-segmented funicle and 4-segmented clava (*cf.* Fig. 177). Propleura fused into carapace. Protibial calcar short and straight (Fig. 210). Forewing disc with hair-like setae; posterior margin with short marginal setae over basal half (Figs 207–209). Propodeum posteriorly without complete, ∩-like flange, the foramen protruding as short tube (*cf.* Fig. 94). Male genitalia lacking externally projecting parameres.

Included species.—Palaeomymar succini Meunier, 1901: 289–290.

Remarks.—As discussed above, Duisburg (1868) originally had 13 males and 3 females of which Meunier (1901) examined five males when he established *P. succini*. He obtained the type material from the "Musée Provincial de Koenigsburg" (Albertus Universität in Königsberg). According to Grimaldi and Engel (2005) most of the material stored in the museum was lost or destroyed during World War II, although a surviving portion is preserved in GZG. Search of the GZG Baltic amber collection by its curator, M. Reich, failed to locate any material identified as *P. succini*, and our survey of their unidentified Baltic amber Hymenoptera failed to recover any mymarommatids. The slide-mounted male labelled "33059 Kl." from the GZG "Klebs" collection (see discussion of Tertiary fossils) could not have been one of the five males examined by Meunier (1901). He stated that "embrowning" of the forewings prevented observation of the structure of the "nervus ulnerus" and both wings of the Klebs collection male are perfectly clear within the amber piece.

Because we distinguish three genera for the extant species, all of which are classified in *Palaeomymar*, it is necessary to designate a neotype for *P. succini* to fix use of the generic name. Based on correlated structure of the protibial calcar, forewing marginal setal pattern, and 9-segmented antenna in females, we identify in the ZMUC collection what we believe are associated sexes of the species that was discussed and illustrated by Duisburg (1868) and Meunier (1901). We designate a male as neotype because the original type series of Meunier (1901) consisted only of males and the neotype male is the only specimen that under a dissecting microscope clearly shows a short, straight (needle-like) protibial spine (Fig. 210: ca?). This spine almost certainly is the calcar, but absence of a long, curved calcar is indicated even if it is only a pseudospur (*cf.* Fig. 143: ps). The marginal setae of the forewings are also visible in the male selected and clearly show that the basal setae are all very short (Figs 207, 208). It is easier to differentiate *P. succini* from other species in Baltic amber based on females than males because of additional antennal features. We therefore also provide descriptive features for the ZMUC female labelled as 16-1/1961, which is the best preserved of all the specimens. It is almost the same size as the neotype male and also lacks a long protibial calcar.

Neotype designation: *Neotype data*: Fossil male, deposited in ZMUC with the following label data: two white labels with "Vesterhav, S. Nielsen, Skjoldelev, Min. Mus. [Mineralogisk Museum] 1890-108"

and "Mymarommidae Mymaromma: O.B. 1964", plus our red neotype label with "Neotype *Palaeomymar succini* Meunier, 1901 designated by Gibson, Read and Huber".

The maximum size of the amber block containing the neotype is 5.5 × 3.75 × 3.25 mm, though it narrows slightly in all dimensions in the direction toward the dorsal surface of the specimen. The sides of the block are smooth except one side has a missing section, which partly obscures observation of the specimen in ventrolateral view. The specimen is obliquely angled with the head directed more or less dorsally (Fig. 207) when the block is set on its side with the missing section.

Neotype description.—Male. Body length about 0.35 mm excluding antennae (length probably underestimated slightly because of foreshortening). Forewing 0.36 mm long × 0.12 mm wide; marginal fringe with longest setae as long as maximum wing width, the exact number of marginal setae uncertain but with about 15 shorter setae along posterior margin basally (these setae increasing in length distally) and about 35–40 much longer setae over apical half; disc membrane longitudinally convoluted. Head with ocelli.

Female description.—Antenna (Fig. 179) with combined length of pedicel and flagellum subequal to body excluding second petiolar segment and gaster; scape 4x as long as wide and 1.6x as long as pedicel; relative length of pedicel: funicle: clava = 1: 4: 3; funicle with basal four segments tubular, apical two segments increasingly more distinctly widened ventrally, and apical segment with dorsal attachment to base of clava; clava 3.75x as long as wide, the dorsal margin apparently without strong bent sensilla. Face very finely sculptured, shiny; malar space distinct. Eye moderately large, with numerous ommatidia. Mandibles comparatively slender, closed with apices apparently widely separated medially. Mesosoma with complete but fine metapleural suture; propodeum posteriorly without complete ∩-like flange, the foramen protruding as short tube that is longer ventrally than dorsally; in lateral view, first petiolar segment with basal constriction clearly visible and inserting into tubular propodeal foramen, the segment subequal in length to metacoxa and twice as long as second petiolar segment. Forewing elongate-spatulate, 1.4x as long (measured from apex of venation) as maximum width, with about 15 shorter setae basally along anterior margin, about 45 much longer setae distally along anterior, apical and posterior margins, and an uncertain number of shorter setae along posterobasal margin.

Mymaromma Girault, revised status

Mymaromma Girault, 1920: 38. Type species: *Mymaromma goethei* Girault; original designation. Synonymy under *Palaeomymar* Meunier by Doutt (1973: 225).

Petiolaria Blood and Kryger, 1922: 229. Type species: *Petiolaria anomala* Blood and Kryger; by monotypy. Synonymy under *Mymaromma* by Girault (1930: 4).

Description.—Head with or without ocelli; interorbital region of face with 10 setae, including 2 setae paramedially above oral margin (Figs 18, 20); occipital plate bare except for ventrolateral seta at each corner (Figs 14, 23, 42). Mandible usually tridentate with variably large and distinct subapical angle or tooth projecting above oral margin (Figs 26–30), though rarely bidentate (Fig. 31). Labiomaxillary plate with labium about twice as wide as maxilla (Figs 19–22, 28) except very rarely (Fig. 31, insert); maxilla with palpal spine apically on stipes and with galea internalized and apically pustulate (Figs 19–22). Female flagellum with 6 or 7 funicular segments and 1-segmented clava; clava with 2 s4-type sensilla on outer surface near dorsal margin (Figs 58, 59). Male flagellum 12- or 13-segmented with single s4-type sensillum apically on fl_9 and fl_{10} (Figs 60, 61). Propleura fused into carapace (Fig. 18). Mesopleuron and metapleuron usually

fused (Figs 80, 81, 83), rarely partly (Fig. 87: mms) or completely separated by suture (Fig. 82), but with curved furrow extending from posteroventral margin of mesothorax to distinct metapleural pit near propodeal spiracle (Figs 81, 87). Metathoracic-propodeal complex with metapleuron, at least dorsally, distinctly smoother than more coarsely sculptured propodeum (Figs 80–83); spiracular aperture oval to slit-like and connected to anterior margin of propodeum by slit-like peritreme, in lateral view the peritreme and dorsal margin of metapleuron forming acute angle directed between scutellum and propodeum (Figs 82–84); metanotum separated from propodeum by peritreme but fused with metapleuron (Fig. 84); prespiracular setae within angle formed by dorsal margin of metanotum and peritreme (Figs 84, 85) and postalar sensillum at extreme dorsal margin of metapleuron (Figs 84, 85). Propodeum posteriorly reflexed into ∩-like flange over petiolar insertion, the posteroventral margin of flange and projection of metapleuron forming pincer-like structure (Figs 81, 83, 86, 87). Forewing often appearing more or less lanceolate, the disc longitudinally convoluted with hair-like setae aligned along folds on dorsal and ventral surfaces (Figs 113–115), and sometimes densely hairy if setae very long (Fig. 116); posterior margin usually with basal seta conspicuously longer than adjacent short setae (Figs 113–115). Femora without bumps on posterior surface. Protibial calcar short, straight and simple (Figs 142, 144a, 145a). Metasoma with Mt_1 longer than Mt_2 but their relative length variable; Mt_1 dorsally variable in sculpture, almost smooth (Fig. 83) to strongly reticulate (Fig. 88), and only very rarely with lateral seta; Mt_2 finely sculptured, usually almost smooth (Fig. 83); Mt_7 with spiracle and seta mesal to spiracle (Fig. 152); syntergum with cerci, the cercus differentiated as subcircular structure (*cf.* Fig. 150) or variably fused with tergite as part of its surface (Fig. 152), and with 1–4 setae. Male genitalia without externally evident parameres.

Included species.—*Mymaromma anomalum* (Blood and Kryger), **rev. comb.** *Petiolaria anomala* Blood and Kryger, 1922: 229–230. Holotype ♂, BMNH (not examined).

Mymaromma buyckxi Mathot, 1966: 236–237, **rev. comb.** Holotype ♀, ISNB (examined).

Mymaromma goethei Girault, 1920: 38–39, **rev. comb.** Holotype ♀, QMBA (examined).

Mymaromma mirissimum (Girault), **n. comb.** *Mymaromella mirissima* Girault, 1935: 3. Holotype ♀, QMBA (examined).

Mymaromma ypt (Triapitsyn and Berezovskiy), **n. comb.** *Palaeomymar ypt* Triapitsyn and Berezovskiy, 2006: 5–7. Holotype ♀, Zoological Museum of Moscow State University, Moscow, Russia (not examined). Paratype ♀ and ♂, CNC (examined).

Distribution.—We have seen individuals and/or species have been reported in the literature from the following areas: **Afrotropical** — Congo (Mathot 1966), Gabon, Madagascar, Nigeria. **Australasian** — Australia (Girault 1920), Chatham Island, Christmas Island, Hawaii (Beardsley et al. 2000), Indonesia (Ceram), New Caledonia, New Zealand, Norfolk Island, Papua New Guinea. **Nearctic** — Canada, Mexico. **Neotropical** — Bermuda, Brazil, Colombia. **Oriental** — China (Lin 1994) [Fujian, Yunan], Indonesia [Kalimantan, Sulawesi, Sumatra], Malaysia [Sabah], Nepal, Philippines (Gallego 1986), Taiwan, Thailand. **Palaearctic** — Belgium (Debauche 1948), Bulgaria (Donev 1982), Czech Republic (Kalina 1989), Denmark (Blood and Kryger 1936), England (Blood and Kryger 1922), France, Germany (Vidal 2001), Hungary, Italy (Viggiani 1966), Japan, Norway (Hansen 1997), Poland (Soyka 1937), Romania (Andriescu and Suciu 1963), Russia (Triapitsyn and Berezovskiy 2000), South Korea (Triapitsyn and Berezovskiy 2006), Spain (Askew et al. 2001), Sweden, Switzerland (Ferrière 1948).

Remarks.—All described species are extant, but species likely existed in the Tertiary.

Mymaromella Girault, revised status

Mymaromella Girault, 1931: 4. Type species: *Mymaromella mira* Girault; by monotypy. Synonymy under *Mymaromma* Girault by Annecke and Doutt (1961: 14) and under *Palaeomymar* Meunier by Doutt (1973: 225).

Description.—Head with or without ocelli; interorbital region of face with 6–10 setae, including 2 (Fig. 36) or 4 (*cf.* Fig. 56) setae above oral margin; occipital plate with 2 paramedial setae (Figs 45, 46: ms) in addition to ventrolateral seta at each corner. Mandible bidentate with both teeth acutely angled (Figs 34, 48, 49), the dorsal tooth much longer than ventral subapical tooth. Labiomaxillary plate with labium narrow, only about as wide as maxilla (Figs 41, 41, 44, 47–49); maxilla with palpal spine subapical and with galea a longer, fleshy lobe exterior to spine (Fig. 41). Female flagellum with 7 funicular segments and 1-segmented clava; clava with 2 or 3 s4-type sensilla on outer surface near midline (Figs 62, 63, 65, 67, 69). Male flagellum 13-segmented with single s4-type sensillum apically on fl_9 and fl_{10} or fl_8–fl_{10} (corresponding to number of sensilla on female clava) (Figs 66, 68). Propleura abutting medially or at least distinguished by median line of differentiated sculpture (Figs 43, 44). Mesopleuron and metapleuron separated by suture (Figs 95–97, 99, 101), without a distinct metapleural pit though sometimes with a very tiny hole about midway between ventral margin of pleuron and propodeal spiracle (Figs 97, 101), and without curved furrow extending dorsally from posteroventral margin of mesothorax. Metathoracic-propodeal complex with sculpture of propodeum and metapleuron quite similar even if pleural sculpture somewhat finer (Figs 95–97, 99, 101); spiracular aperture circular to oval and connected to anterior margin of propodeum by slit-like peritreme, in lateral view the peritreme and dorsal margin of metapleuron forming evenly convex arc (Figs 95–102); metanotum fused with propodeum, but separated from metapleuron by peritreme such that metanotal-propodeal complex form variably long angle directed anteriorly between scutellum and dorsal margin of metanotum (Figs 98, 100, 102); prespiracular setae within dorsolateral angle of metanotal-propodeal complex and postalar sensillum either at extreme anterior angle of complex (Figs 98, 100) or sometimes appearing anterior to it (Fig. 102). Propodeum posteromedially constricted into short tube anterior to reflexed foraminal margin (Figs 90–97, 99, 101), and with posterolateral margin more or less distinctly reflexed as flange on either side of constriction (Figs 92, 94: pf) to form pincer-like structure with projection of metapleuron (Figs 92, 94, 96, 97, 101). Forewing variable in shape (Figs 117–121) though often spatulate (Fig. 119) or broadly rounded apically (Figs 118, 166), the disc with or without distinct longitudinal convolutions but with short, spine-like setae; length of marginal setae highly variable and posterior margin with (Figs 118, 1119) or without (Figs 117, 120, 166, 121) a conspicuously long basal seta. Femora without bumps on posterior surface. Protibial calcar long, apically curved and bifurcate (Figs 137–139a). Metasoma with Mt_1 longer than Mt_2 but their relative length variable; Mt_1 dorsally more or less transversely strigose-coriaceous and with lateral seta within basal half (Figs 90, 92, 94); Mt_2 variable in sculpture dorsally, usually transversely strigose; Mt_7 with spiracle and seta mesal to spiracle (Figs 149–151); syntergum with cerci, the cercus differentiated as subcircular structure (Figs 149–151) or variably fused with tergite as part of its surface (*cf.* Fig. 152), and with 2–4 setae. Male genitalia without externally evident parameres.

Included species.—*Mymaromella chaoi* (Lin), **n. comb.** *Palaeomymar chaoi* Lin, 1994: 123–124. Holotype ♀, FAUF (not examined).

Mymaromella cyclopterus (Fidalgo and De Santis), **n. comb.** *Palaeomymar cyclopterus*

Fidalgo and De Santis, 1982: 3–4. Holotype ♀, MLPA (examined).

Mymaromella duerrenfeldi[1] (Schlüter and Kohring), **n. comb.** *Palaeomymar duerrenfeldi* Schlüter and Kohring, 1990: 117–118. Holotype ♂, ZMB (examined).

Mymaromella mira Girault, 1931: 4. **rev. comb.** Holotype ♀ photograph, QMBA, USNM (examined).

Distribution.—We have seen individuals and/or species have been reported in the literature from the following areas: **Afrotropical** — Ivory Coast. **Australasian** — Australia (Girault 1931). **Nearctic** — Canada (Clouâtre et al. 1989), United States. **Neotropical** — Argentina (Fidalgo and De Santis 1982), Brazil, Trinidad, Venezuela (reported as *Palaeomymar* by García 2000). **Oriental** — China (Fujian, Guangxi). **Palaearctic** — South Korea (Triapitsyn and Berezovskiy 2006), Sweden.

Remarks.—We newly classify *M. duerrenfeldi* in *Mymaromella* because of the relatively recent age (about 5 mya) of this Tertiary species and because it has bidentate mandibles, a long and curved protibial calcar, and broadly rounded forewings with short discal setae.

Lin (1994, fig. 4) illustrated the bidentate mandibles of *M. chaoi* as having a short dorsal tooth and a long ventral tooth. Study of topotypic material shows this to be erroneous and the short tooth is ventral as in other *Mymaromella*.

Mymaromella mira was described from a photograph of a female "collected at Canterbury, Victoria in April" (Dahms 1984), which is in the QMBA. According to Girault's unpublished manuscript, the photograph is the "type" and a "paratype" photograph dated "January 4, 1931 (4-1-31)" that was sent to the USNM (Dahms 1984). The USNM photograph (Fig. 168) is identical to the QMBA photograph and has the data "[?] Girault letter to Gahan Nov. 1934". Because the two photographs are identical this suggests that *M. mira* was based on a unique specimen. The discrepancy between the collection date of the "type" and the date given for the "paratype" may simply reflect the date the photographs were printed or perhaps is a misinterpretation of the month *vs.* the day, i.e., "4-1-31" either representing April 1 or 4 January, 1931. Close examination of the photographs show that there is a comparatively long posterobasal seta on the forewings (*cf.* Fig. 118).

Zealaromma n. gen.

Type species.—*Mymaromma insulare* Valentine, 1971: 331–333; present designation.

Etymology.—A combination of New Zealand, the only country from which species of the genus are known, and *Mymaromma*, the genus in which the type species was first described.

Description.—Head with or without ocelli; interorbital region of face with 8 setae, including 4 setae above oral margin (Fig. 56); occipital plate bare except for ventrolateral seta at each corner (Fig. 50). Mandible bidentate with both teeth acutely angled and dorsal tooth much longer than ventral subapical tooth (Figs 52, 54). Labiomaxillary plate with labium narrow, only about as wide as maxilla (Figs 50, 52); maxilla with palpal spine apical on stipes and with galea internalized and apically pustulate (Figs 55–57). Female flagellum with 7 funicular segments and 2-segmented clava (Figs 71, 172); terminal claval segment with 2 s4-type sensilla on outer surface near dorsal margin (Fig. 71). Male flagellum 12-segmented with single s4-type sensillum near apex of fl_9 and fl_{10} (Fig. 73). Propleura abutting medially. Mesopleuron and metapleuron fused except for short suture below base of forewing, without evident metapleural pit, but with shallow groove extending dorsally from posteroventral margin of mesothorax to propodeal spiracle (Figs 103, 108). Metathoracic-propodeal complex with distinct smooth region between much more coarsely sculptured propodeum and metapleuron ventrally (Figs 104, 107, 108);

spiracular peritreme circular and without slit-like peritreme between aperture and anterior margin of propodeum; metanotum either independent from both propodeum and metapleuron (Figs 105, 106) or fused with propodeum and metapleuron (Figs 109, 110), but with postalar sensillum (Figs 105, 110: pas) separated from apparent "metanotum" anterior to prespiracular setae (Figs 105, 110: pss). Propodeum posteromedially constricted into short tube anterior to reflexed foraminal margin (Figs 103, 104, 107, 108), and with posterolateral margin reflexed as distinct vertical flange beside tubular constriction (Figs 104, 107). Forewing variably distinctly spatulate (Fig. 165) to lanceolate (Figs 122, 164), but disc longitudinally convoluted and with hair-like setae aligned along folds on dorsal and ventral surfaces; marginal setae comparatively short and stiff (spine-like) (Figs 122, 164) or very long and hair-like (Fig. 165), the posterobasal seta sometimes long but if so then not distinctly differentiated in length from adjacent setae (Fig. 165). Femora, particularly mesofemur, with bumps on posterior surface (Fig. 146). Protibial calcar long, apically curved and deeply bifurcate with very long inner tine (Fig. 140). Metasoma with Mt_1 nearly twice as long as Mt_2; Mt_1 with subbasal lateral seta (Fig. 104) and Mt_1 and Mt_2 dorsally very finely sculptured (Figs 104, 107); Mt_7 without spiracle (Figs 153–155) and usually bare (Figs 153, 155); syntergum without cerci (Figs 153, 155). Male genitalia with elongate-digitiform paramere bearing long terminal seta projecting externally from between syntergum and hypopygium (Figs 154–156).

Included species.—Zealaromma insulare (Valentine, 1971), **n. comb.**

Zealaromma valentinei Gibson, Read and Huber, **n. sp.**

Remarks.—Valentine (1971) stated that he recognized five species from mainland New Zealand in addition to *Z. insulare*, which differed in the form and fusion of the mesothoracic segments, simple or divided clava, size and shape of the forewings (one being apterous), and presence or absence of ocelli. Noyes and Valentine (1989) also stated that there were five undescribed species in New Zealand, including a brachypterous and apparently an apterous species. We did not locate any brachypterous or apterous specimens and from the material we examined from New Zealand recognize only three species: *Z. insulare*, *Z. valentinei* and an undescribed species of *Mymaromma*. This species, *M.* sp. 10, is represented by a single female from the South Island (NZAC) and several other specimens (Appendix II) that differ from all other mymarommatids in their extremely long and dense forewing discal setae (Fig. 116).

KEY TO SPECIES OF *ZEALAROMMA*

1. Forewing with about 10 stiff, relatively short (needle-like) and widely spaced distal marginal setae originating from wing margin (Figs 122, 164); head without ocelli; metanotum fused with both metapleuron and propodeum (Figs 108–110) ..... *Zealaromma insulare* (Valentine)

- Forewing with numerous fine, very long (hair-like) and closely spaced distal marginal setae originating distinctly from within wing periphery (Fig. 165); head with ocelli (Fig. 53); metanotum separated from metapleuron and propodeum by sutures (Figs 105, 106) ..... *Zealaromma valentinei* **n. sp.**

Zealaromma valentinei n. sp.

Type material.—**Holotype**. Female. "NEW ZEALAND BR [South Island: Buller] Lake Rotoiti 610m; 26 Dec 1979 - 4 Jan 1980 A.K. Walker" / "Holotype *Zealaromma valentinei* Gibson, Read and Huber" (NZAC). **Paratypes** (15♀, 5♂). NEW ZEALAND, North Island: **ND** [Northland] Waipoua Kauri Forest, 11-12.XII.1983, L. Masner, s.s. (1♀ CNC). **TK** [Taranaki]: Mt. Egmont N.P., 16.XII.1983, L. Masner, s.s. (1♀ CNC). NEW ZEALAND, South Island: **BR** 1♀, same data as holotype (NZAC). Lower Buller R., Norris Ck., 14.X.1970, J.I. Townsend, litter 70/158 (2♀ on one card NZAC). Punakiki, 28.XII.1983, L. Masner, s.s. (1♀, 1♂ CNC). Tuttys Plateau, Mawhera, 20.IX.1972, J.S. Dugdale, moss 72/178 (1♀ NZAC). **MC** [Mid Canterbury], Banks Peninsula, Prices Valley, II.1981, R.P. Macfarlane, malaise trap, edge of native bush (1♀ NZAC). Banks Peninsula, Prices V, 19-27.X.1988, J.W. Early (5♀, 2♂ CNC; 1♀ gold coated for SEM). **NN** [Nelson], Wooded peak Dun Track Sdle, 14.IX.1971, G.W. Ramsay, litter 71/110 (1♀ NZAC). **SL** [Southland], Longwood Forest, Purakino picnic area, 24-28.I.1999, L. LeSage, Nothofagus forest, YPT 99-57 (1♀, 2♂ CNC).

Etymology.—Named in honour of Dr. Errol Valentine, who first published on New Zealand mymarommatids.

Description.—Length, 0.55 mm (air-dried holotype). Body yellow except small triangular region below base of forewing and ocellar triangle dark brown, gaster sometimes brownish dorsally; hind leg with apices of basal three tarsal segments very narrowly brown; forewing disc with middle third to basal half of mesh-like lineations and the marginal setae behind this region brown (Fig. 165).

Head with ocelli (Fig. 53). Face with supraclypeal region finely strigose, otherwise with distinctive mesh-like sculpture, the sculpture narrowed toward midline so as to more or less form a median carina (Fig. 52). Eye moderately large, with about 20–25 ommatidia in female and 30–35 ommatidia in male; separated from oral margin by distinct malar space of similar width as mandible (Figs 52, 54). Antenna of female as in Fig. 172.

Mesosoma with propleura completely divided medially (Fig. 112). Forewing as in Fig. 165, with 43–48 very long and thin (hair-like), evenly spaced marginal setae over about apical half of wing, 12–15 much shorter setae basally along anterior margin, and with 6 or 7 variably shorter setae basally along posterior margin, of which at least the basal 3 setae are comparatively long and at least the distal seta (sometimes distal 1–3 setae) are quite short. Metanotum separated from metapleuron laterally and from propodeum posterolaterally (Figs 105, 106).

Metasoma of male without seta on Mt_7 (Fig. 155).

Remarks.—Body length varies from about 0.5 mm in air-dried individuals to about 0.7 mm in some critical-point dried females. The difference appears to be mostly because the gaster remains inflated in critical-point dried specimens. Females with the gaster neither shrunken nor obviously over-inflated are about 0.65 mm. The species description of *Z. valentinei* is brief because it mostly includes only those features that readily differentiate it from *Z. insulare*.

SUPRAFAMILIAL RELATIONSHIPS

One of the objectives of this study was to determine whether any additional morphological evidence could be found to help resolve the suprafamilial relationships of Mymarommatoidea. Mymarommatoidea has been proposed as the sister group of either Serphitoidea (Kozlov and Rasnitsyn 1979) or Chalcidoidea (Gibson 1986). We therefore included fossils of Serphitidae in our study, but our observations are based on only seven Taimyr and nine Canadian Cretaceous specimens. Our study of mymarommatoids revealed that they are much more diverse morphologically than thought previously. Consequently, the inferences made below should all be considered as tentative until character-state dis-

tribution and groundplan features of Serphitidae are determined more accurately through an equally comprehensive study.

A Mymarommatoidea + Serphitoidea sister-group relationship is supported by common possession of a similarly structured 2-segmented petiole (Kozlov and Rasnitsyn 1979), whereas common possession of axillar phragmata as the sites of origin for tubular mesotergal-mesotrochanteral muscles is the principal evidence for a Mymarommatoidea + Chalcidoidea relationship (Gibson 1986). Vilhelmsen and Krogmann (2006, figs 12–14) showed that the prophragma of *M. anomalum* has rod-like structures similar to axillar phragmata. They suggested that this apparent "serial" homology and the different structure of the axillar phragmata in mymarommatids and chalcids (tubular *vs.* flat) might indicate that the phragmata evolved independently in the two taxa. However, Mymarommatoidea and Chalcidoidea are still the only known apocritans having the mesotrochanteral depressor muscle consisting only of a notal portion that originates at least partly from an axillar phragma. Our study shows that Cretaceous mymarommatids also had tubular mesotrochanteral depressor muscles originating from rod-like axillar phragmata (Fig. 206: axp). Knowledge of the structure of this muscle in Serphitidae would therefore be valuable for inferring relationships. Serphitids are much more highly sclerotized and melanized than are mymarommatids and we did not see any specimen in which the internal musculature was visible.

As noted by Vilhelmsen and Krogmann (2006), the presence or absence of an exposed prepectus and the position of the mesothoracic spiracle are other phylogenetically informative features for inferring relationships of Chalcidoidea. The position of the mesothoracic spiracle in Chalcidoidea is autapomorphic, being at or above the dorsal margin of the prepectus between the pronotum and mesoscutum (Gibson 1986, figs 18–29). Other parasitic Hymenoptera have the spiracle ventral to the level of the dorsal margin of the pronotum, either between the pronotum and mesopleuron or secondarily on the pronotum in the same relative position. Furthermore, the prepectus or its remnant extends dorsally behind the spiracle, between it and the mesopleuron (Gibson 1985, figs 19–26), except in Stephanidae (Gibson 1985, fig. 16) and Ichneumonoidea (Gibson 1985, figs 27, 28). Although a pronotal notch was not observed in any fossil mymarommatoid or in *Zealaromma* (Figs 103, 108), the incision on the posterior margin of the pronotum of some mymarommatids (Figs 16, 82: pn; 99, 101) could indicate the position of the mesothoracic spiracle before it was lost. If so, the ancestor of mymarommatoids had the mesothoracic spiracle in the symplesiomorphic position for parasitic Hymenoptera. It therefore is not useful for establishing relationships of Mymarommatoidea, but supports the hypothesis of autapomorphy for Chalcidoidea.

In lateral view, one specimen of Serphitidae from Taimyr amber (PIN: 3730/31) very clearly has a white, globular mesothoracic spiracle ventral to the dorsal margin of the pronotum between the pronotum and mesopleuron (Figs 220, 221: sp). The spiracle appears to lie partly within the excised posterodorsal margin of the pronotum (most clearly visible from a somewhat ventral view, Fig. 222: sp). In lateral (Figs 220, 221) or ventrolateral (Fig. 222) view, about the dorsal third of the posterior margin of the pronotum abuts the anterior margin of the mesopleuron, but ventrally a slender, spindle-shaped region (Figs 220–222: pre?) separates the posterior margin of the pronotum from the mesopleuron between the spiracle and procoxa. This intervening region appears to be a separate sclerite because its anterior margin is delimited by a distinct suture and it is on a lower level than the posterior margin of the pronotum, because it is separated from the mesopectus by a distinct

suture at least ventrally, and because its sculpture is different from the putative pronotum and mesopectus (with longitudinal rugae compared to rugose pronotum and mesopectus). The region could be a differentiated part of the mesopectus, but more likely it is a relatively long and slender prepectus. In lateral view, the mesothoracic spiracle extends over the anterior margin of the mesopleuron (Figs 220–222) and appears to be on a slightly higher level than the mesopleuron. This is because the mesopleuron posterior to the spiracle is slightly concave. The concave region is distinct because it is delineated by carinae (Fig. 221: c). Many extant platygastroid (Gibson 1985, figs 23, 24) and some proctotrupoid (Gibson 1985, figs 19a, 20a, 25a) taxa also have the spiracle on a slightly higher level than the mesopleuron because the posterior pronotal inflection extends dorsally under and behind the spiracle. This suggests that if the slender region of PIN: 3730/31 is the prepectus then it likely also extends dorsally behind the spiracle. If so, the prepectal structure is more similar to that of Monomachidae (Gibson 1985, fig. 15) than Stephanidae (Gibson 1985, fig. 16). Because of the intervening region, the posterior margin of the pronotum is somewhat sinuate (Figs 220–222). The posterior margin of the pronotum is similarly sinuate in many Scelionidae (Platygastroidea) having a netrion (Gibson 1985, fig. 23). Rasnitsyn (1980) hypothesized that the netrion in scelionids is the prepectus fused with the pronotum. The similarity between the putative sclerite of PIN: 3730/31 and the netrion of some scelionids suggests that it might be fused with the pronotum internal to the external suture (*cf.* Figs 220–222 with Gibson 1985, fig. 23 and Masner 1979, figs 4–8). If so, it is structurally the same as a netrion and therefore a possible synapomorphy for Serphitoidea + Platygastroidea.

The other serphitids we examined did not have such a distinctly differentiated mesopectal region, though the specimen in PIN: 3311/80 and the largest of the three specimens in PIN: 3730/28-30 has an obscurely differentiated region between the pronotum and mesopectus, at least on the right side from direct ventral view. The region is less distinct in these two specimens partly because it is quite smooth, similar in sculpture to the pronotum and mesopleuron. The posterior margin of the pronotum of the holotype of *Microserphites parvulus* Kozlov and Rasnitsyn was also stated as having a narrow border (Kozlov and Rasnitsyn 1979, fig. 7), which may be equivalent to the region we observed in PIN: 3730/31. Further study is necessary to determine whether all Serphitidae have a slender mesopectal region differentiated below the mesothoracic spiracle, whether this region is a free prepectus or a netrion, and whether the posterior margin of the pronotum is free from the mesopleuron or connected by a posterior pronotal inflection. These observations could be complicated because the pronotum is somewhat moveable relative to the mesothorax in extant apocritans with a prepectus (e.g. Monomachidae). The pronotum could overlie and partly or entirely conceal the sclerite in some fossils if the slender region in PIN: 3730/31 is a free prepectus rather than a fused netrion. The margin of the sclerite adjacent to the pronotum appears to be on a slightly lower level than the pronotum in PIN: 3730/31, which suggests that the pronotum can override the sclerite. Study of other individuals of the same species as in PIN: 3730/31 could help determine whether the pronotum is moveable, and therefore whether the sclerite is more likely a prepectus or a netrion. The species is readily identified by the presence of a distinct setal patch on the mesopectus near the procoxa (Figs 220, 222: sep).

Rasnitsyn et al. (2004, p. 128) stated that "monophyly of Khutelchalcididae within Chalcidoidea is very likely" based on presence of a spiracular excision in the pronotum (as an indicator of the chalcid

synapomorphy of a dorsal spiracular position) and a free prepectus. However, if their interpretation of the unique fossil comprising the family is correct, then the comparatively large incision in the posterodorsal margin of the pronotum (Rasnitsyn et al. 2004, fig. 6) shows that the spiracle is in the symplesiomorphic position relative to chalcids. This placement of the putative spiracle and the vertical structure ventral to it, which they interpret as the prepectus (Rasnitsyn et al. 2004, fig. 6), resemble the structure of the serphitid (Fig. 222) in PIN: 3730/31. As noted above, the presence of a free prepectus is symplesiomorphic and does not support monophyly of Khutelchalcididae + Chalcidoidea. The thoracic structure of Monomachidae, Serphitidae, Khutelchalcididae and some Aculeata suggest that one or more early lineages of Apocrita had a free prepectus that was visible ventral to the spiracle depending on position of a somewhat mobile pronotum. The ancestor of Platygastroidea may have had a similar structure, but it is only in Chalcidoidea that the prepectus was enlarged secondarily to intervene between the pronotum and mesopleuron dorsally. This prepectal structure apparently was derived concurrently with the dorsal shift in position of the mesothoracic spiracle. Of critical importance in taxa with a prepectus, whether this is free or secondarily fused with the pronotum, is whether it extends behind and above the level of the mesothoracic spiracle. Unfortunately, this can usually be determined only by dissecting the pronotum from the mesothorax and therefore is not readily apparent in fossils. However, the exact structure of the prepectus/netrion in Serphitidae may be determined if a fossil is discovered with the pronotum or prothorax detached from the mesothorax.

Mymarommatoidea, Serphitoidea, Platygastroidea and most parasitic Hymenoptera other than Chalcidoidea have a more ore less gibbous mesoscutum and the pronotum triangular in lateral view (Gibson 1985, figs 21, 23, 27, 29). These features are not evidence of relationships. Gibson (1986) showed that structure of the pronotum and mesonotum is correlated with presence or absence of a free prepectus and relative mobility of the pronotum. Examination of the serphitids we could observe in ventral view shows a propleural structure (Fig. 222: ppm) very similar to extant mymarommatids with the propleura abutting along their entire length (Fig. 112). Vilhelmsen and Krogmann (2006) correctly stated that most Chalcidoidea have the prosternum partly exposed because the ventral margins of the propleura are more or less divergent. Mymarommatids are therefore more similar to serphitids than to chalcids in their propleural structure. However, this structure is shared with most Hymenoptera excluding Chalcidoidea and the most basal symphytan lineages (Vilhelmsen and Krogmann 2006). The basal symphytan lineages with chalcid-like propleura also have the pronotum comparatively mobile relative to the mesothorax. Further study is required to determine whether there is a correlation between propleural structure and pronotal mobility similar to that of the pronotal-mesonotal complex. Such a study should include Aculeata with an independent prepectus and a relatively mobile pronotum as well as aculeates with a rigidly attached pronotum.

Most apocritans have a curved, apically bifurcate protibial calcar (Basibuyuk and Quicke 1995). Only Chalcidoidea and Mymarommatoidea have some members with this calcar structure and others with a short, straight, needle-like calcar. Because Chalcidoidea and Mymarommatoidea are both well substantiated as monophyletic taxa, the reduced calcar shared by some members of both groups must be convergent. For the same reason, the similar forewing and hind wing structures of mymarommatoids and most *Mymar* (*cf.* Figs 1–7 with 129–136) are certainly convergent.

Kozlov and Rasnitsyn (1979) did not provide the tibial spur formula for *Microserphites* or *Aposerphites* Kozlov and Rasnitsyn, but stated that this was 1:2:2 for *Serphites* Brues. Most of the serphitids we examined had two distinct meso- and metatibial spurs, though these were not visible in all examined inclusions. Naumann and Masner (1985) listed the tibial spur formula as 1:2:2 for 9 of the 11 families they treated as the "proctotrupoid complex" of families. The formula was listed as 1:2:2 or 1:1:1 for Scelionidae and Platygastridae, but Austin and Field (1997) stated that members of the most primitive tribes of Platygastroidea are plesiomorphic in having two mesotibial spurs. The number of mesotibial spurs is also variable in Ceraphronoidea. Members of Megaspilidae have two and members of Ceraphronidae one mesotibial spur (Gauld and Bolton 1988). We found that the tibial spur formula is 1:0:2 for Stephanidae and 1:1:2 for Megalyridae and most Chalcidoidea. A few Chalcidoidea only have a single metatibial spur, but the exceptions include some of the tiniest Mymaridae, such as species of *Alaptus* Westwood and *Camptoptera* Förster. At least extant mymarommatids lack both meso- and metatibial spurs, though the tibiae have socketed setae ventroapically (pseudospurs) that can be mistaken for tibial spurs (Figs 139b, c; 141b, c; 144b, c: ps). Absence of meso- and metatibial spurs from mymarommatids and the loss of one mesotibial spur from more derived Platygastroidea and in Ceraphronidae might be correlated with very small body size. If so, the presence of only a single mesotibial spur in Chalcidoidea could indicate that their common ancestor was very small. This would support the hypothesis that the chalcid ancestor was an egg parasitoid rather than a parasitoid of a wood-boring insect (Gibson et al. 1999). However, even though most Cynipoidea have two mesotibial spurs, some species of *Ibalia* Latreille (Ibaliidae) have only a single mesotibial spur (Ronquist and Nordlander 1989, Liu and Nordlander 1992). This, along with loss of one mesotibial spur from Megalyridae and both mesotibial spurs from Stephanidae, suggests that there could be some correlation between parasitism of wood-boring insects and the loss of mesotibial spurs. The single mesotibial spur shared by Chalcidoidea and Megalyridae presumably is convergent, but further study of the number of mesotibial spurs throughout Apocrita is warranted for phylogenetic inference.

The similar forewing venation of most Chalcidoidea and Scelionidae has often been cited as possibly indicating a sister-group relationship between Chalcidoidea and Platygastroidea. The venation is reduced to single vein complex near the anterior margin of the wing in most members of both groups. Typically, there is a "submarginal", "marginal", "stigmal" and "postmarginal" vein, and often also a short "uncus" projecting from the stigmal vein (Huber and Sharkey 1993, fig. 14; Gibson 1997, fig. 5). Rasnitsyn et al. (2004) stated that the forewing pterostigma was not prominent and possibly was absent from Khutelchalcididae, unlike in an undescribed fossil they identified as a scelionid from the lowermost Cretaceous. The photograph of this putative scelionid shows a costal vein (Rasnitsyn et al. 2004, fig. 7: c) and a longitudinal pterostigma distal to a "pre-pterostigmal break", plus an oblique r-rs (= stigmal vein) projecting from the pterostigma near its middle. Another photograph of the same impression sent to us by Alex Rasnitsyn (PIN) more clearly shows the venation (Fig. 227). The presence of a pterostigma suggests that the marginal vein of extant scelionids evolved through a gradual narrowing of the pterostigma into an only somewhat thickened vein-like structure (A. Rasnitsyn, pers. comm.). However, the groundplan venation of extant Platygastroidea is controversial. Masner et al. (in press) reinterpreted the groundplan forewing venation of Scelionidae based on the putative basal

extant lineages of the group. They noted that members of these lineages lack a marginal vein. Rather, the submarginal vein (R) bifurcates distally before attaining the anterior margin of the wing so that the stigmal vein (r-rs) originates within the membrane and is separated from the wing margin by a short R_1 (Masner et al. in press, figs 41–43, 45–47). Based on this, they concluded that a marginal vein evolved secondarily in Scelionidae and is convergent with the marginal vein of Chalcidoidea. They did not state explicitly how the marginal vein of some scelionids evolved, but they illustrated a distal extension of R_1 along the wing margin in some scelionids as producing the postmarginal vein (Masner et al. in press, figs 46, 47). Presumably, secondary proximal lengthening of R along the wing margin resulted in the marginal vein of some scelionids (Masner et al. in press, fig. 44).

Masner et al. (in press, fig. 49) compared their interpretation of the groundplan venation of Platygastroidea with Cynipoidea to illustrate presumed symplesiomorphic features. The groundplan venation of Platygastroidea, as interpreted from basal extant lineages, can also be derived readily from the venation characteristic of Serphitidae. Kozlov and Rasnitsyn (1979, fig. 2; Rasnitsyn et al. 2004, fig. 8) described and illustrated a costal vein and a distinct pterostigma in *Serphites*, but indicated that the costal vein was missing and the pterostigma was indistinct in *Microserphites parvulus* (Kozlov and Rasnitsyn 1979, fig. 6). A specimen of *Serphites* from Canadian Cretaceous amber (MCZ: 5330) has a distinct pterostigma but lacks a costal vein. Vein R bifurcates before the anterior margin of the wing so that R_1 constitutes the anterobasal and anterior margins of the pterostigma and r-rs constitutes the posterior margin of the pterostigma (Fig. 226). Except for the pterostigma, this venation is very similar to the possible groundplan venation of Platygastroidea. However, the unusually large "pterostigma" of serphitids may be because of autapomorphic secondary melanization of the wing membrane in the region between R_1 and r-rs (Fig. 226).

The precursor of the marginal vein of Chalcidoidea is uncertain. The chalcid marginal vein may have evolved through a narrowing of a pterostigma in a transformation similar to that proposed for Scelionidae by A. Rasnitsyn. Alternatively, it may have evolved through anterior elongation of vein R along the wing margin similar to the transformation series proposed for Scelionidae by Masner et al. (in press). If the latter, the marginal vein of chalcids consists only of R, not C+R (Huber and Sharkey 1993, fig. 14; Masner et al. in press, fig. 48) or Sc_2+R_1 (Bradley 1955) or R_1 (Burks 1938). Regardless of the correct interpretation of the groundplan venation of extant Platygastroidea, both hypotheses suggest that the marginal vein of Scelionidae is secondarily derived and therefore convergent to that of Chalcidoidea. Mymarommatoidea also have a recognizable marginal vein (Figs 127, 129, 185: mv) that appears to have a very short stigmal vein distally (Fig. 185: stv). These features may be synapomorphic for Mymarommatoidea + Chalcidoidea, but if so they are homoplastic relative to the venation of some Platygastroidea.

The presence of a costal vein in some fossils assigned to Scelionidae (Fig. 227: cv) and the lack of a costal vein in some Serphitidae (Fig. 226) indicates that loss of this vein occurred independently in the two taxa. Both taxa are known from the earliest Cretaceous or latest Jurassic (Rasnitsyn et al. 2004) so perhaps it is unremarkable that both families exhibit a diversity of wing venation. However, the earliest fossil "scelionids" are impression fossils, from which far less morphological information can be deduced than from amber fossils. The putative scelionids with a pterostigma and a costal vein may only resemble and not actually be closely

related to extant Scelionidae. Further research is necessary to establish this and to resolve the true groundplan venation of extant Scelionidae.

Further study of the external and internal structure of the different types of claval sensilla of mymarommatids and other apocritans is also required. Mymaridae (Figs 8–10: s4) have sensilla that in external structure are very similar to the s4-type sensilla of mymarommatids (Figs 58, 60, 62–64, 66, 68, 70, 71: s4). In Mymaridae they have been called "basiconic" (Baaren et al. 1999, figs 2F, 4A, 4B, 4F, 5F), "grooved peg" (Chiappini et al. 2001, figs 1a, 1c, 16) or "sickle-shaped" (Huber and Fidalgo 1997, figs 47, 48) sensilla. Chiappini et al. (2001) stated that the clava of *Anagrus atomus* (L.) (Mymaridae) has a single such sensillum near its ventral margin almost at its middle, and 1–3 sensilla distally on the apical three (of five) funicular segments. Baaren et al. (1999) reported that in *Anaphes listronoti* Huber and *Anaphes victus* Huber (Mymaridae) all but the first of six funicular segments have one or two of the sensilla distally and both claval segments each have two sensilla. There is at least one s4-type sensilla ventroapically on the female clava of *Polynema striaticorne* Girault (Mymaridae) (Isidoro et al. 1996, fig. 8c). Consequently, mymarids appear to differ from mymarommatids in having the sensilla not only on the clava but also distally on some funicular segments (Figs 9, 10: s4) in a position similar to those of the claval segments of male mymarommatids (*cf.* Figs 60, 61, 66, 68). Female mymarids have the sensilla ventrally (Fig. 8), dorsally (Fig. 9) or both ventrally and dorsally (Huber and Fidalgo 1997, fig. 48), and in some specimens they can be present on a segment of one antenna but missing from the same segment of the other antenna (Huber and Fidalgo 1997). In addition to mymarids and mymarommatids, individuals of both described genera of Rotoitidae (Chalcidoidea) have apically projecting, lanceolate sensilla originating from a depression distally on the claval and funicular segments (Figs 75–77), and according to John Heraty (UCRC, pers. comm.) they are also present in some Aphelinidae (e.g. *Cales* Howard). We are not aware of any reports of similarly shaped sensilla in other Chalcidoidea, although so called basiconic, campaniform, capitate peg or multiporous grooved sensilla reported in Agaonidae (Ware and Compton 1992, fig. 3), Eulophidae (Veen and Wijk 1985, fig. 9c), Encyrtidae (Baaren et al. 1996, figs 1, 5f), Pteromalidae (Miller 1972, figs 3, 4), and Trichogrammatidae (Voegelé et al. 1975, pl. III figs 1–4; Olson and Andow 1993, figs 1, 11) likely are homologous with s4-type sensilla. Even though they have a different external structure, they all originate from a circular depression and usually at least some are positioned distally on the funicular segments similar to s4-type sensilla in mymarids and mymarommatids. A reduction in the length and globular enlargement of the apex of a lanceolate s4-type mymarid or mymarommatid sensillum would result in a petiolate, mushroom-like sensillum similar to those of the other chalcid families listed above. The presence of lanceolate s4-type sensilla in Mymaridae and Rotoitidae suggest that these are groundplan features of Chalcidoidea, but that the shape of the sensillum likely was modified secondarily in other chalcids. Chiappini et al. (2001, figs 1c, 18) called a small peg-like sensillum that is ventroapical in position on the clava of *Anagrus atomus* (*cf.* Fig. 8: s4?) a "sunken peg sensillum". Our very limited survey of the sensilla in Mymaridae suggests that the sunken peg sensillum in *A. atomus* may be nothing more than a modified s4-type sensillum (*cf.* Figs 8, 9). More comprehensive surveys are required to determine the exact distribution of lanceolate s4-type sensilla in Chalcidoidea, whether such sensilla occur in other apocritan groups, and whether it is possible to demonstrate structural transformation series from

which phylogenetic inferences can be made.

Further study of the different types of dorsal (s2-type) and ventral (s3-type) claval sensilla are also warranted for phylogenetic inference. Mymarid females have a row or rows of specialized trichoid sensilla along the ventral surface of the clava (Fig. 9: s3), which Baaren et al. (1999) called "sensilla chaetica". These sensilla are similar to the s3-type sensilla of mymarommatoids (Figs 64: s3; 181b). Baaren et al. (1999) described four different types of sensilla chaetica in *Anaphes listronoti*, including an apical sensillum (their type 1), which at least some female mymarommatids have (*cf.* Figs 8, 9 with Fig. 64: as; 67, 69). They also differentiated three other morphological types of ventral sensilla chaetica. Isidoro et al. (1996, fig 8d) suggested that a double row of robust sensilla ventrally on the clava of female *P. striaticorne* are multiporous gustatory sensilla. Although we did not study the morphology of the ventral row or rows of sensilla in mymarommatids in detail, more than one structure of s3-type sensilla is evident for at least some species (Fig. 72, insert).

Barlin (1978) proposed that the uniquely structured multiporous plate sensilla (mps) of Chalcidoidea evolved from bent multiporous setiform (s2-type) sensilla that became attached to the cuticle. The pore-canal opening in the proximal end of the mps and the unattached distal end of the mps were cited as possible evidence. Kozlov and Rasnitsyn (1979) further suggested that the thick, basally curved sensilla on the clava of female mymarommatids (Figs 63, 64: s2) might be precursors of the mps of Chalcidoidea (Figs 9, 10: mps). They also proposed that the latter evolved through accretion of the ventral surface of the sensillum to the surface of the segment (see also, Basibuyuk and Quicke 1999). Our study supports such an "accretion" hypothesis for the origin of the unique, chalcid-like mps (Gibson 1986 fig. 4; Basibuyuk and Quicke 1999, fig. 5d). However, parasitic Hymenoptera other than Mymarommatidae also have long, thick, basally bent sensilla. Basibuyuk and Quicke (1999) stated that Ceraphronoidea, Platygastroidea (Isidoro et al. 1996, fig. 2) and some Proctotrupoidea, particularly Diapriidae (Basibuyuk and Quicke 1999, fig. 5a), have distinctive, curved, multiporous setiform sensilla. Maamingidae also have such sensilla, each recessed into a shallow longitudinal groove (Early et al. 2001) and with the apices of some of the sensilla extending beyond the apex of the segment (Fig. 74). Fusion of the lower surface of the sensillum within the longitudinal groove would result in a mps external structure very similar to that characteristic of chalcids (*cf.* Figs 74, 77). As noted by Basibuyuk and Quicke (1999, p. 53), mps vary in shape, but are "always embedded in a chamber in the antennal integument".

A comprehensive survey of the mps structure of chalcids is required to determine their diversity more accurately, but the mps of Mymaridae appear to be quite typical for Chalcidoidea. The mps are structurally diverse in Rotoitidae. Those of *R. basalis* (Fig. 76) are somewhat intermediate between a typical chalcid-like mps and a s2-type sensillum. The sensilla are non-socketed, as for chalcid mps, but they resemble a very thick s2-type sensillum because only the oval base is confluent with the surface and the longer and more slender curved portion, rather than just the apex, is free above the surface. Furthermore, under higher magnification there is a fine groove around the base of the sensillum (Fig. 76) reminiscent of a socket. The mps of *Chiloe micropteron* Gibson and Huber (Fig. 75) are more similar to typical chalcid-like mps. An undescribed species of *Rotoita* near *R. basalis* also has chalcid-like mps, except that on the funicular segments at least some of the convex mps have a distinct groove on either side (Fig. 77), and on the clava the mps originate more distinctly within a longitudinal

depression. Both the funicular and claval segments of the undescribed *Rotoita* also have much more slender, curved sensilla that resemble s2-type sensilla except that they are non-socketed (Fig. 77: s2/mps). Kozlov and Rasnitsyn (1979) partly differentiated serphitids from mymarommatids based on the absence of strong, curved sensilla from the clava of serphitids. The serphitids we examined also lacked s2-type sensilla. The flagellar segments of serphitids (Figs 218, 219) appear to be more or less uniformly covered with suberect, curved, trichoid sensilla, though these could be multiporous setiform sensilla.

Even if chalcid mps were derived from s2-type sensilla, the wide distribution of s2-type sensilla in parasitic Hymenoptera indicates their presence is synapomorphic for a larger group of taxa than just Mymarommatoidea + Chalcidoidea. In Chalcidoidea, both sexes have mps and they are on the funicular as well as the claval segments. Therefore, their immediate common ancestor may also have had s2-type sensilla in both sexes on all the flagellar segments, unlike Mymarommatidae. Rasnitsyn et al. (2004, fig. 5) suggested that lines on the flagellar segments of Khutelchalcididae were internal apertures of long mps and that these were a synapomorphy for Khutelchalcididae + Chalcidoidea. It is also possible that the lines are remnants of elongate s2-type sensilla similar to those in Maamingidae (Fig. 74). According to Barlin (1978), the internal aperture extends the length of the mps in Chalcidoidea and in some subfamilies of Braconidae (Ichneumonoidea). Cynipoidea also have elongate mps, but with long internal apertures only in Cynipidae (Rasnitsyn et al. 2004). According to Barlin (1978), the pore canal for entry of the dendrites occurs at the proximal end of the sensillum in Chalcidoidea but near the center of the sensillum in Cynipoidea and Ichneumonoidea. Although the irregular lines on the flagellar segments of Khutelchalcididae might be elongate internal apertures of mps, they do not show the unique features of chalcid mps — internally, the proximal position of the pore canal and, externally, the sensillum being raised, ridge-like, above the surface of the cuticle, without an encircling groove, and with the distal end free (Basibuyuk and Quicke 1999, fig. 5d). Additional study is necessary to confirm the presence of mps in other fossil impressions of Khutelchalcididae, to determine the internal structure of the mps in Rotoitidae, and to assess more thoroughly the internal and external structure of the flagellar sensilla throughout parasitic Hymenoptera. A comprehensive survey of the setation/sensilla of the metanotum and around the wing bases throughout parasitic Hymenoptera might also provide additional characters and transformation series for phylogenetic inference.

Except for Serphitidae, mymarommatids are unique in having the second metasomal segment tubular (Figs 88, 89). The functional or ecological significance of a tubular second metasomal segment is unknown. The post-petiolar metasoma (gaster) of Mymarommatoidea is quite similar to that of Chalcidoidea. Similarities include cerci on the syntergum and absence of spiracles from all but the penultimate tergite in the groundplan of Mymarommatoidea, tergites smoothly overlapping the sternites, the hypopygium being able to separate widely from the syntergum in females, and an ovipositor that rotates and extends ventrally from the gaster rather than being extended posteriorly. However, all of these features have a much wider distribution in Apocrita and at best support the monophyly of a much larger group of taxa than just Mymarommatoidea + Chalcidoidea.

Kozlov and Rasnitsyn (1979) stated that the gastral tergites protrude laterally somewhat and the sternites form a longitudinal fold in *Microserphites*. A serphitid in Canadian Cretaceous amber (MCZ: 5343) has what we interpret as a similar gastral structure. This specimen belongs to

Serphites based on its wing venation and position of the posterior ocellus. In ventral view, the gaster is strongly flattened with the ventrolateral aspect of each tergite extending on either side of the sternum for a short distance before being abruptly angled back toward the sternum. Consequently, the gaster is uniformly carinately margined laterally and ventrally has distinctly differentiated "laterotergites" forming a narrow band on either side of the sternum (*cf.* Fig. 224: ltt). The abruptly folded tergal structure is most distinct for the basal gastral tergites because both the dorsal and ventral surfaces are visible, but it is not possible to determine whether the laterotergites articulate with differentiated laterosternites. The gastral sternum is composed of six sternites that form a uniformly low convex surface; the second gastral sternite is transverse-rectangular and is the largest sternite, though only slightly longer than the first gastral sternite. Several Taimyr amber serphitids (PIN: 3311/80, PIN: 3730/28-30 (Fig. 224), PIN: 3731) have gastral structures very similar to that described for the MCZ: 5343 specimen. These Taimyr specimens represent a species different from MCZ: 5343 based on a very different length of the second petiolar segment. All the Taimyr amber specimens had been identified as "*Serphites* sp.". Kozlov and Rasnitsyn (1979) did not describe laterally differentiated tergites for *Serphites* or their new genus *Aposerphites*. Some fossils we examined and identify as *Serphites* have the gaster subcircular in cross-section rather than flattened. It usually is not possible to be certain whether the tergites have differentiated laterotergites when the gaster is subcircular. However, one specimen (MCZ: 5256) with an inflated gaster has a whitish line laterally. This line superficially divides the tergites from the sternites, but under some angles of light what appears to be quadrate plates and the true ventral margins of the tergites are visible below the whitish line. Another specimen (MCZ: 5330) has an inflated gaster with the tergites and sternites separated by a distinct, white, membranous band (Fig. 225). Under some angles of light, the tergites are slightly angled along a straight line so that there is a slender region along the tergum above the narrow membranous band (Fig. 225: ltt), which we consider as a band of differentiated laterotergites. Even less distinct is a slender band laterally along the sternites (Fig. 225: lst) that is similar in width to the putative laterotergites. This region appears to consist of a slightly depressed part of each sternite that the respective laterotergite would override if the gaster was not inflated. Based on serphitids with a flattened gaster and deeply inflexed laterotergites, our assumption is that the differentiated lateral part of the sternites can flex so as to lie over the laterotergites, and thus constitute "laterosternites". Regardless, the membranous band separating the sternites and tergites is straight in MCZ: 5330 (Fig. 225), unlike the irregular line of separation between the tergites and sternites in taxa that lack laterotergites, such as mymarommatids (Fig. 147) and chalcids. The latter two Canadian Cretaceous serphitids (MCZ: 5256 and 5330) suggest that laterotergites are present in serphitids, but that they are not obvious when the gaster is inflated. Observation of a differentiated lateral region on the sternites is only possible when the gaster is inflated and the tergites and sternites are separated.

Austin et al. (2005) stated that monophyly of Platygastroidea is supported by two character systems, gustatory sensilla on the claval segments and structure of the gaster. In Platygastroidea, the gastral tergites and sternites are connected by laterotergites and the spiracles are reduced and non-functional. Vanhorniidae (Proctotrupoidea) also lack gastral spiracles but do not have laterotergites (Naumann and Masner 1985), whereas Ambositrinae (Diapriidae) have spiracles on the penultimate gastral tergite and laterotergites (Masner

1961). Most of the serphitids we examined were inappropriately preserved or positioned to be confident of the presence or absence of spiracles, but under some angles of light MCZ: 5330 has a small, smooth, circular structure laterally on Mt_7, which led Gibson (1985) to code metasomal spiracles as present in Serphitidae. There also appears to be a circular structure laterally on Mt_7 of PIN: 3730/31 that may be a spiracle, which is in a transversely-oval depression that is margined anteriorly. The hypopygium was extended ventrally in most female serphitids we examined similar to mymarommatids and chalcids. Consequently, if the presence of metasomal spiracles is verified for other serphitids, then their gastral structure is more similar to Ambositrinae (Diapriidae) than Platygastroidea, which have a tubular, telescoping ovipositor extension system. The ambositrine gaster differs by having Mt_2 composed of two or three fused terga (Masner 1993).

Masner et al. (in press) discussed four genera of Scelionidae that apparently lack laterotergites, but at least three of the genera have longitudinal sublateral keels on the tergites. These keels may represent vestiges of the lateral fold that differentiates the laterotergites of other platygastroids. Furthermore, the ventral margins of the tergites and the dorsal margins of the sternites form straight lines (Masner et al. in press, fig. 3), which are separated by membrane when the gaster is inflated (Masner et al. in press, fig. 1). This "multisegmented carapace" structure is very similar to that of other platygastroids with laterotergites and of the MCZ: 5330 serphitid (Fig. 225). Relationships of the four scelionid genera that apparently lack laterotergites need to be clarified because they are all characterized by a single mesotibial spur rather than the groundplan two mesotibial spurs (see above).

The MCZ: 5343 serphitid is a male. The metasoma in ventral view has symmetrical, elongate-digitiform processes that have at least one long terminal seta (Fig. 223: par?). The processes extend from either side of the sternum at the line of junction between Ms_7 and Ms_8 and in posterior view appear to originate laterally between the apical tergite and sternite. The processes resemble what we consider to be parameres in male *Zealaromma* (Figs 154, 156: par) and *Maaminga* (Fig. 157: par). Rasnitsyn (1988, node 65) postulated that a tubular male genital capsule with both the volsellae and parameres fused with the aedeagus was synapomorphic for Chalcidoidea + Mymarommatidae + Serphitidae + Platygastroidea and, possibly, the extinct family Juraprii-dae. This hypothesis appears to be falsified by the presence of moveable parameres in the male genitalia of *Zealaromma* and, likely, Serphitidae, but the fused condition remains a possible synapomorphy for Chalcidoidea + Platygastroidea.

The metasoma of MCZ: 5343 has seven distinct, melanized tergites in dorsal view and a small, lighter coloured apical eighth tergite that in posterior view originates somewhat under Mt_7. Laterally on this apical tergite is a circular, somewhat convex structure with several projecting setae, which likely is a cercus. Two females (PIN: 3730/31; MCZ: 5330) also have setose digitiform processes (*cf.* Gibson 2003, figs 26, 42) basolaterally on Mt_8 that likely are the cerci (Gibson 1985). The left process of PIN: 3730/31 appears to have at least four and probably six projecting setae.

The serphitid head in lateral (Fig. 218) or frontal (Fig. 219) view has the antennae inserted very low on the face close to the oral cavity. In well preserved specimens there is a distinctly differentiated clypeus and the antennal toruli are separated from a linear epistomal suture by a distance similar to the diameter of a torulus. This is typical of the head structure that characterizes Platygastroidea (Naumann and Masner 1985) and contrasts with the higher, possibly plesiomorphic position of the toruli in Mymarommatoidea and Chalcidoidea. The mandibles of most serphitids

we examined are quite broad with three long and slender teeth (Fig. 218; Alonso et al. 2000, fig. 2), though the holotype of *Microserphites parvulus* appears to have only two slender teeth (Kozlov and Rasnitsyn 1979, fig. 7). Distinct maxillary and labial palpi are often visible in serphitids, unlike in mymarommatids, though this represents another symplesiomorphy. A feature that may be phylogenetically informative is the presence of an acetabular carina or at least an anteriorly differentiated region of the mesopectus ventrally behind the procoxae (Fig. 220: acc). This carina is absent from mymarommatids (Fig. 86), mymarids and most other chalcids. Although Naumann and Masner (1985) indicated that an acetabular carina was absent in Platygastroidea this was an error — absence or presence of an acetabular carina in Platygastridae and Scelionidae should have been listed (see Masner 1979).

CONCLUSIONS

Several structural similarities suggest a close relationship between Serphitoidea and Platygastroidea, though at present there are no unequivocal synapomorphies for the two taxa. Some similarities, such as presence and position of the mesothoracic spiracle and two mesotibial spurs are obvious symplesiomorphies, but other shared features are not studied sufficiently for confident hypotheses of character-state distribution and polarity in Serphitidae or Apocrita. These features include a similarly structured gaster having laterotergites and possibly laterosternites, a differentiated mesopectal region that might be homologous with a netrion or the ancestral structure (prepectus exposed ventral to mesothoracic spiracle) from which a netrion evolved, a forewing venation that could be similar to the groundplan venation of Scelionidae, position of the toruli relative to the epistomal suture, and similar mesosomal sclerotization and sculpture, including an acetabular carina.

Other than the common possession of a 2-segmented petiole, we found no evidence supporting a Serphitoidea + Mymarommatoidea sister-group relationship. The petiolar segments are similar in both taxa, though in some serphitids they are longitudinally strigose and/or extensively setose, unlike the petiolar segments of mymarommatids. Newly discovered similarities, such as medially abutting propleura and independent parameres in the male genitalia have much wider distribution and therefore are indicated as symplesiomorphies.

Common possession of lanceolate s4-type flagellar sensilla and one or two rows of s3-type sensilla ventrally on the clava of females could provide additional support for monophyly of Mymarommatoidea and Chalcidoidea. However, the diverse external and internal structures of different claval and flagellar sensilla found by Isidoro et al. (1996) in parasitic Hymenoptera demonstrate that a much more comprehensive comparative study is required prior to reliable hypotheses. It seems likely that the marginal veins of at least Chalcidoidea and Scelionidae are convergent, though common possession of a marginal vein could be synapomorphic for Mymarommatoidea + Chalcidoidea. Study of the male from lower Cretaceous Spanish amber that Alonso et al. (2000) stated has a 2-segmented petiole but non-mymarommatid wing features, and which they postulated may be the sister taxon of Mymarommatidae + Chalcidoidea (Mymaridae), could provide valuable information for resolving character-transformations and relationships.

The extinct Cretaceous taxon Khutelchalcididae is indicated to be at most the sister-group of Chalcidoidea rather than a "basal chalcidoid". The pronotum has an incision in the posterodorsal margin that suggests the mesothoracic spiracle was in the plesiomorphic position and even though it may have had a slender, externally visible prepectus ventrally, this did not

extend dorsally to the mesoscutum as in Chalcidoidea.

Future studies of higher-level relationships of Chalcidoidea or Mymarommatoidea should include Maamingidae as well as Platygastroidea and Serphitidae as outgroups. Inclusion of Maamingidae is warranted because of the structure of their s2-type antennal sensilla (Fig. 74) compared to the uniquely structured mps of Chalcidoidea, the presence of independent, rod-like parameres in the male genitalia, a forewing venation (Early et al. 2001, fig. 19) similar to that of *Rotoita* (Gibson and Huber 2000, fig. 46), other similarities between the taxa discussed by Early et al. (2001), and relationships indicated by molecular analyses (Castro and Dowton 2006).

ACKNOWLEDGEMENTS

We thank the individuals and institutions listed under Materials and Methods for the loan of specimens on which our study was based. We also thank Lars Vilhelmsen and Lars Krogmann for providing us with their complete file of SEM images of *M. anomalum*, and Alex Rasnitsyn (PIN), Norman Johnson (Ohio State University, Columbus) and Lubomir Masner (CNC) for discussions concerning serphitid and platygastroid morphology. Thomas Schlüter kindly granted permission to reproduce Fig. 215, Alex Rasnitsyn supplied us with Fig. 227 and Bob Wharton (Texas A&M University, College Station) provided us with a copy of the PhD thesis of Margaret Barlin. Klaus Bolte (CNC) photographed several of the amber inclusions used to illustrate the text. Andrew Bennett and Henri Goulet (CNC), Lars Vilhelmsen, and an anonymous reviewer provided many useful comments for improvement of a previous version of the manuscript. This research was conducted as part of the Hymenoptera Tree of Life initiative (National Science Foundation grants DEB-0334945 and EF-0337220).

LITERATURE CITED

Andriescu, I. and I. Suciu. 1963. *Mymaromma anomala* (Blood et Kryger), reprezentantă unei familii de himenoptere (Chalcidoidea) nouă pentru fauna R. P. R. *Analele Stiintifice ale Universitatii "Al. I. Cuza" din Iasi (Seria Noua)* 9: 251–255 + 1 pl.

Alonso, J., A. Arillo, E. Barrón, J. Carmelo Corral, J. Grimalt, J. F. López, R. López, X. Martínez-Delclòs, V. Ortuño, E. Peñalver, and P. R. Trincao. 2000. A new fossil resin with biological inclusions in lower Cretaceous deposits from Álava (northern Spain, Basque-Cantabrian basin). *Journal of Paleontology* 74: 158–178.

Annecke, D. P. and R. L. Doutt. 1961. The genera of the Mymaridae. Hymenoptera: Chalcidoidea. *Entomology Memoirs, Department of Agricultural Technical Services, Republic of South Africa* 5: 1–71.

Askew, R. R., J. Blasco-Zumet, and J. Pujade-Villar. 2001. Chalcidoidea y Mymarommatoidea (Hymenoptera) de un sabinar de *Juniperus thurifera* L. en Los Monegros, Zaragoza. *Monografias de la Sociedad Entomológica Aragonesa* 4: 1–76.

Austin, A. D. and S. A. Field. 1997. The ovipositor system of scelionid and platygastrid wasps (Hymenoptera: Platygastroidea): comparative morphology and phylogenetic implications. *Invertebrate Taxonomy* 11: 1–87.

———, N. F. Johnson, and M. Dowton. 2005. Systematics, evolution, and biology of scelionid and platygastrid wasps. *Annual Review of Entomology* 50: 553–582.

Baaren, J. van., R. Barbier, and J.-P. Nénon. 1996. Female antennal sensilla of *Epidinocarsis lopezi* and *Leptomastix dactylopii* (Hymenoptera: Encyrtidae), parasitoids of pseudococcid mealybugs. *Canadian Journal of Zoology* 74: 710–720.

———, G. Boivin, J. Le Lannic, and J.-P. Nénon. 1999. Comparison of antennal sensilla of *Anaphes victus* and *A. listronoti* (Hymenoptera, Mymaridae), egg parasitoids of Curculionidae. *Zoomorphology* 119: 1–8.

Bakkendorf, O. 1948. A comparison of a mymarid from Baltic amber with a recent species, *Petiolaria anomala* (Micro-Hym.). *Entomologiske Meddeleleser* 25: 213–218.

Barlin, M. R. 1978. *Multiporous plate sensilla in parasitic Hymenoptera: their ultrastructure and phylogenetic relationship*. PhD Dissertation, Texas A&M University, College Station, Texas. 126 pp.

Basibuyuk, H. H. and D. L. J. Quicke. 1995. Morphology of the antenna cleaner in the Hymenoptera with particular reference to non-aculeate families (Insecta). *Zoologica Scripta* 24: 157–177.

——— and ———, 1997. Hamuli in the Hymenoptera (Insecta) and their phylogenetic implications. *Journal of Natural History* 31: 1563–1585.

——— and ———, 1999. Gross morphology of multiporous plate sensilla in the Hymenoptera (Insecta). *Zoologica Scripta* 28: 51–67.

———, ———, A. P. Rasnitsyn, and M. G. Fitton. 2000. Morphology and sensilla of the orbicula, a sclerite between the tarsal claws, in the Hymenoptera. *Annals of the Entomological Society of America* 93: 625–636.

Beardsley, J. W., J. T. Huber, and W. D. Perreira. 2000. Mymarommatoidea, a superfamily of Hymenoptera new for the Hawaiian Islands. *Proceedings of the Hawaiian Entomological Society* 34: 61–63.

Blood, B. N. and T. P. Kryger. 1922. A new mymarid from Brockenhurst. *Entomologist's Monthly Magazine* 58: 229–230.

——— and ———, 1936. *Petiolaria anomala* Bl. & Kr. (Hym., Chalcid.): description of the female. *Journal of the Society for British Entomology* 1: 115–116 + plate III.

Bradley, J. C. 1955. The wing-venation of Chalcidoidea and of some allied Hymenoptera. *Mémoires de la Société Royale d'Entomologie de Belgique* 27: 127–138.

Brues, C. T. 1937. Superfamilies Ichneumonoidea, Serphoidea, and Chalcidoidea. Pp. 27–44 *in* Carpenter, F. M., J. W. Folsom, E. O. Essig, A. C. Kinsey, C. T. Brues, M. W. Boesel, and H. E. Ewing. Insects and arachnids from Canadian amber. *University of Toronto Studies, Geological Series* 40: 7–62.

Burks, B. D. 1938. A study of chalcidoid wings (Hymenoptera). *Annals of the Entomological Society of America* 31: 157–161.

Campbell, B., J. M. Heraty, J.-Y. Rasplus, K. Chan, J. Steffen-Campbell, and C. Babcock. 2000. Molecular systematics of the Chalcidoidea using 28S-D2 rDNA. Pp. 59–73 *in* Austin, A. D., and M. Dowton, eds. *Hymenoptera: evolution, biodiversity and biological control*. CSIRO publishing, Collingwood. 468 pp.

Castro, L. R. and M. Dowton. 2006. Molecular analyses of the Apocrita (Insecta: Hymenoptera) suggest that the Chalcidoidea are sister to the diaprioid complex. *Invertebrate Systematics* 20: 603–614.

Chiappini, E. and E. Mazzoni. 2000. Differing morphology and ultrastructure of the male copulatory apparatus in species-groups of *Anagrus* Haliday (Hymenoptera: Mymaridae). *Journal of Natural History* 34: 1661–1676.

———, C. Solinas, and M. Solinas. 2001. Antennal sensilla of *Anagrus atomus* (L.) (Hymenoptera: Mymaridae) female and their possible behavioural significance. *Entomologica, Bari* 35: 51–76.

Clouâtre, A., D. Coderre, and D. Gagnon. 1989. Habitat of a new Mymarommatidae found in southern Quebec, Canada (Hymenoptera: Terebrantes). *The Canadian Entomologist* 12: 825–826.

Dahms, E. C. D. 1984. A checklist of the types of Australian Hymenoptera described by Alexandre Arsene Girault: III. Chalcidoidea species F–M with advisory notes. *Memoirs of the Queensland Museum* 21: 579–842.

Debauche, H. R. 1948. Étude sur les Mymarommidae et les Mymaridae de la Belgique (Hymenoptera Chalcidoidea). *Mémoires du Musée Royal d'Histoire Naturelle de Belgique* 108: 1–248 + 24 plates.

Donev, A. 1982. Mymarommidae. Nauchni Trudove, Biologiya. *Plovdivski Universitet "Paissi Hildenarski"* 20: 483–484.

Doutt, R. L. 1973. The fossil Mymaridae. *Pan-Pacific Entomologist* 49: 221–228.

Dowton, M. and A. D. Austin. 2001. Simultaneous analysis of 16S, 28S, CO1 and morphology in the Hymenoptera: Apocrita – evolutionary transitions among parasitic wasps. *Biological Journal of the Linnean Society* 74: 87–111.

Duisburg, P. von. 1868. Zur Bernstein-Fauna. *Schriften der Physikalisch-ökonomischen Gesellschaft zu Königsberg* 9: 23–28.

Early, J. W., L. Masner, I. D. Naumann, and A. D. Austin. 2001. Maamingidae, a new family of proctotrupoid wasp (Insecta: Hymenoptera) from New Zealand. *Invertebrate Taxonomy* 15: 341–352.

Ferrière, C. 1948. Un curieux Mymaride: *Petiolaria anomala* Bl. et Kr. *Mitteilungen der Schweizerischen Entomologischen Gesellschaft* 21: 555–556.

Fidalgo, P. and L. De Santis. 1982. Una nueva especie de mimarido de la subfamilia Mymaromminae (Insecta, Hymenoptera). *Revista del Museo de La Plata (Nueva Serie), Zoologia* 13 (127): 1–6.

Fursov, V., Y. Shirota, T. Nomiya, and K. Yamagishi. 2002. New fossil mymarommatid species, *Palaeomymar japonicum* sp. nov. (Hymenoptera: Mymarommatidae), discovered in Cretaceous amber from Japan. *Entomological Science* 5: 51–54.

Gallego, V. C. 1986. Notes on the parasitoid complex of the coconut leafminer *Promecotheca cumingii* Baly in some Mindanao provinces, Philippines. *Philippine Journal of Coconut Studies* 11: 4–7.

García, J. L. 2000. Nuevos registros genéricos para Venezuela de Hymenoptera Parasitica. *Boletín de Entomología Venezolana* 15: 113–117.

Gauld, I. D., and B. Bolton, eds. 1988. *The Hymenoptera*. Oxford University Press, Oxford. 332 pp.

Gibson, G. A. P. 1985. Some pro- and mesothoracic structures important for phylogenetic analysis of Hymenoptera, with a review of terms used for the structures. *The Canadian Entomologist* 117: 1395–1443.

———. 1986. Evidence for monophyly and relationships of Chalcidoidea, Mymaridae, and Mymarommatoidea (Hymenoptera: Terebrantes). *The Canadian Entomologist* 118: 205–240.

———. 1993. Superfamilies Mymarommatoidea and Chalcidoidea. Pp. 570–655 *in* Goulet, H., and J. Huber, eds. *Hymenoptera, an identification guide to families*. Agriculture Canada Research Branch Monograph No. 1894E, Ottawa. 668 pp.

———. 1997. Chapter 2. Morphology and terminology. Pp. 16–44 *in*: Gibson, G. A. P., J. T. Huber, and J. B. Woolley, eds. *Annotated Keys to the Genera of Nearctic Chalcidoidea (Hymenoptera)*. NRC Research Press, Ottawa, Ontario. 794 pp.

———. 2003. Phylogenetics and classification of Cleonyminae (Hymenoptera: Chalcidoidea: Pteromalidae). *Memoirs on Entomology, International* 16: i–v + 339 pp.

——— and J. T. Huber. 2000. Review of the family Rotoitidae (Hymenoptera: Chalcidoidea), with

description of a new genus and species from Chile. *Journal of Natural History* 34: 2293–2314.

———, J. M. Heraty, and J. B. Woolley. 1999. Phylogenetics and classification of Chalcidoidea and Mymarommatoidea — a review of current concepts (Hymenoptera, Apocrita). *Zoologica Scripta* 28: 87–124.

Girault, A. A. 1920. New genera and species of chalcid-flies from Australia. *Insecutor Inscitiae Menstruus* 8: 37–50.

———. 1930. *New pests from Australia, VIII.* Privately printed, Brisbane. 5 pp.

———. 1931. *A new habit in an old insect. Homo pudicus and new Eurytomidae.* Privately printed, Brisbane. 4 pp.

———. 1935. *Microhymenoptera Australiensis nova, mostly Chalcididae.* Privately printed, Sydney. 4 pp.

Grimaldi, D. A. and M. S. Engel. 2005. *Evolution of the Insects.* Cambridge University Press, Cambridge, etc. 772 pp.

———, ———, and P. C. Nascimbene. 2002. Fossiliferous Cretaceous amber from Myanmar (Burma): its rediscovery, biotic diversity, and paleontological significance. *American Museum Novitates* 3361: 1–72.

Hansen, L. O. 1997. *Palaeomymar duisburgi* (Stein, 1877) (Hym., Mymarommatoidea): a species and superfamily new to the Norwegian fauna. *Fauna Norvegica, Series B* 44: 81–82.

Huber, J. T. 1987. Première mention en Suisse de la famille Mymarommatidae (Hymenoptera). *Mitteilungen der Schweizerischen Entomologischen Gesellschaft* 60: 82.

———. 2005. The gender and derivation of genus-group names in Mymaridae and Mymarommatidae (Hymenoptera). *Acta Societatis Zoologicae Bohemoslovenicae* 69: 167–183.

——— and P. Fidalgo. 1997. Review of the genus *Stephanodes* (Hymenoptera: Mymaridae). *Proceedings of the Entomological Society of Ontario* 128: 27–63.

——— and M. J. Sharkey. 1993. Chapter 3. Structure. Pp. 13–59 *in*: Goulet, H., and J. Huber, eds. *Hymenoptera, an identification guide to families.* Agriculture Canada Research Branch Monograph No. 1894E, Ottawa. 668 pp.

Isidoro, N., F. Bin, S. Colazza, and S. B. Vinson. 1996. Morphology of antennal gustatory sensilla and glands in some parasitoid Hymenoptera with hypothesis on their role in sex and host recognition. *Journal of Hymenoptera Research* 5: 206–239.

Kalina, V. 1989. Checklist of Czechoslovak Insects III (Hymenoptera). Chalcidoidea. *Acta Faunistica Entomologica Musei Nationalis Pragae* 19: 127.

Königsmann, E. 1978. Das phylogenetische System der Hymenoptera. Teil 3: "Terebrantes" (Unterordung Apocrita). *Deutsche Entomologische Zeitschrift (N. F.)* 25: 1–55.

Kozlov, M. A. and A. P. Rasnitsyn. 1979. On the limits of the family Serphitidae (Hymenoptera, Proctotrupoidea). *Entomologischeskoe Obozrenie* 58: 402–416. [In Russian.]

Lin, N. 1994. First discovery of Mymarommatidae (Hymenoptera) from China, with description of a new species. *Entomotaxonomia* 16: 120–126.

Liu, Z. and G. Nordlander, G. 1992. Ibaliid parasitoids of siricid woodwasps in North America: two new *Ibalia* species and a key to species (Hymenoptera: Cynipoidea). *Proceedings of the Entomological Society of Washington* 94: 500–507.

Masner, L. 1961. Ambositrinae, a new subfamily of Diapriidae from Madagascar and Central Africa. *Mémoirs de l'Instutute Scientifique de Madagascar, Série E* 12: 289–295.

———. 1979. Pleural morphology in scelionid wasps (Hymenoptera: Scelionidae) — an aid in higher classification. *The Canadian Entomologist* 111: 1079–1087.

———. 1993. Superfamily Proctotrupoidea. Pp. 537–557 *in*: Goulet, H., and J. Huber, eds. *Hymenoptera, an identification guide to families.* Agriculture Canada Research Branch Monograph No. 1894E, Ottawa. 668 pp.

———, N. F. Johnson, and A. D. Polaszek. 2007. Redescription of *Archaeoscelio* Brues and description of three new genera of Scelionidae (Hymenoptera): a challenge to the definition of the family. *American Museum Novitates* 3550: 1–24.

Mathot, G. 1966. Contribution a la connaissance des Mymaridae et Mymarommidae d'Afrique Centrale (Hymenoptera Chalcidoidea). *Bulletin and Annales Societe Royal d'Entomologie de Belgique* 102: 213–239.

Meunier, F. 1901. Contribution à la faune des Mymaridae ou 'atomes ailés' de l'ambre. *Annales de la Société Scientifique de Bruxelles* 25: 282–292.

Miller, M. C. 1972. Scanning electron microscope studies of the flagellar sense receptors of *Peridesmia discus* and *Nasonia vitripennis* (Hymenoptera: Pteromalidae) *Annals of the Entomological Society of America* 65: 1119–1124.

Naumann, I. D. and L. Masner. 1985. Parasitic wasps of the proctotrupoid complex: a new family from Australia and a key to world families (Hymenoptera: Proctotrupoidea *sensu lato*). *Australian Journal of Zoology* 33: 761–783.

Nikol'skaya, M. N. 1978. Family Serphitidae (Serphitida). Pp. 1179–1180 *in* Medvedev, G. S. ed.-in-chief. 1987. *Keys to the insects of the European part of the USSR. Vol. III, Hymenoptera, Part II.* Amerind Publishing Co., New Dehli 1341 pp. [Translated from Russian original.]

Noyes, J. S. and E. W. Valentine. 1989. Chalcidoidea (Insecta: Hymenoptera) — introduction, and review of genera in smaller families. *Fauna of New Zealand* 18: 91 pp.

Olson, D. M. and D. A. Andow. 1993. Antennal sensilla of female *Trichogramma nubilale* (Ertle and Davis) (Hymenoptera: Trichogrammatidae) and comparisons with other parasitic Hymenoptera. *International Journal of Insect Morphology and Embryology* 22: 507–520.

Rasnitsyn, A. P. 1980. The origin and evolution of hymenopterous insects. *Trudy Paleontologicheskogo Instituta. Akademiya Nauk SSSR* 174: 1–190. [In Russian.]

———. 1988. An outline of evolution of the hymenopterous insects (Order Vespida). *Oriental Insects* 22: 115–145.

———. 2002. Superorder Vespida Laicharting, 1781. Order Hymenoptera Linné, 1758. Pp. 242–254 *in* Rasnitsyn, A. P., and D. L. J. Quicke, eds. *History of Insects*. Kluwer Academic Publishers, Dordrecht, etc. 517 pp.

———, H. H. Basibuyuk, and D. L. J. Quicke. 2004. A basal chalcidoid (Insecta: Hymenoptera) from the earliest Cretaceous or latest Jurassic of Mongolia. *Insect Systematics and Evolution* 35: 123–135.

Ronquist, F. and G. Nordlander. 1989. Skeletal morphology of an archaic cynipoid, *Ibalia rufipes* (Hymenoptera: Ibaliidae). *Entomologica Scandinavica*, Supplement 33: 1–60.

———, A. P. Rasnitsyn, A. Roy, K. Eriksson, and M. Lindgren. 1999. Phylogeny of the Hymenoptera: a cladistic reanalysis of Rasnitsyn's (1988) data. *Zoologica Scripta* 28: 13–50.

Schlüter, T. 1978. Zur Systematik und Palökologie harzkonservierter Arthopoda einer Taphozönose aus dem Cenomanium von NW-Frankreich. *Berliner Geowissenschaftliche Abhandlungen (A)* 9: 1–150.

——— and R. Kohring. 1990. Sie zwergwespengattung *Palaeomymar* (Hymenotpera: Proctotrupoidea: Serphitidae) aus dem mio/pliozänen Simetit Siziliens. *Berliner Geowissenschaftliche Abhandlungen (A)* 124: 115–121.

Soyka, W. 1937. *Mymaromma anomala* (Kryger) ♀ (Erstbeschreibung des ♀) (Mymaridae, Chalc. Hym.). *Natuurhistorisch Maandblad, Maastricht* 26: 23–24.

Stein, J. P. E. F. 1877. Drei merkwürdige Bernstein-Insekten. *Mitteilungen der Münchener entomologischen Verhandlung* 1: 28–30.

Triapitsyn, S. V. and V. V. Berezovskiy. 2000. Superfam. Mymarommatoidea 27. Fam. Mymarommatoidea. *Opredeliteli nasekomikh dalinego vostoka Rossii* 4: 579. [In Russian.]

——— and ———, 2006. A new species of the genus *Palaeomymar* Meunier, 1901 (Hymenoptera: Mymarommatidae) from the Russian Far East, with notes on other Palaearctic species. *Far Eastern Entomologist* 159: 1–8.

Valentine, E. W. 1971. Entomology of the Aucklands and other islands south of New Zealand. *Pacific Insects Monographs* 27: 327–333.

Veen, J. C. van. and L. E. van Wijk. 1985. The unique structure and functions of the ovipositor of the non-paralyzing ectoparasitoid *Colpoclypeus florus* Walk. (Hym., Eulophidae) with special reference to antennal sensilla and immature stages. *Zeitschrift für angewandte Entomologie* 99: 511–531.

Vidal, S. 2001. Entomofauna Germanica. Band 4. Verzeichnis der Hautflügler Deutschlands. Chalcidoidea. *Entomologische Nachrichten und Berichte Beiheft* 7: 61.

Viggiani, G. 1966. Ricerche sugli Hymenoptera Chalcidoidea. VI. Generi e specie nuovi per l'entomofauna italiana (Encyrtidae, Aphelinidae, Mymarommatidae). *Bollettino del Laboratorio di Entomologia Agraria 'Filippo Silvestri', Portici* 24: 84–105.

Vilhelmsen, L. and L. Krogmann. 2006. Skeletal anatomy of the mesosoma of *Palaeomymar anomalum* (Blood & Kryger, 1922) (Hymenoptera: Mymarommatidae). *Journal of Hymenoptera Research* 15: 290–306.

Voegelé, J., J. Cals-Usciati, J.-P. Pihan, and J. Daumal. 1975. Structure de l'antenne femelle des Trichogrammes. *Entomophaga* 20: 161–169.

Ware, A. B. and S. G. Compton. 1992. Repeated evolution of elongate multiporous plate sensilla in female fig wasps (Hymenoptera: Agaonidae: Agaoninae). *Proceedings Nederlandse Akademie van Wetenschappen* 95: 275–292.

Yoshimoto, C. M. 1975. Cretaceous chalcidoid fossils from Canadian amber. *The Canadian Entomologist* 107: 499–528.

———. 1984. *The insects and arachnids of Canada, Part 12. The families and subfamilies of Canadian chalcidoid wasps*. Publication 1760, Canadian Government Publishing Centre, Supply and Services Canada, Ottawa. 149 pp.

Appendix I. Abbreviations used for structures in the illustrations.

acc:	acetabular carina
aea:	aedeagal apodeme
aed:	aedeagus
am:	anterior margin
an:	anus
anp:	anal plate
as:	apical sensillum of clava
asc:	anterior scutellum
axp:	axillar phragma
bc:	basicoxite of metacoxa
c:	carina
ca:	calcar
cc:	costal cell
cer:	cercus
cl:	clava
cl_n:	claval segment
cs:	campaniform sensillum

ct: coxal trough
cv: costal vein
cx: coxa
d: dorsal mandibular surface
dig: digitus
dis: digital spine
dms: dorsal metapleural sensillum
dsc: disc of forewing
dt: dorsal tooth of mandible
fc: fine comb
fs: flagellar setae
frp: frontal plate of head capsule
fs: flagellar setae
fu: funicle
fu_n: funicular segment
gp: gonopore
ham: hamulus
hp: humeral plate
hwb: base of hind wing
hyp: hypopygium
i: inner mandibular surface
isp: intersegmental pit
lab: labium
lbr: labrum
lpm: prementum of labium
lst: laterosternite
ltt: laterotergite
max: maxilla
mb: membrane
mc: macrochaeta of forewing
mg: mandibular groove
mms: mesopleural-metapleural suture
mn: mesopleural notch
mnd: mandible
mps: multiporous plate sensillum
ms: paramedial setae of occipital plate
msc: mesoscutum
Mt_n: metasomal tergite
mv: marginal vein
mxg: galea of maxilla
mxp: maxillary palpus
mxs: stipes of maxilla
no_3: metanotum
o: outer mandibular surface
ocp: occipital plate of head capsule
op: opposing process of hind wing
opp: pit on occipital plate
ov: ovipositor
ovs: ovipositor sheath
paa: parameral apodeme
pap: process of labiomaxillary complex
par: paramere
pas: postalar sensillum
pf: propodeal flange
pgp: postgenal plate of head capsule
pl_3: metapleuron
pl_2p: mesopleural pit
pl_3p: metapleural pit
pn: pronotal notch
ppm: propleural margin
pro: propodeum
pre: prepectus
prs: propodeal seta
psc: posterior scutellum
ps: pseudospur
pss: prespiracular sensillum
pst: pterostigma
pt_n: petiolar segment
ptp: posterior tentorial pits
ret: retinaculum
s1–4: type 1, 2, 3 or 4 flagellar sensillum
sa: subalar area
sas: subalar sensilla of mesopleuron
sbt: subbasal tooth
sep: setal patch
smv: submarginal vein
sp: spiracle
spa: spiracular aperture
spp: spiracular peritreme
sps: suprapleural sensillum
std: forewing stalk, distal part
stk: forewing stalk
stp: forewing stalk, proximal part
stv: stigmal vein
syn: syntergum
tg: tegula
tra: trachea
voa: volsellar apodeme
vol: volsella
vt: ventral tooth of mandible

Appendix II. Synopsis of extant material examined.

Mymaromma Blood and Kryger

1. *Mymaromma anomalum* (Blood and Kryger) (numerous individuals, CIRAD, CNC, NHRS, UCRC): **Nearctic** — Canada (ON). **Palaearctic** — Czech Republic, England, France, Germany, Hungary, Italy, Japan, Poland, Russia, Sweden.
2. *Mymaromma buyckxi* Mathot (7♀, 4♂; CNC, ISNB): **Afrotropical** — Congo, Gabon, Madagascar, Nigeria.
3. *Mymaromma goethei* Girault (numerous individuals, ANIC, BPBM, CNC, UCRC): **Australasian** — Australia (QLD, NT, WA), ?Hawaii, Papua New Guinea.
4. *Mymaromma mirissimum* Girault (numerous individuals, ANIC, CNC): **Australasian** — Australia (ACT, QLD, NT, WA), Christmas Island, Norfolk Island.
5. *Mymaromma ypt* (Triapitsyn & Berezovskiy) (33♀, 11♂; CNC, UCRC): **Oriental** — China (Fujian). **Palaearctic** — Russia, South Korea.
6. *Mymaromma* sp. (numerous individuals, CNC, UCRC): **Oriental**: Taiwan, Thailand.

7. *Mymaromma* sp. (numerous individuals, CNC): **Australasian** — Indonesia (Ceram), New Caledonia. **Oriental** — Indonesia (Sulawesi, Sumatra), Malaysia (Sabah), ?Nepal, Philippines (Luzon, Negros), Taiwan, Thailand.
8. *Mymaromma* sp. (3♀, 2♂; CNC, UCRC): **Neotropical** — Bermuda, Colombia, Mexico.
9. *Mymaromma* sp. (1♀, 2♂; CNC): **Neotropical** — Brazil.
10. *Mymaromma* sp. (22♀, 26♂; ANIC, NZAC): **Australasian** — Chatham Island, New Zealand, Norfolk Island.

Mymaromella Girault

11. *Mymaromella chaoi* (Lin) (2♀; FAUF): **Oriental** — China.
12. *Mymaromella cyclopterus* (Fidalgo and De Santis) (1♀, MLPA): **Neotropical** — Brazil.
13. *Mymaromella mira* Girault (20♀, 35♂; ANIC, CNC, UCR): **Australasian** — Australia (ACT, SA, WA).
14. *Mymaromella* sp. (43♀, 2♂; CNC, USNM): **Nearctic** — Canada (ON), USA (GA, NC, NY, MD, MI, SC, VA).
15. *Mymaromella* sp. (6♀; CNC): **Nearctic** — Canada (NB, ON, PQ).
16. *Mymaromella* sp. (3♀; CNC, UCRC): **Australasian** — Australia (ACT).
17. *Mymaromella* sp. (11♀; ANIC, BMNH): **Australasian** — Australia (TAS, WA).
18. *Mymaromella* sp. (7♀, 1♂; ANIC, BMNH, UCRC): **Australasian** — Australia (SA, WA).
19. *Mymaromella* sp. (7♀; CNC): **Neotropical** — Brazil, Trinidad, Venezuela.
20. *Mymaromella* sp. (1♀; BMNH): **Afrotropical** — Ivory Coast.
21. *Mymaromella* sp. (6♀; BMNH): **Afrotropical** — Ivory Coast.
22. *Mymaromella* sp. (2♀; CNC): **Palaearctic** — Sweden.
23. *Mymaromella* sp. (1♀; ANIC): **Australasian** — Australia (WA).

Zealaromma Gibson, Read and Huber

24. *Zealaromma insulare* (numerous individuals; CNC, NZAC): **Australasian** — New Zealand.
25. *Zealaromma valentinei* (16♀, 5♂; CNC, NZAC): **Australasian** — New Zealand.

Appendix III. Character state summary of Mymarommatoidea.

1. Head capsule: (0) uniformly sclerotized, a single structure; (1) with a hyperoccipital band of pleated membrane differentiating moveable occipital plate from frontal plate.
2. Mandibular structure: (0) laterally thin, with outer surface convex and apices broadly overlapping when closed; (1) laterally thick, with outer surface convex and apices not meeting when closed (exodont).
3. Number of mandibular teeth: (0) two; (1) three.
4. Paramedial setae on occipital plate: (0) absent; (1) present.
5. Number of supraclypeal interorbital setae: (0) 4; (1) 2.
6. Ocelli: (0) present; (1) absent.
7. Width of labium: (0) about as wide as maxilla; (1) about twice as wide as maxilla.
8. Relative position of maxillary palpus and galea: (0) palpus originating from subapical lobe on inner part of galea; (1) palpus originating apically on lobe ventral to galea.
9. Number of claval segments of female: (0) 4; (1) 3; (2) 2; (3) 1.
10. Structure of multi-segmented clava: (0) segments distinctly separated, forming loosely associated clava; (1) segments compacted, forming tube-like clava.
11. Number of funicular segments of female: (0) 7; (1) 6.
12. Number of s4-type claval sensilla of female: (0) 2; (1) 3.
13. Position of s4-type claval sensilla of female: (0) near dorsal margin; (1) near midline or below.
14. Structure of propleura: (0) abutting, but separated or distinguished medially by distinct line; (1) fused into carapace.
15. Condition of meso- and metapleuron: (0) separated by suture; (1) completely fused or separated by suture only ventrally.
16. Condition of metanotum: (0) independent from metapleuron and propodeum; (1) fused laterally to metapleuron; (2) fused posterolaterally to propodeum; (3) fused to both metapleuron and propodeum.
17. Metapleural pit: (0) present; (1) absent.
18. Position of metapleural pit when present: (0) distinctly nearer spiracle than ventral margin of pleuron; (1) about midway between spiracle and ventral margin of pleuron.
19. Propodeal flange: (0) present laterally as vertical flange but incomplete dorsally; (1) complete laterally and dorsally, ∩-like.
20. Spiracular peritreme: (0) slit-like; (1) evident only as slender, smooth band of cuticle.
21. Spiracular aperture: (0) circular to oval; (1) elongate, slit-like.
22. Pattern of marginal setae along posterior margin of forewing: (0) with at least three moderately long basal setae; (1) with conspicuously long basal seta proximal to several very short setae; (2) with all setae very short basally.
23. Foretibial calcar: (0) comparatively long, curved and apically bifurcate; (1) comparatively short, straight and simple.

24. Posterior surface of mesofemur: (0) without bumps; (1) with bumps.
25. Seta laterally on first petiolar segment: (0) present; (1) absent.
26. Metasomal spiracle: (0) present; (1) absent.
27. Cerci: (0) present, though sometimes partly integrated into syntergal surface; (1) absent.
28. Male genitalia: (0) with external parameres; (1) without external parameres.

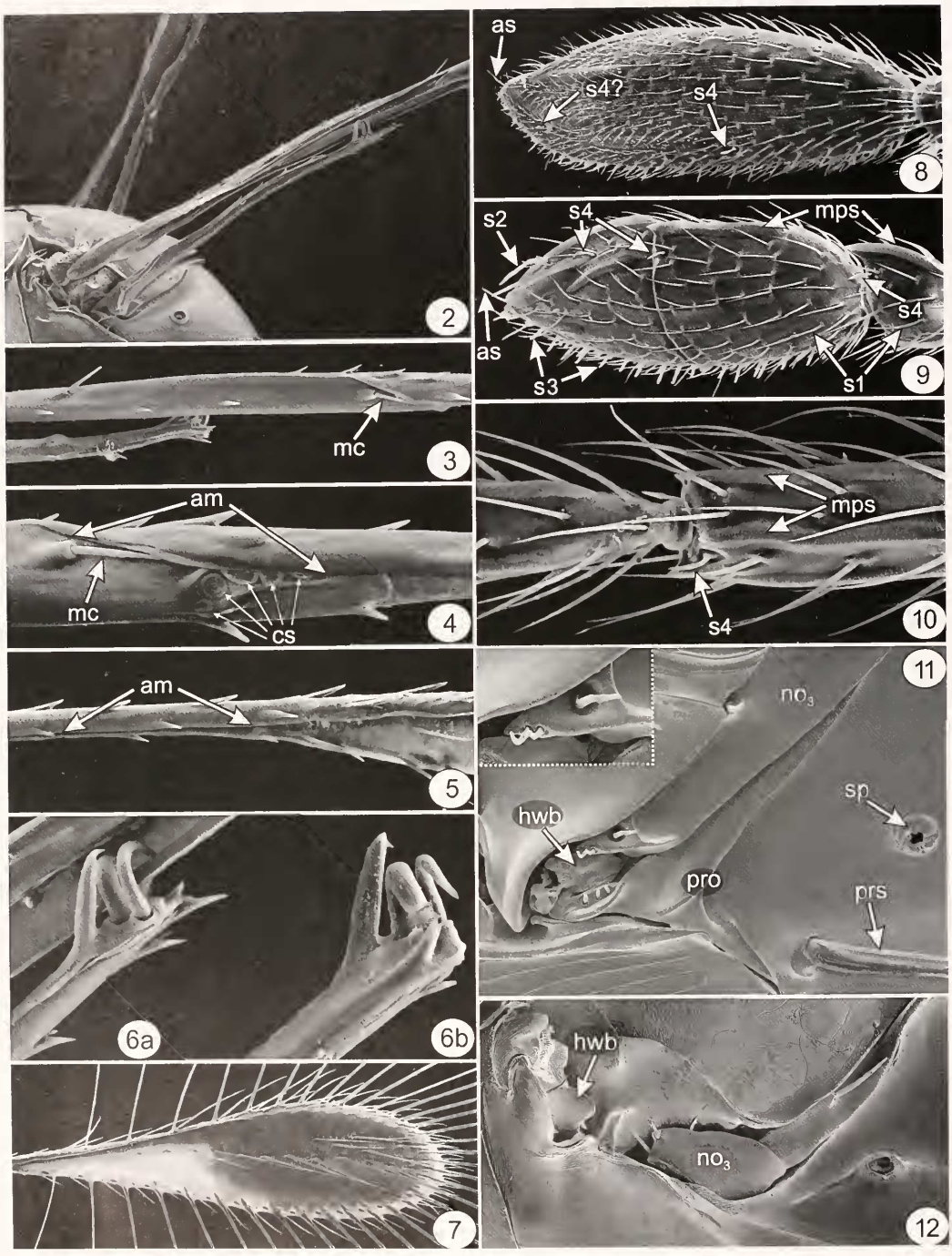

Figs 2–12. **2–7**, *Mymar schwanni*: **2**, forewing stalk and hind wing, ventral; **3**, wing coupling, dorsal; **4**, forewing stalk sensilla; **5**, distal part of forewing stalk; **6**, hind wing apex (**a**: ventral, **b**, dorsal); **7**, forewing disc, dorsal. **8 and 9**, ♀ clava: **8**, *Eustochus atripennis*; **9**, *M. schwanni*. **10**, *M. schwanni*, ♂ flagellar segments. **11 and 12**, dorsolateral view of metanotum, propodeum and base of hind wing: **11**, *Ptilomymar* sp. (insert: enlargement of lateral metanotal setae); **12**, *Mymar taprobanicum*.

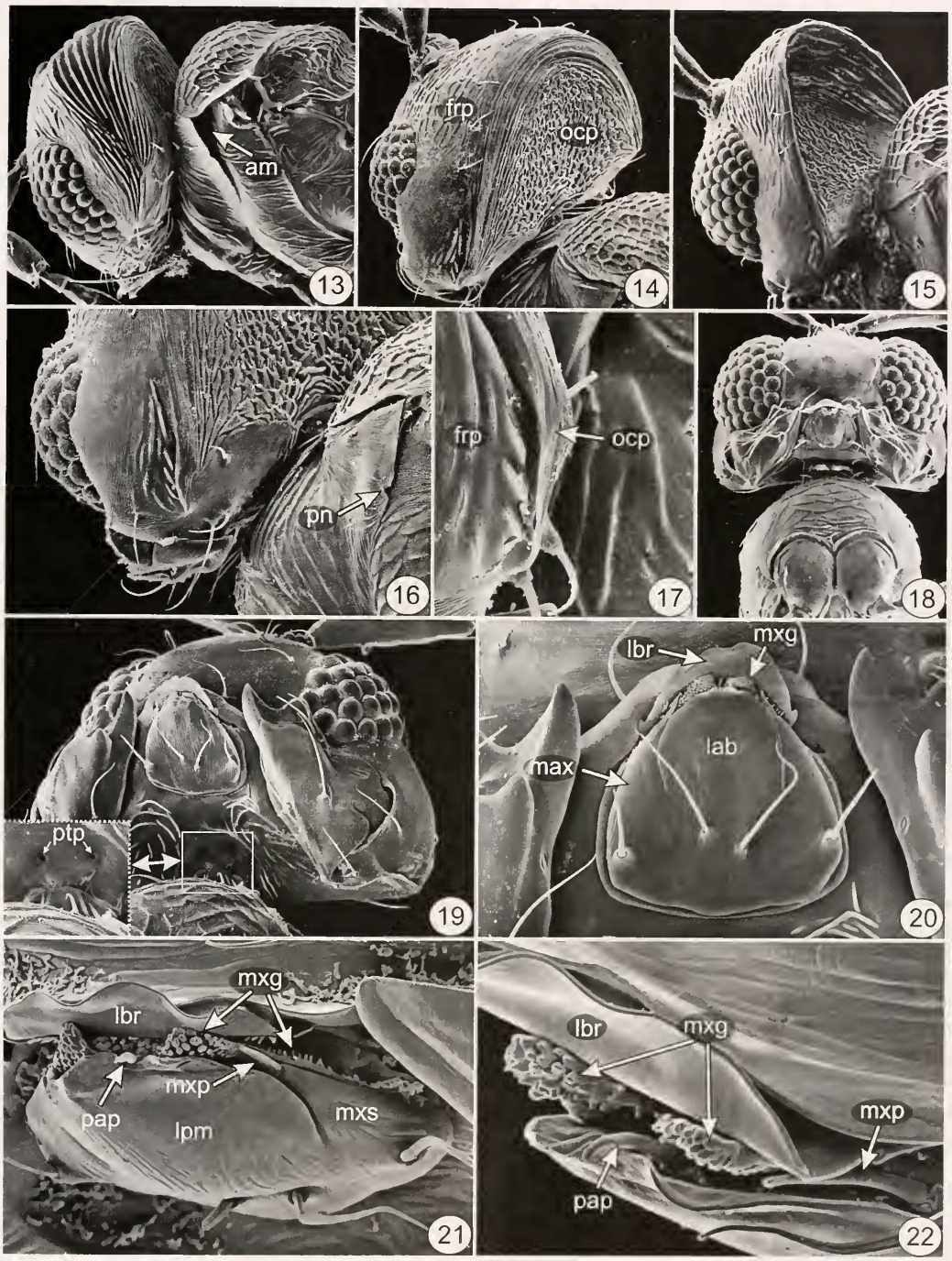

Figs 13–22. **13–15**, head capsule: **13**, *Mymaromella mira* (ocp expanded); **14**, *Mymaromma anomalum* (ocp normal); **15**, *Mymaromma buyckxi* (ocp inflexed). **16 and 17**, *M. anomalum*, articulation of occipital and frontal plates: **16**, posterolateral; **17**, lateral. **18**, *M. buyckxi*, mouthparts and propleura. **19**, *M. anomalum*, head, anteroventral (insert: posterior tentorial pits). **20–22**, *Mymaromma* spp., labiomaxillary complex: **20**, *M. anomalum*, ventral; **21**, *M.* sp. 7, anteroventral; **22**, *M.* sp. 6, anterolateral.

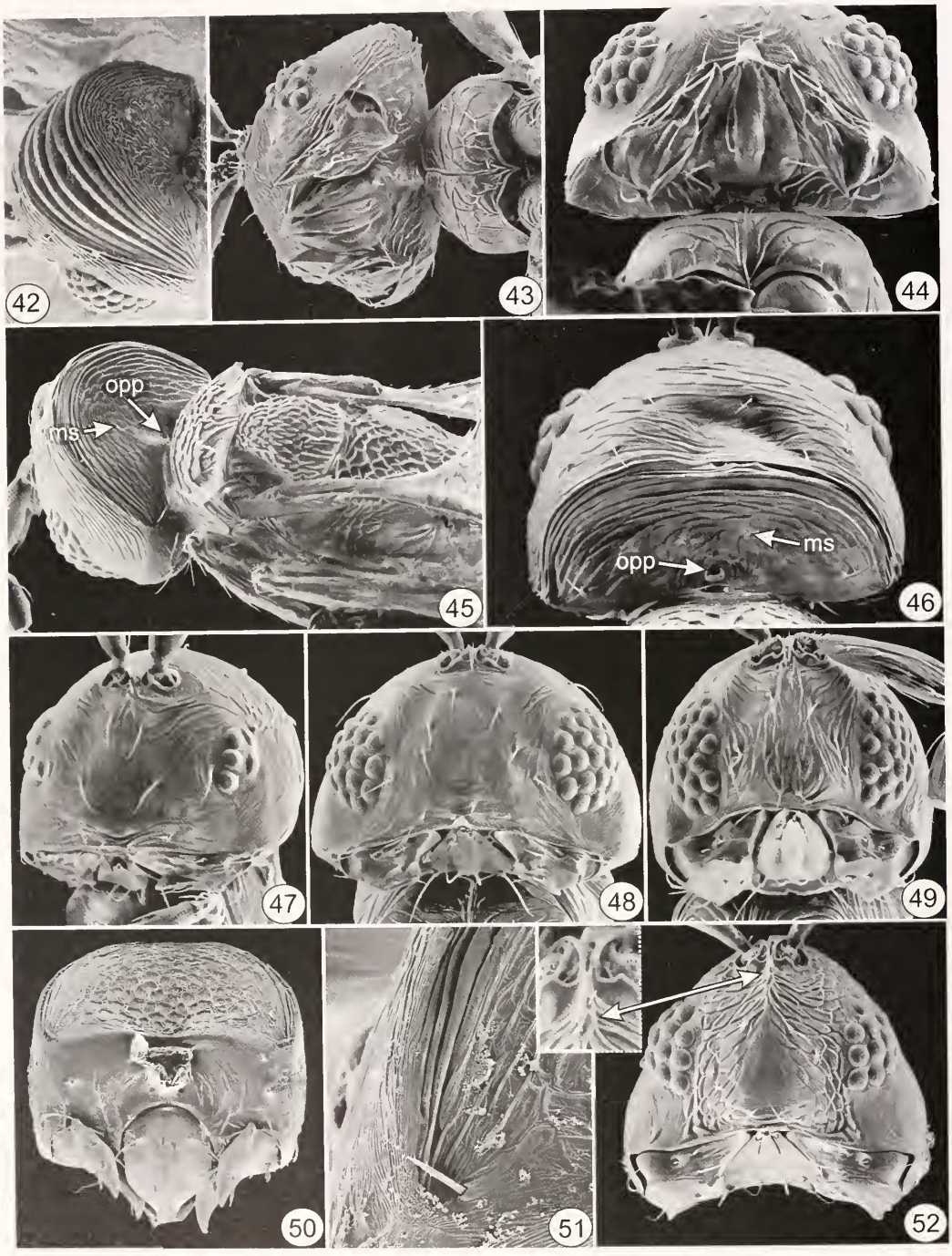

Figs 42–52. **42**, *Mymaromma* sp. 8, occipital plate and pleated membrane. **43 and 44**, *Mymaromella* spp., mouthparts and propleura: **43**, *M.* sp. 15; **44**, *M.* sp. 14. **45**, *Mymaromella* sp. 17, head and mesosoma, dorsolateral. **46**, *Mymaromella* sp. 16, head, dorsal. **47–49**, *Mymaromella* spp., face and mouthparts: **47**, *M.* sp. 20; **48**, *M.* sp. 14; **49**, *M.* sp. 17. **50 and 51**, *Zealaromma valentinei*: **50**, head capsule, posterior; **51**, articulation of occipital and frontal plates, posterior. **52**, *Zealaromma insulare*, face and mouthparts (insert: subtorular setae).

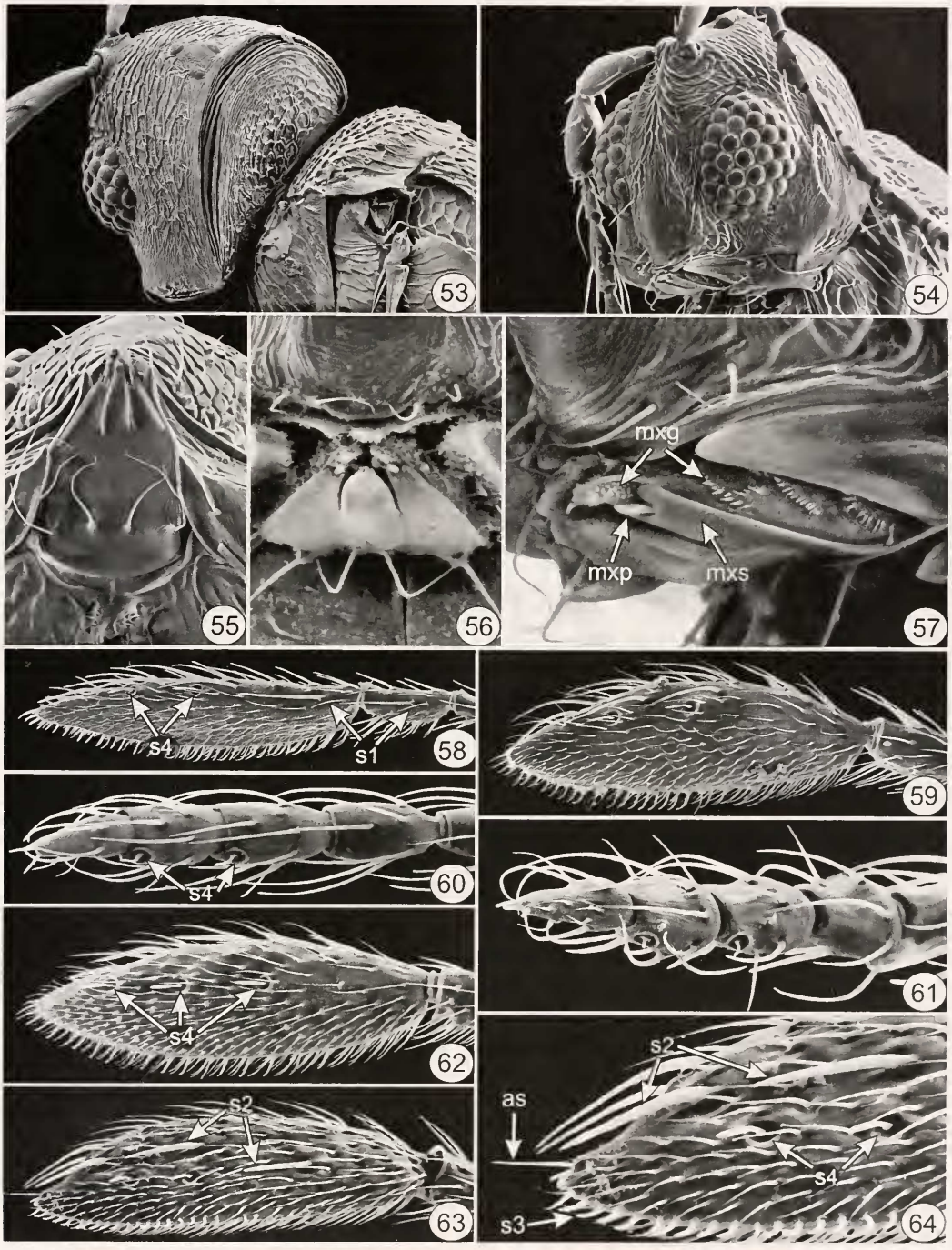

Figs 53–64. **53 and 54**, *Zealaromma valentinei*, head: **53**, posterodorsal; **54**, frontolateral. **55–57**, *Zealaromma* spp., labiomaxillary complex: **55**, *Z. insulare*, ventral; **56**, *Z. valentinei*, anterior; **57**, *Z. valentinei*, lateral. **58–61**, *Mymaromma* spp., clava: **58**, *M.* sp. 9 ♀; **59**, *M.* sp. 10 ♀; **60**, *M. goethei* ♂; **61**, *M. anomalum* ♂. **62–64**, *Mymaromella* spp., clava, outer surface: **62**, *M.* sp. 21 ♀; **63**, *M.* sp. 17 ♀; **64**, *M.* sp. 17 ♀ (apical half).

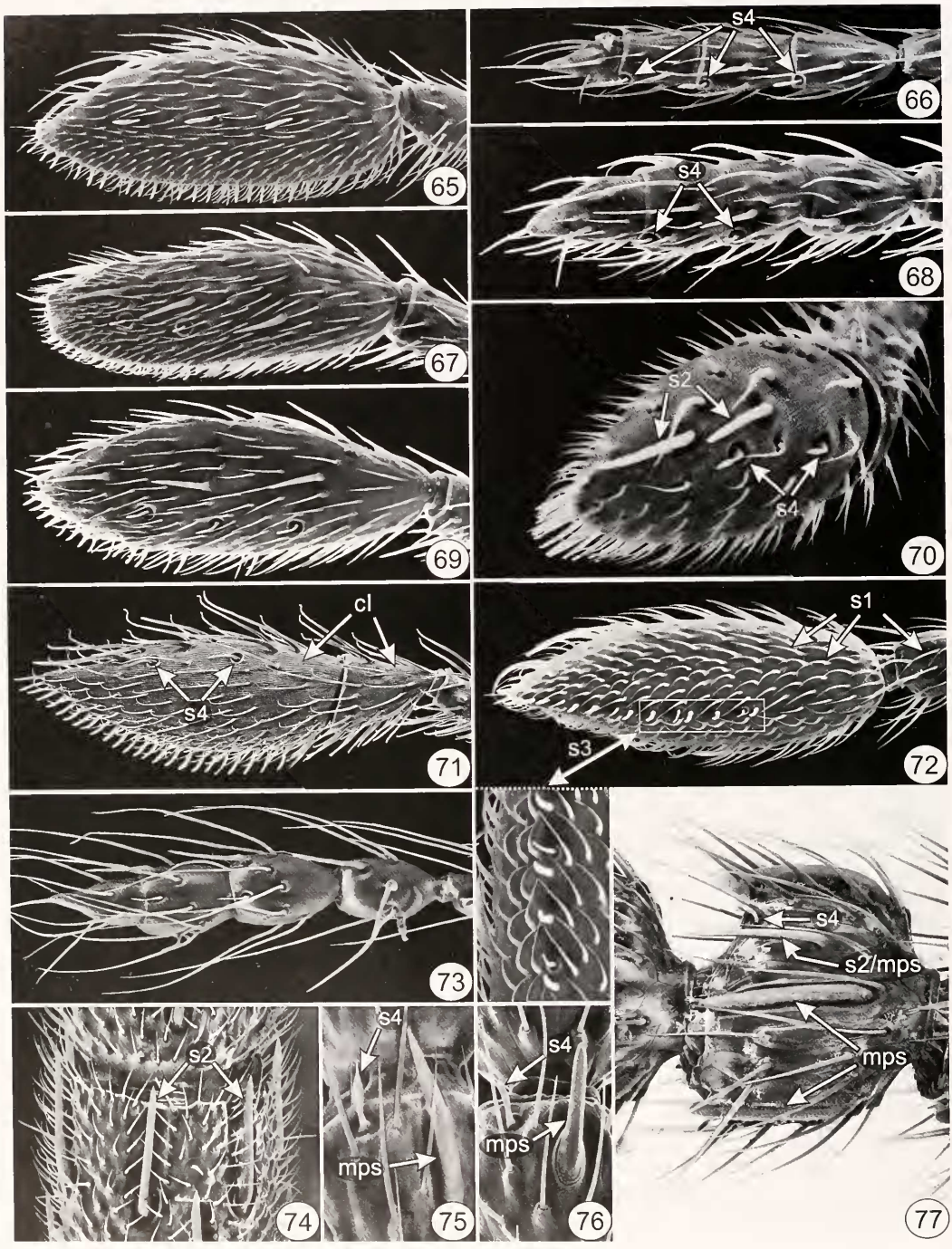

Figs 65–77. **65–69**, *Mymaromella* spp., clava: **65**, *M. mira* ♀, outer; **66**, *M. mira* ♂; **67**, *M.* sp. 18 ♀, outer; **68**, *M.* sp. 18 ♂; **69**, *M.* sp. 23 ♀, outer. **70 and 71**, *Zealaromma valentinei* ♀, clava: **70**, oblique dorsal; **71**, outer. **72**, *Mymaromella* sp. 20 ♀, clava, inner ventral (insert: different structures of s3-type sensilla). **73**, *Z. insulare* ♂, clava. **74–77**, ♀ funicular segment: **74**, *Maaminga rangi*; **75**, *Chiloe micropteron*; **76**, *Rotoita basalis*; **77**, *Rotoita* sp. nr *R. basalis*.

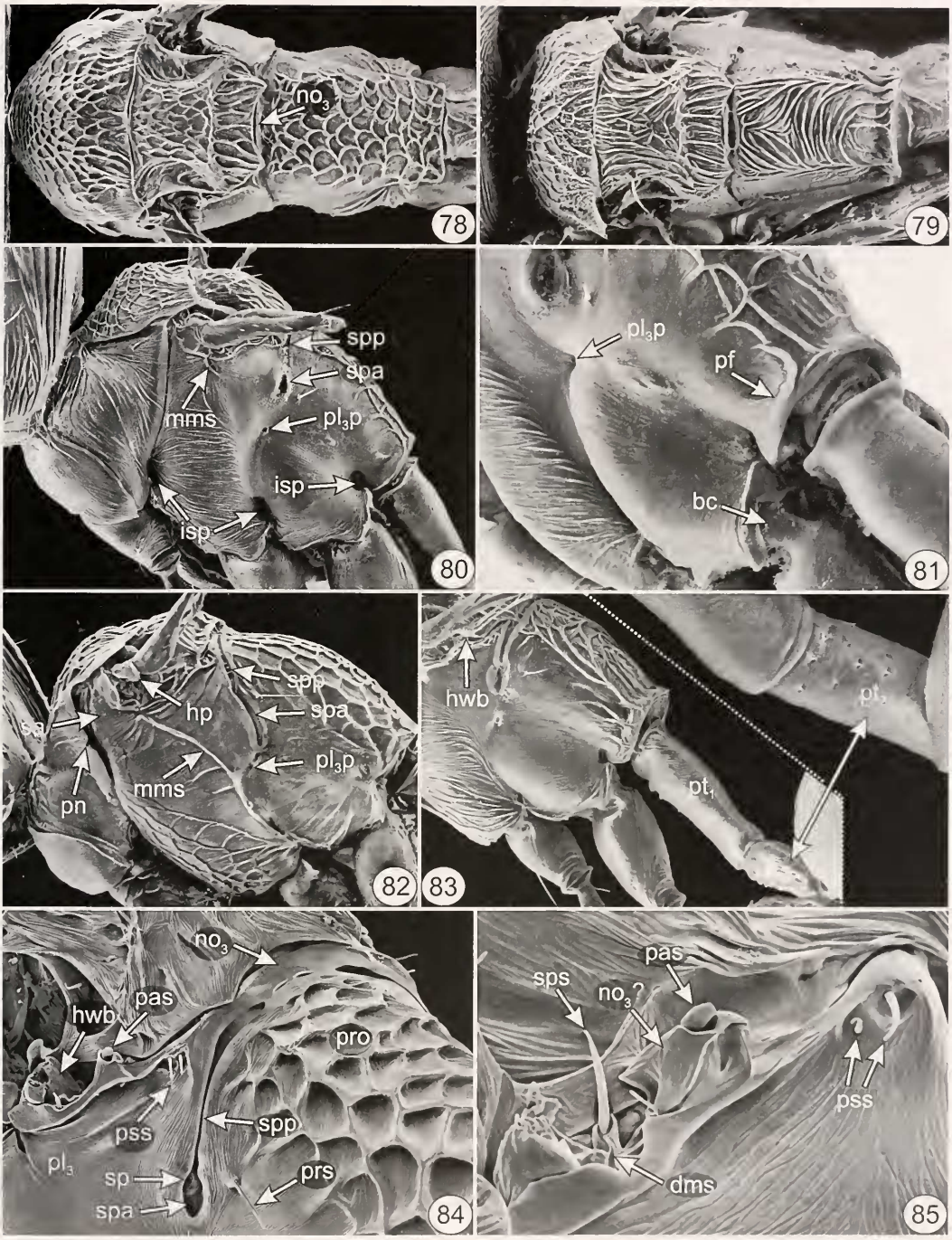

Figs 78–85. **78 and 79**, *Mymaromma* spp., mesosoma, dorsal: **78**, *M. buyckxi*; **79**, *M.* sp. 6. **80 and 81**, *Mymaromma* sp. 10: **80**, mesosoma, lateral; **81**, articulation of mesosoma and petiole, posterolateral. **82 and 83**, *Mymaromma* spp.: **82**, *M.* sp. 9, mesosoma, lateral; **83**, *M. goethei*, posterior of mesosoma and petiole, lateral (insert: second petiolar segment). **84 and 85**, *Mymaromma* sp. 7, metathoracic-propodeal complex: **84**, posterolateral; **85**, sensilla.

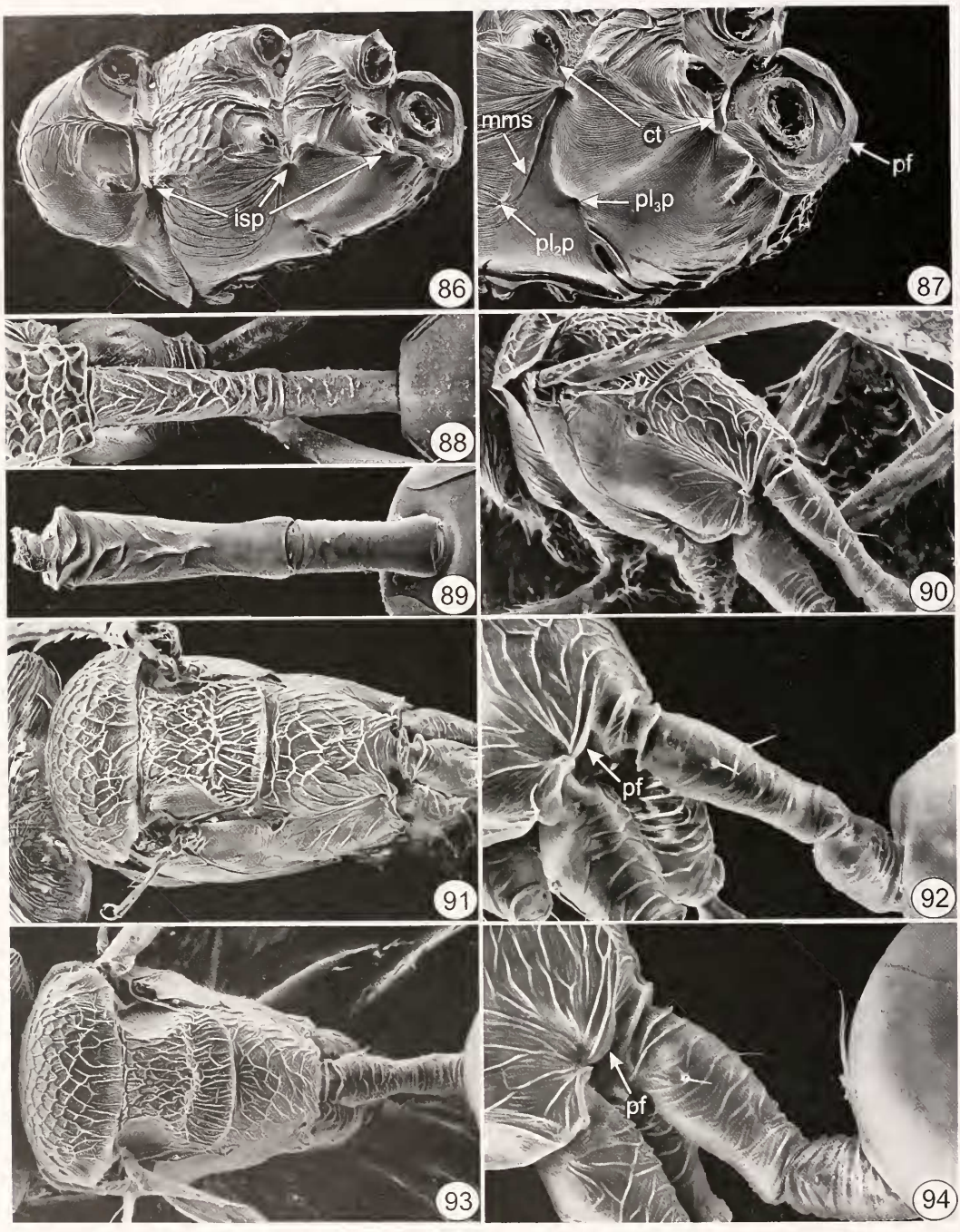

Figs 86–94. **86 and 87**, *Mymaromma* sp. 7: **86**, mesosoma, ventrolateral; **87**; posterior half of mesosoma, ventrolateral. **88 and 89**, *Mymaromma* spp., petiole: **88**, *M. buyckxi*, dorsal; **89**, *M.* sp. 6, ventral. **90**, *Mymaromella* sp. 21, mesosoma and petiole, posterolateral. **91 and 92**, *Mymaromella* sp. 14: **91**, mesosoma, dorsal; **92**, propodeal apex and petiole, lateral. **93 and 94**, *Mymaromella mira*: **93**, mesosoma and petiole, dorsal; **94**, propodeal apex and petiole, lateral.

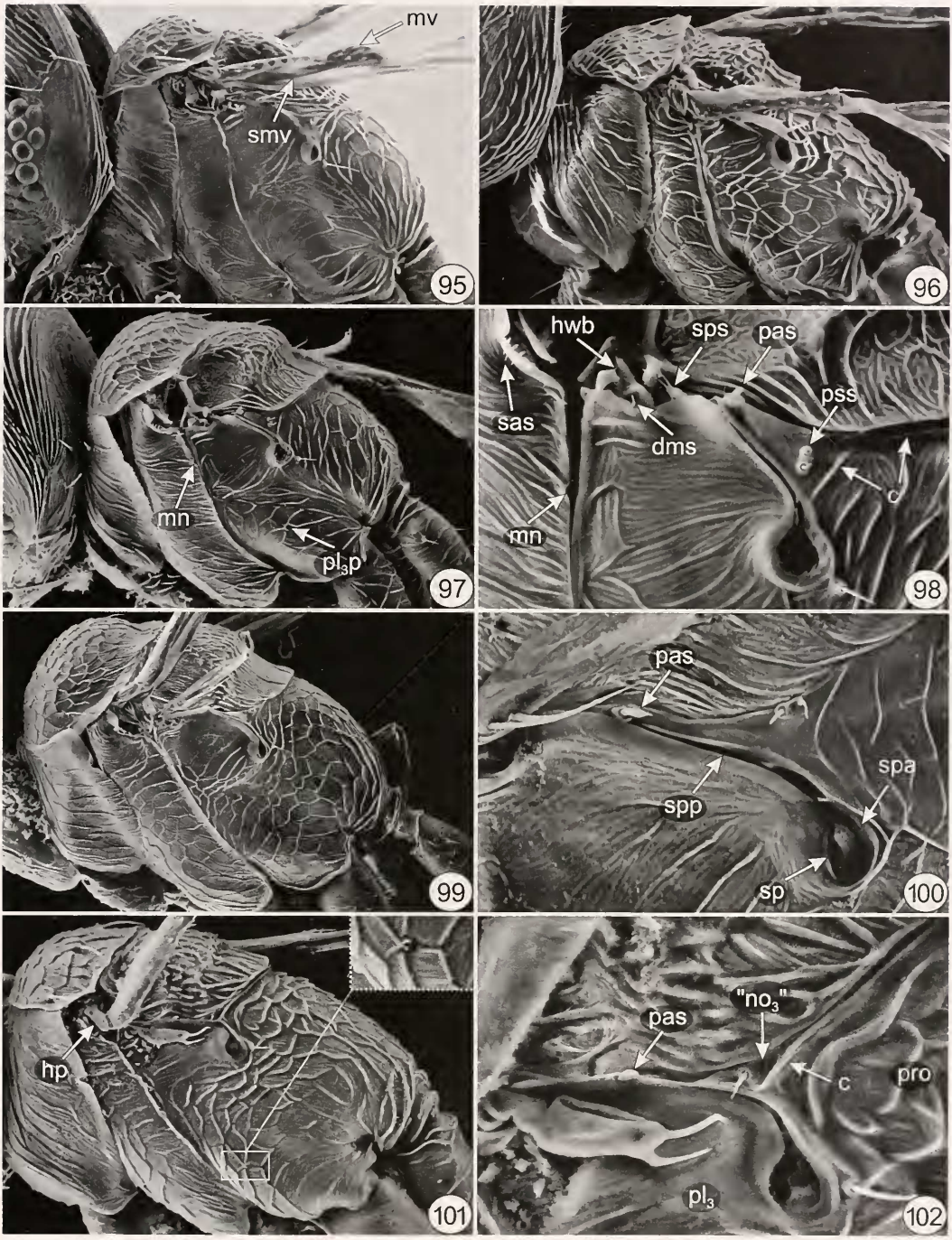

Figs 95–102. **95 and 96**, *Mymaromella* spp., mesosoma, lateral: **95**, *M.* sp. 21; **96**, *M.* sp. 15. **97 and 98**, *Mymaromella mira*: **97**, mesosoma, lateral; **98**, metathoracic-propodeal sensilla. **99 and 100**, *Mymaromella* sp. 23: **99**, mesosoma, lateral; **100**, metathoracic-propodeal sensilla. **101 and 102**, *Mymaromella* sp. 17: **101**, mesosoma, lateral (insert: metapleural pit); **102**; metathoracic-propodeal sensilla.

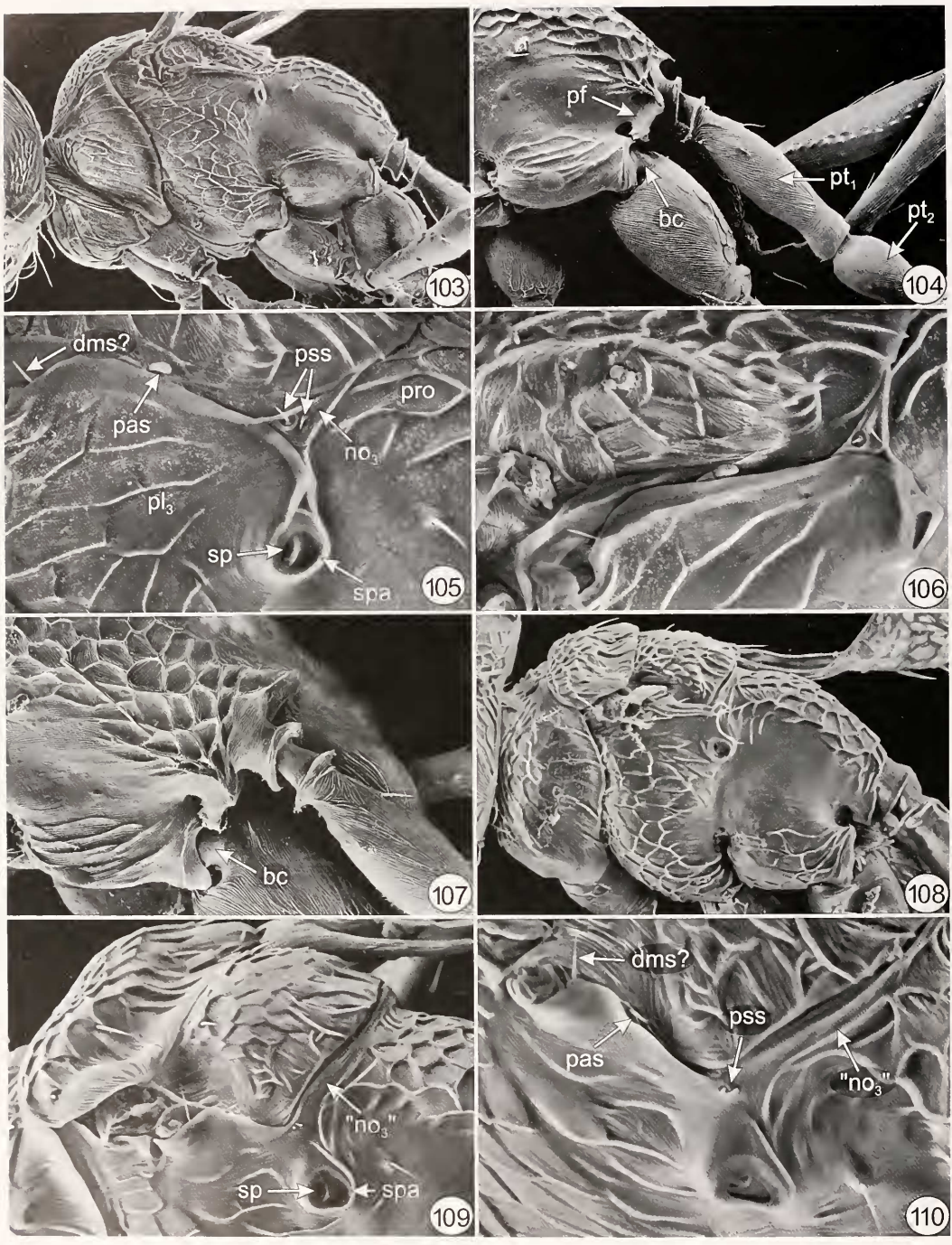

Figs 103–110. **103–107**, *Zealaromma valentinei*: **103**, mesosoma, lateral; **104**, posterior of metasoma, lateral; **105**, metathoracic-propodeal complex, lateral; **106**, metathoracic-propodeal complex, dorsolateral; **107**, posterior of metasoma, dorsolateral. **108–110**, *Zealaromma insulare*: **108**, mesosoma, lateral; **109**, metathoracic-propodeal complex, posterolateral; **110**, metathoracic-propodeal complex, posterodorsal.

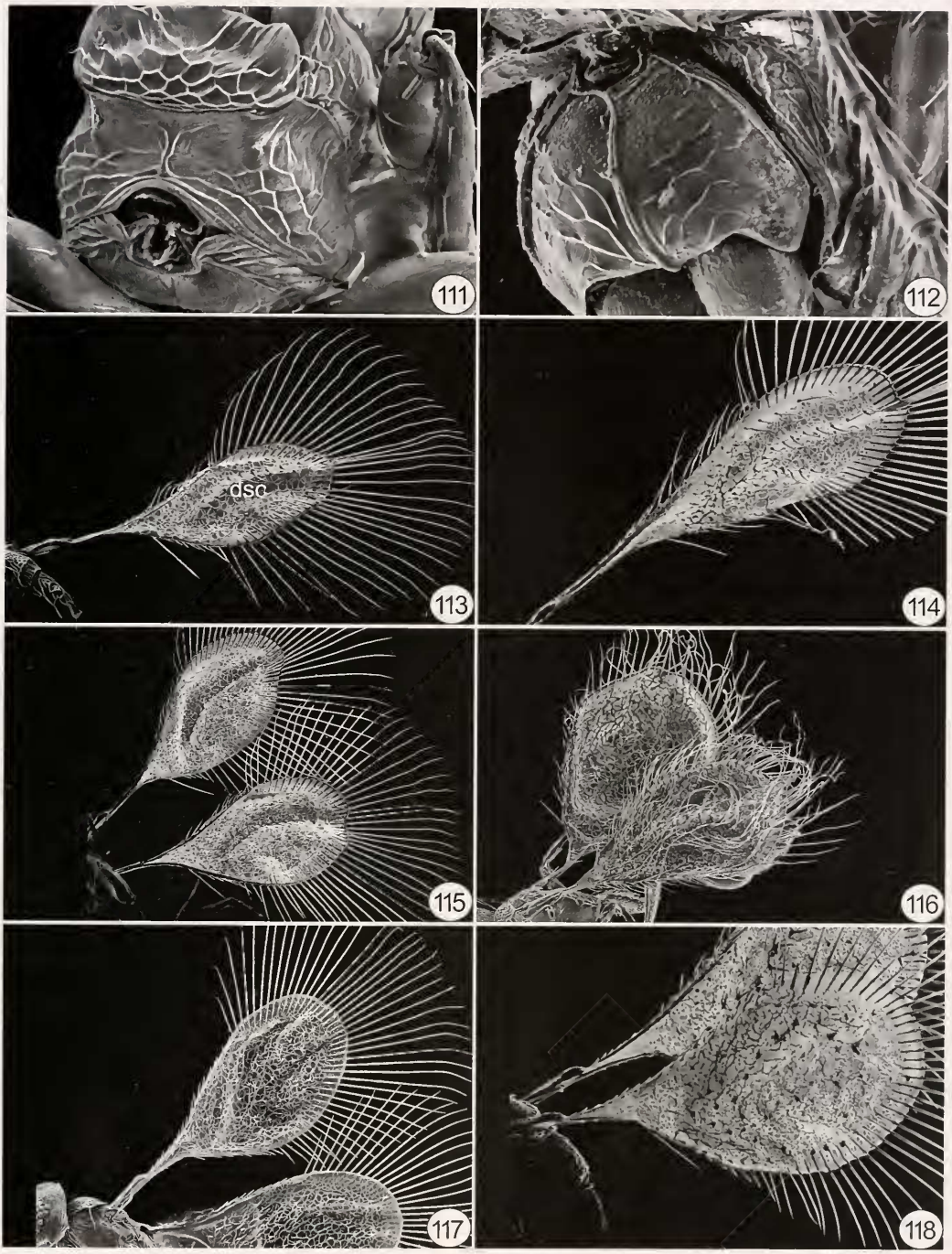

Figs 111–118. **111**, *Zealaromma insulare*, mesosoma, anterior (head removed). **112**, *Zealaromma valentinei*, propleura, anteroventral. **113–116**, *Mymaromma* spp., forewing: **113**, *M. goethei*; **114**, *M.* sp. 9; **115**, *M. buyckxi*; **116**, *M.* sp. 10. **117 and 118**, *Mymaromella* spp., forewing: **117**, *M.* sp. 14; **118**, *M.* sp. 21.

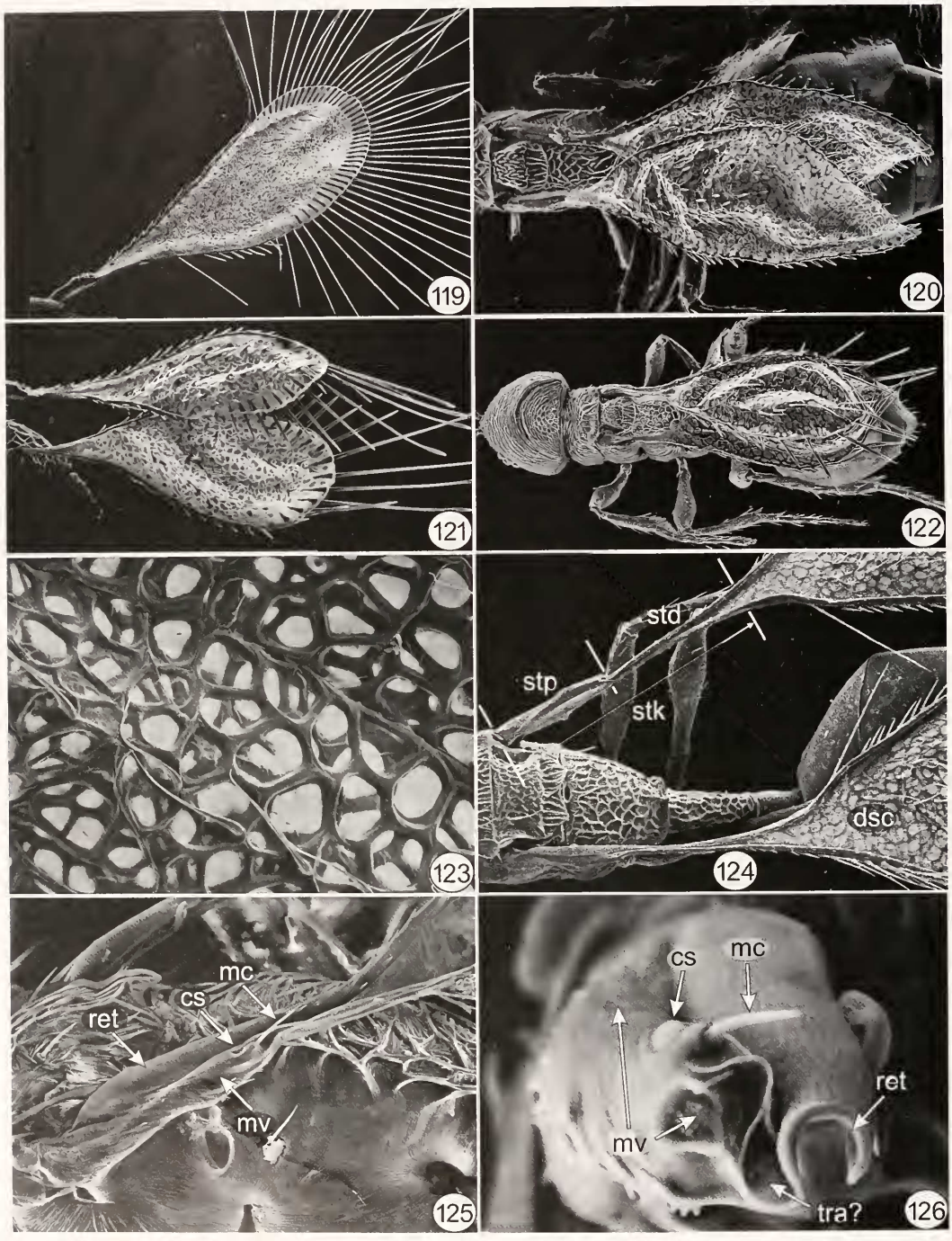

Figs 119–126. **119–121**, *Mymaromella* spp., forewing: **119**, *M.* sp. 18; **120**, *M.* sp. 17; **121**, *M.* sp. 20. **122**, *Zealaromma insulare*, dorsal habitus. **123**, *Zealaromma valentinei*, forewing disc reticulate pattern. **124**, *Mymaromma anomalum*, proximal part of forewing. **125 and 126**, *Mymaromma* sp. 10: **125**, proximal part of forewing; **126**, cross-section of forewing venation.

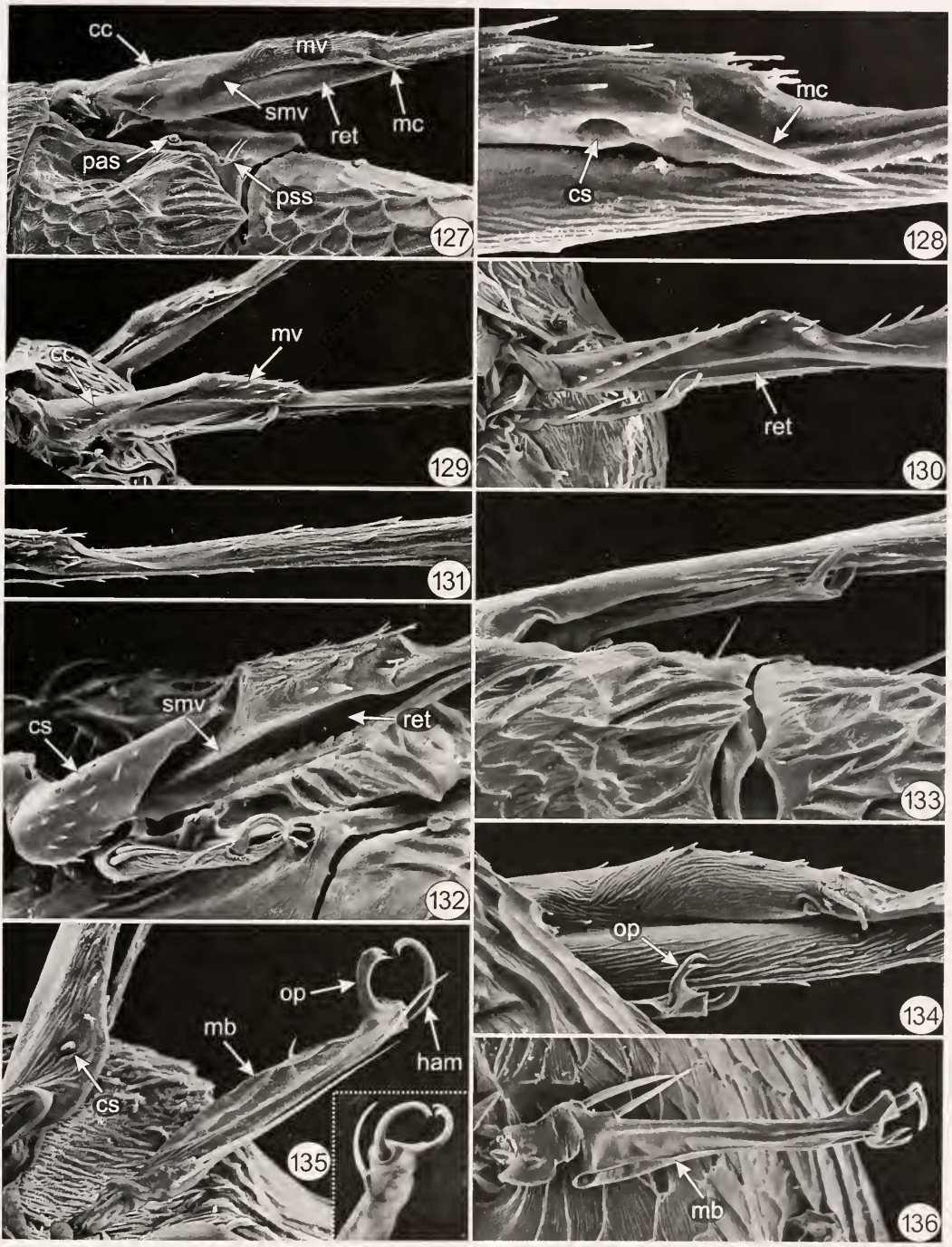

Figs 127–136. **127 and 128**, *Mymaromma anomalum*: **127**, proximal part of forewing stalk, dorsal; **128**, apex of forewing venation. **129 and 130**, proximal part of forewing stalk, ventral: **129**, *Mymaromma goethei*; **130**, *Mymaromella* sp. 14. **131–133**, *M. anomalum*: **131**, distal part of forewing stalk, ventral; **132**, proximal part of forewing stalk, ventral; **133**; wing coupling, dorsal. **134**, *Zealaromma valentinei*, wing coupling. **135 and 136**, hind wing: **135**, *Mymaromella* sp. 23 (insert: apex, *Mymaromella* sp. 18); **136**, *Zealaromma valentinei*.

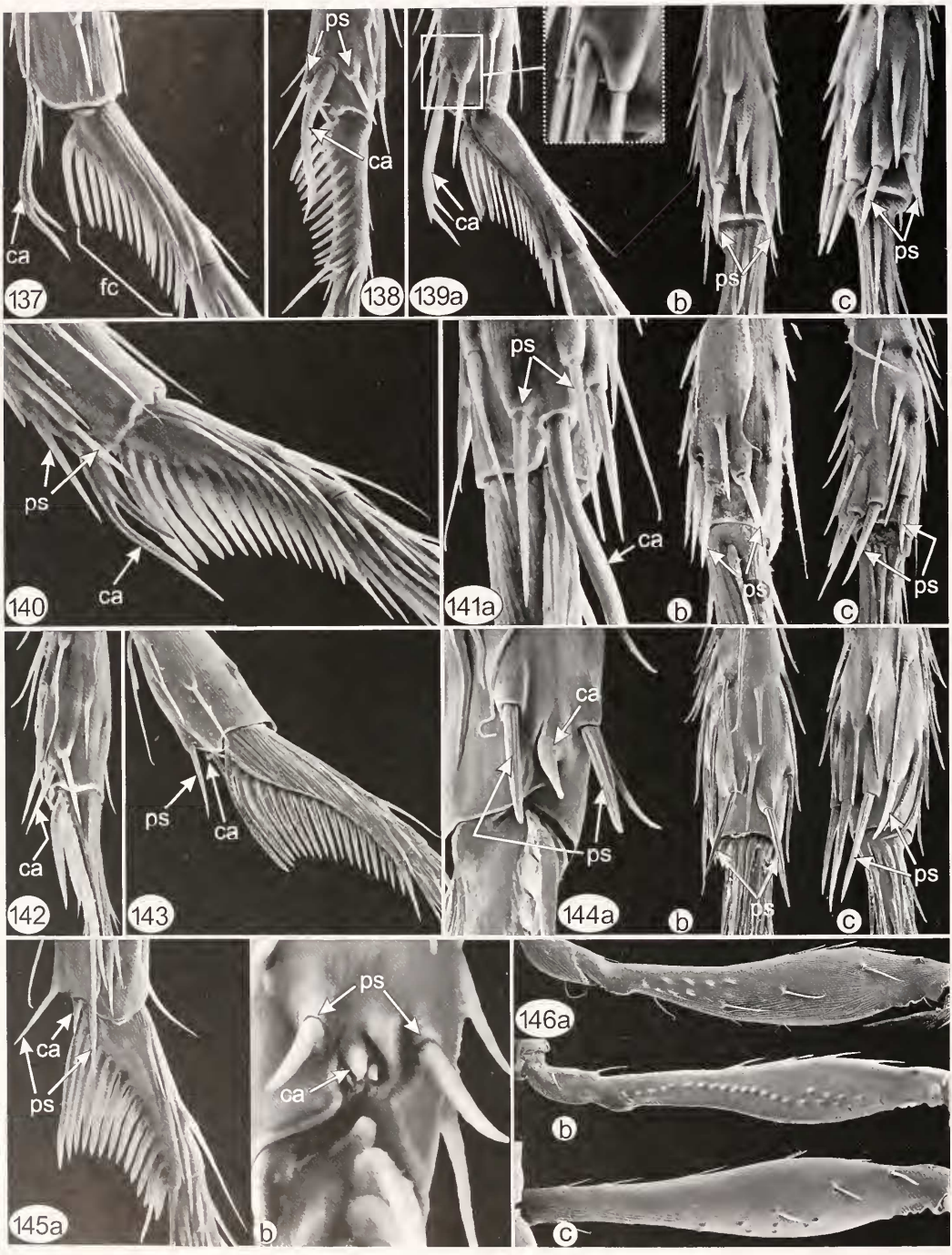

Figs 137–146. **137 and 138**, strigil: **137**, *Mymaromella* sp. 17, lateral; **138**, *Mymaromella* sp. 21, ventrolateral. **139**, *Mymaromella* sp. 14: **a**, strigil, lateral (insert: enlargement of calcar base between pseudospurs); **b and c**, apex of tibia, ventral: **b**, mesotibia; **c**, metatibia. **140 and 141**, *Zealaromma valentinei*: **140**, strigil, lateral; **141**, apex of tibia, ventral: **a**, protibia, **b**, mesotibia, **c**, metatibia. **142**, *Mymaromma goethei*, strigil, ventral. **143 and 144**, *Mymaromma anomalum*: **143**, strigil, lateral; **144**: apex of tibia, ventral: **a**, protibia, **b**, mesotibia, **c**, metatibia. **145**, *Mymaromma* sp. 10: **a**, strigil, lateral, **b**, apex of protibia, ventral (calcar foreshortened). **146**, *Z. valentinei*, femur, posterior surface: **a**, profemur; **b**, mesofemur; **c**, metafemur.

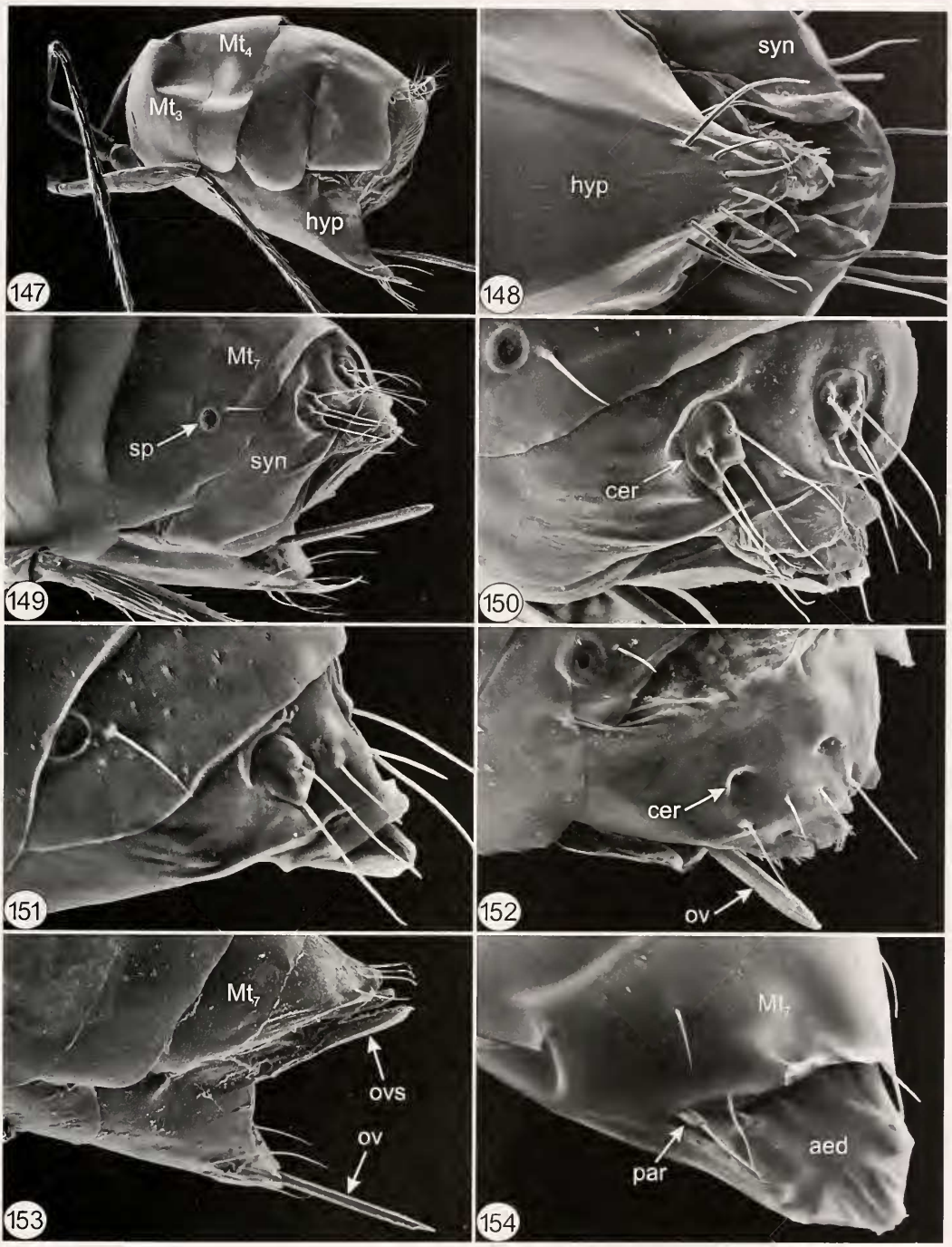

Figs 147–154. **147**, *Mymaromella* sp. 23 ♀, gaster. **148**, *Mymaromma* sp. 6 ♀, hypopygium. **149 and 150**, *Mymaromella* sp. 18 ♀: **149**, apex of gaster; **150**, apical two gastral tergites. **151 and 152**, ♀ apical two gastral tergites: **151**, *Mymaromella* sp. 17; **152**, *Mymaromma* sp. 10. **153 and 154**, *Zealaromma* spp.: **153**, *Z. valentinei* ♀, apex of gaster; **154**, *Z. insulare* ♂, penultimate gastral tergite and aedeagus (syntergum concealed under Mt_7).

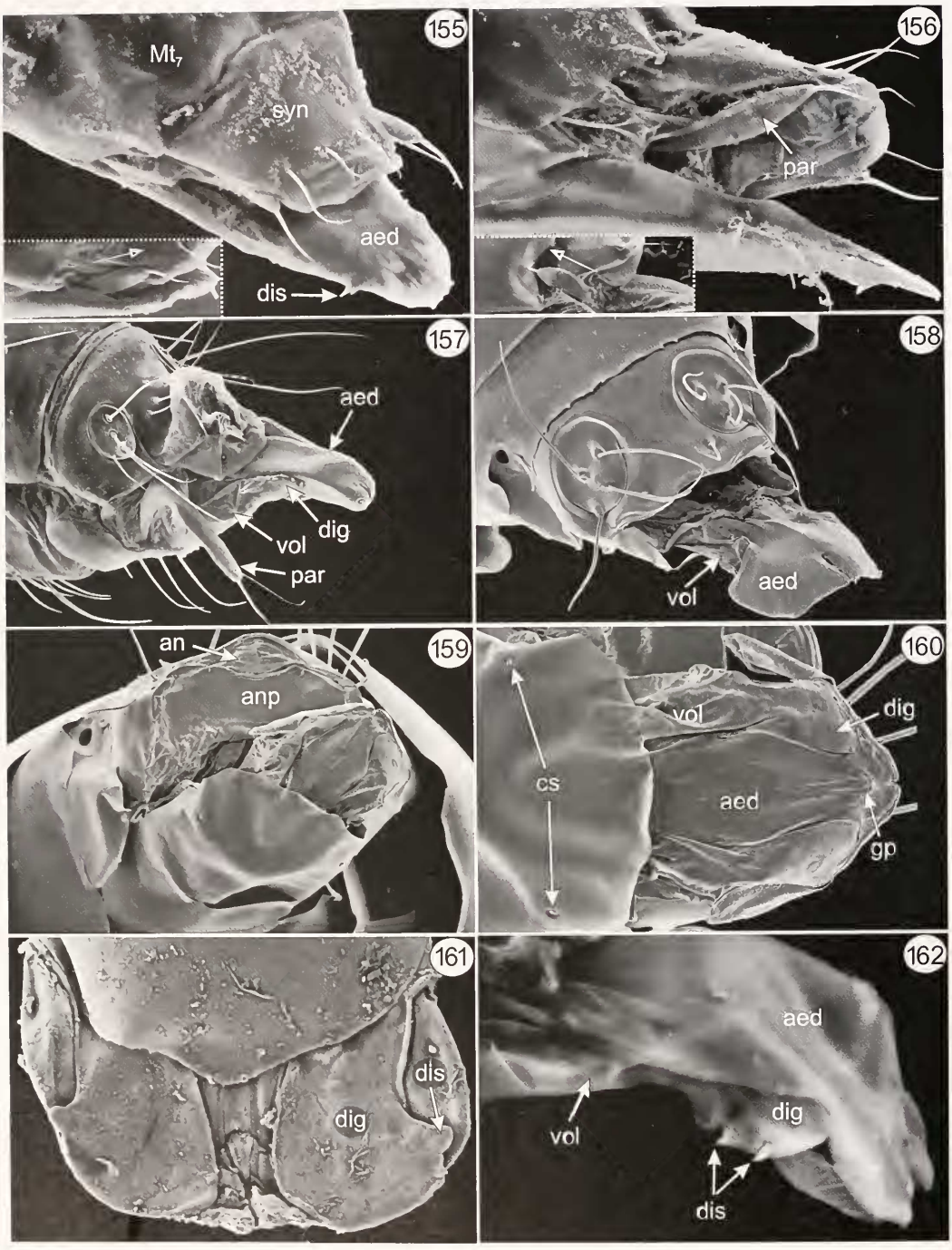

Figs 155–162. **155 and 156**, *Zealaromma valentinei* ♂, apex of gaster (insert: paramere, arrows indicate direction): **155**, dorsolateral; **156**, ventrolateral. **157**, *Maaminga rangi* ♂, Mt_8 and genitalia. **158–160**, *Mymaromma* sp. 7 ♂, apex of gaster and genitalia: **158**, dorsolateral; **159**, ventrolateral; **160**, ventral. **161**, *Mymaromma* sp. 6 ♂, parameres, ventral. **162**, *Mymaromella mira* ♂, genitalia, dorsolateral.

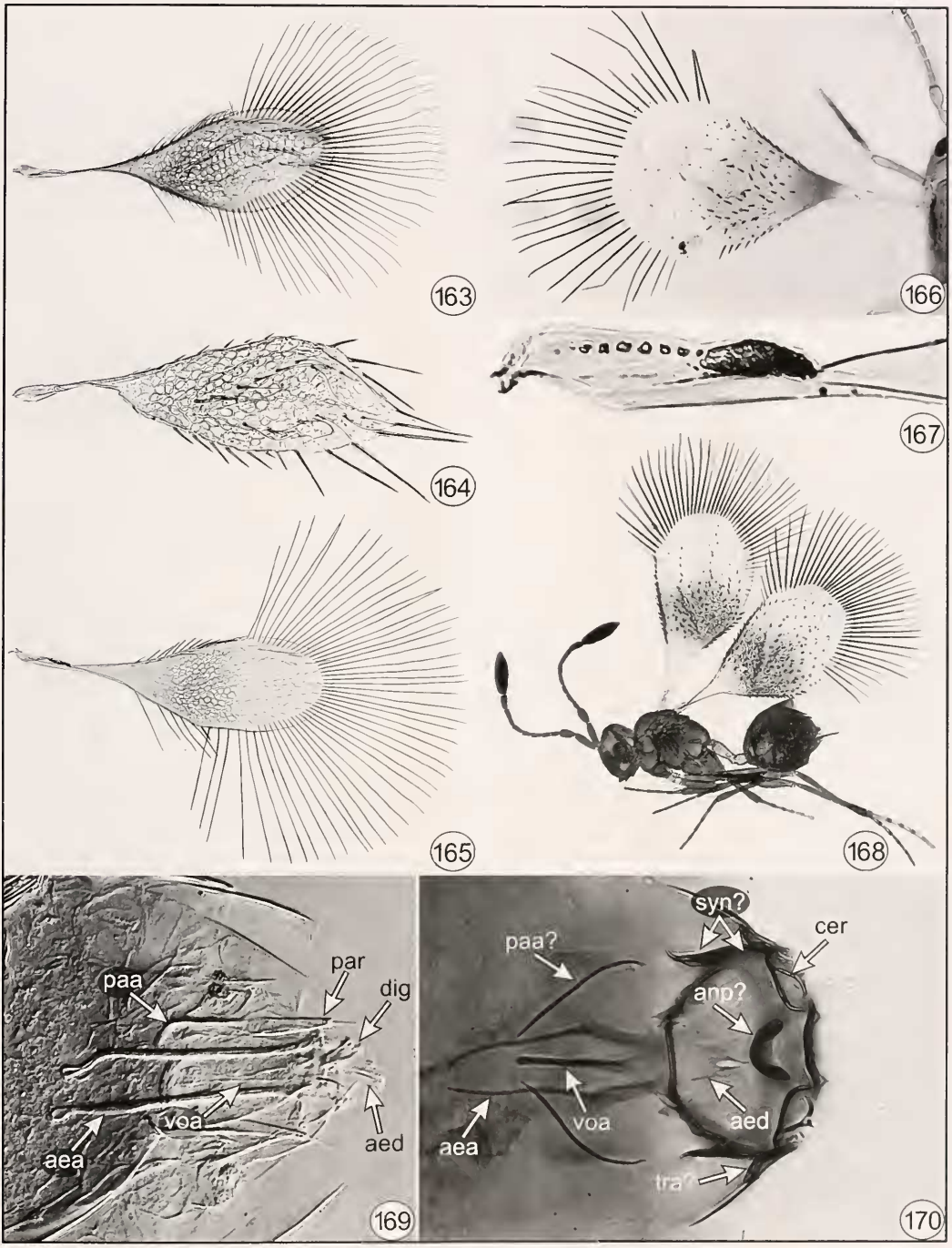

Figs 163–170. **163–166**, forewing: **163**, *Mymaromma anomalum* (Sweden); **164**, *Zealaromma insulare*; **165**, *Z. valentinei*; **166**, *Mymaromella cyclopterus* (holotype ♀). **167**, *Mymaromella* sp. 14, forewing stalk. **168**, *Mymaromella mira* (USNM type photograph). **169 and 170**, ♂ genitalia: **169**, *Z. insulare*; **170**, *M. anomalum* (Japan).

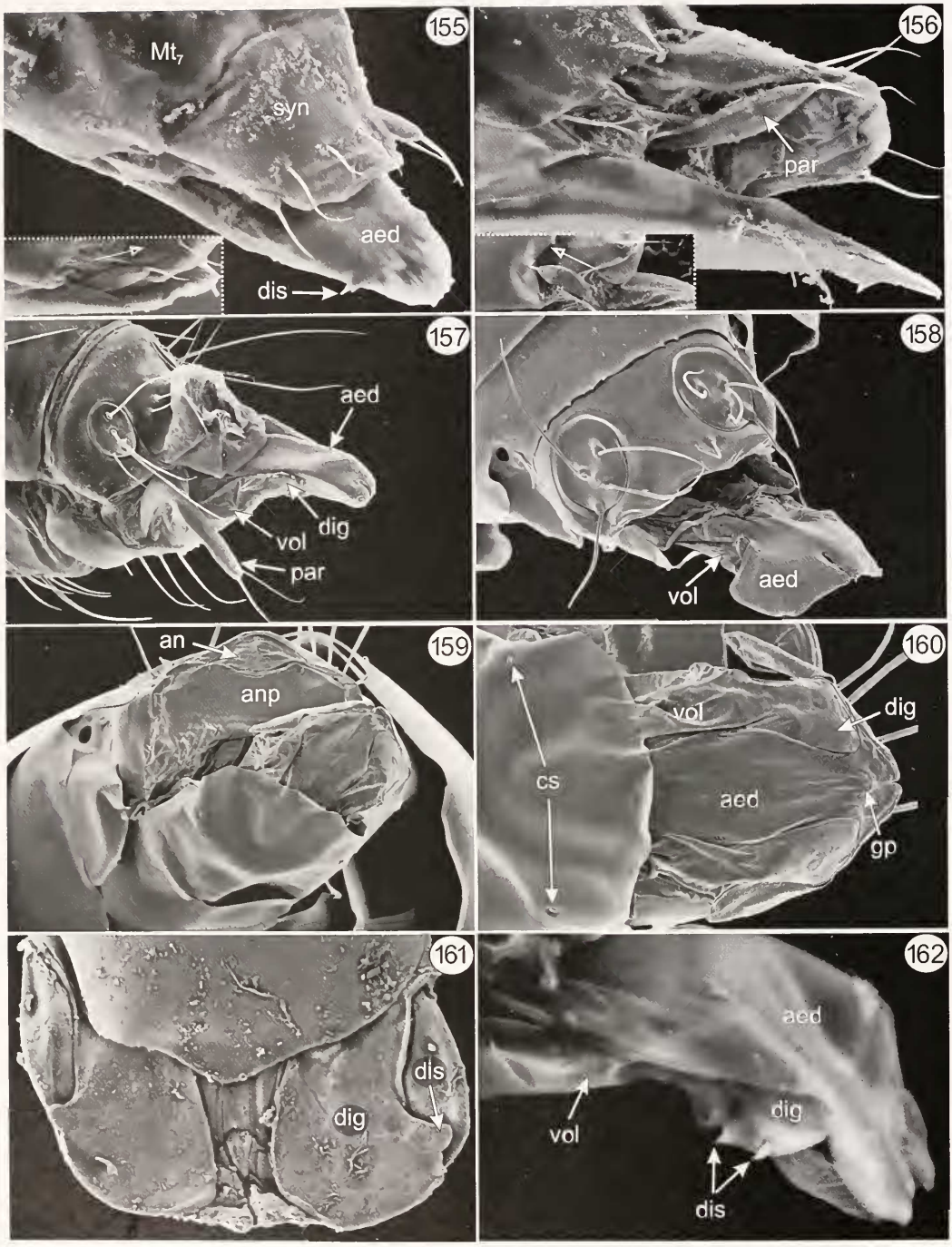

Figs 155–162. **155 and 156**, *Zealaromma valentinei* ♂, apex of gaster (insert: paramere, arrows indicate direction): **155**, dorsolateral; **156**, ventrolateral. **157**, *Maaminga rangi* ♂, Mt_8 and genitalia. **158–160**, *Mymaromma* sp. 7 ♂, apex of gaster and genitalia: **158**, dorsolateral; **159**, ventrolateral; **160**, ventral. **161**, *Mymaromma* sp. 6 ♂, parameres, ventral. **162**, *Mymaromella mira* ♂, genitalia, dorsolateral.

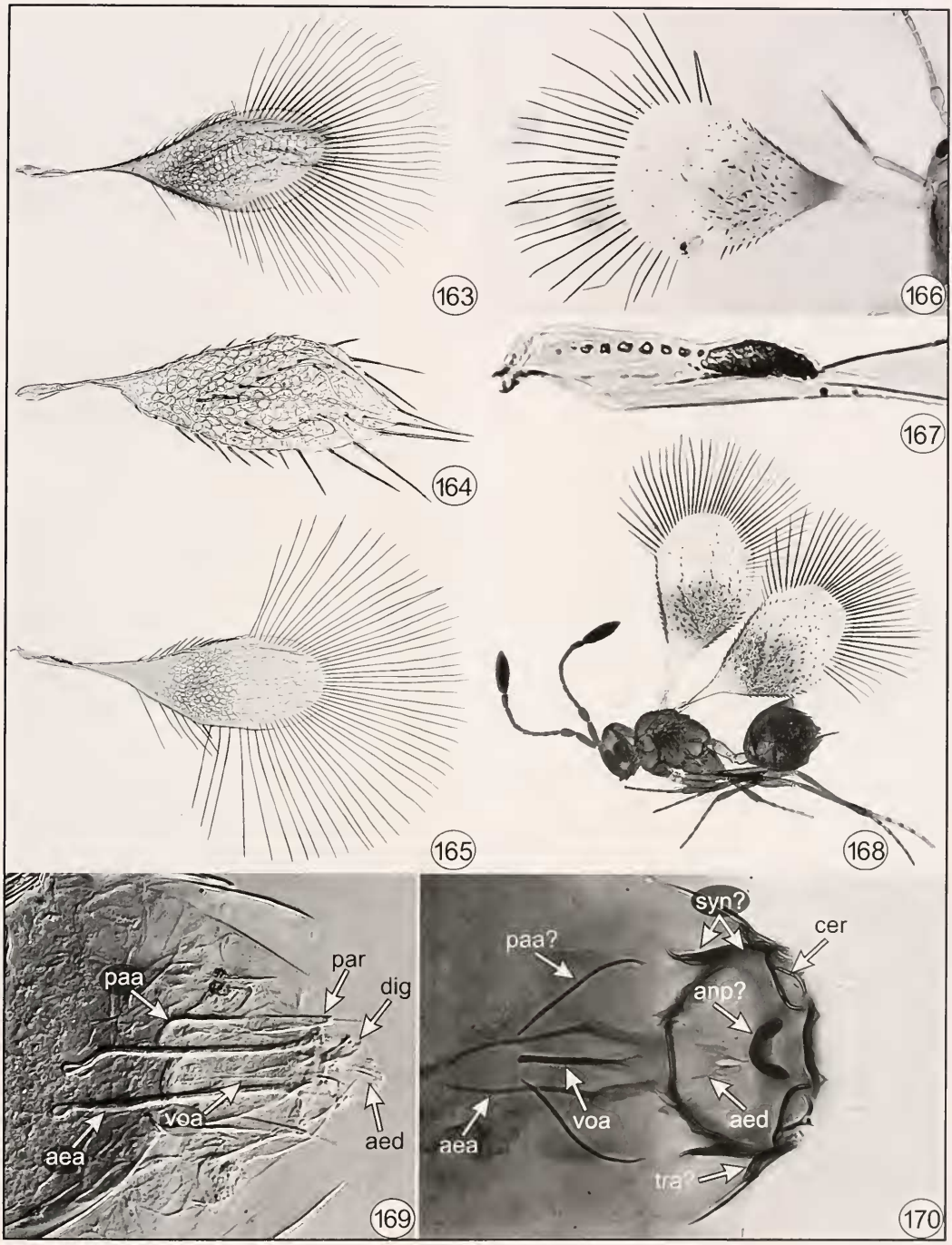

Figs 163–170. **163–166**, forewing: **163**, *Mymaromma anomalum* (Sweden); **164**, *Zealaromma insulare*; **165**, *Z. valentinei*; **166**, *Mymaromella cyclopterus* (holotype ♀). **167**, *Mymaromella* sp. 14, forewing stalk. **168**, *Mymaromella mira* (USNM type photograph). **169 and 170**, ♂ genitalia: **169**, *Z. insulare*; **170**, *M. anomalum* (Japan).

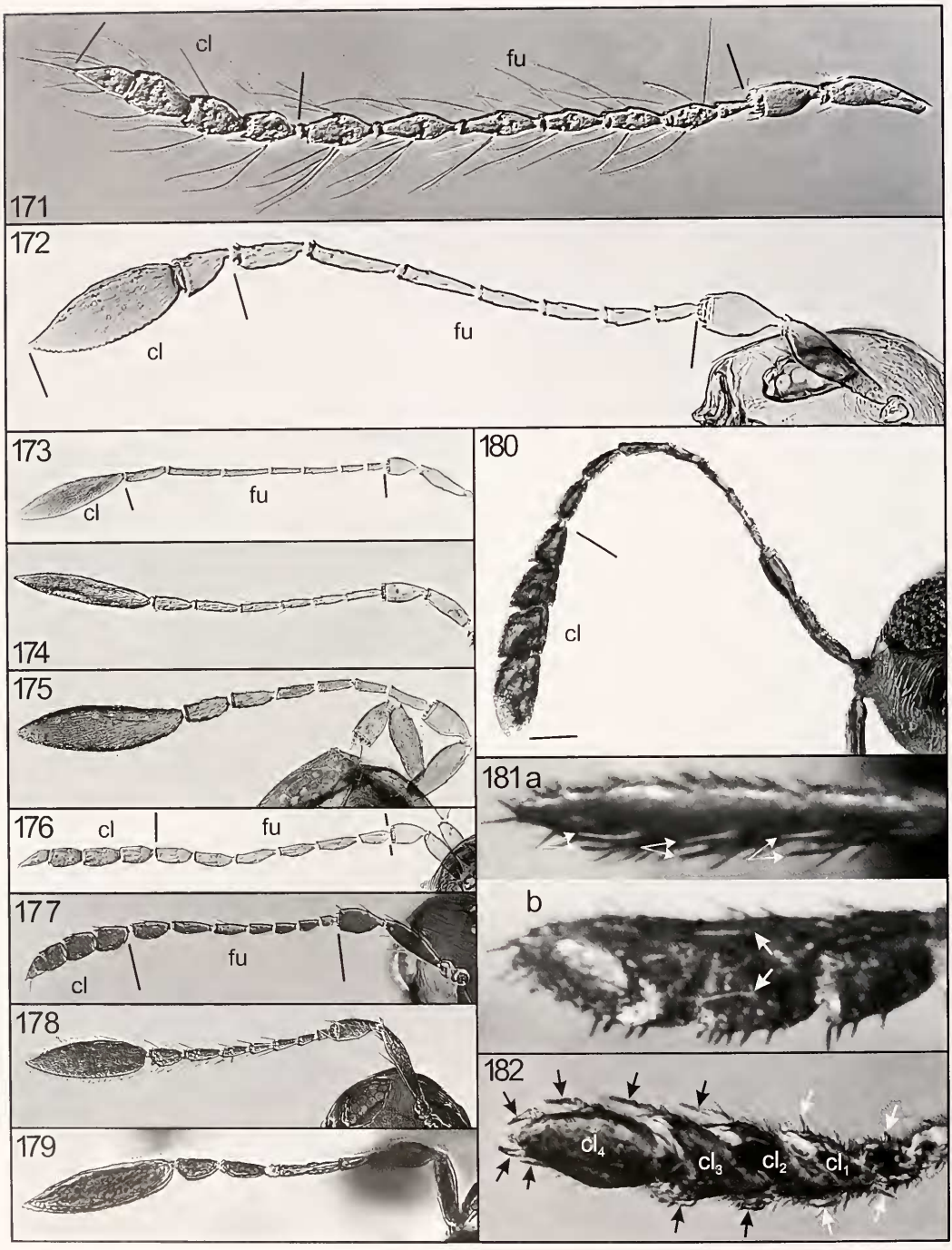

Figs 171–182. **171 and 172**, *Zealaromma* spp., antenna: **171**, *Z. insulare* ♂; **172**, *Z. valentinei* ♀. **173–176**, *Mymaromma* spp., antenna: **173**, *M. anomalum* ♀; **174**, *M. goethei* ♀; **175**, *M.* sp. nr *goethei* ♀; **176**, *M.* sp. nr *goethei* ♂. **177 and 178**, *Mymaromella* sp. 14, antenna: **177**, ♀; **178**, ♂. **179**, *Palaeomymar succini* ♀, antenna. **180 and 181**, *Gallorommа agapa* (holotype ♀): **180**, left antenna; **181**, apical three claval segments (**a**, right clava, dorsal view; **b**, left clava, outer surface). **182**, *Gallorommа* sp. ♀, clava (GPPC: HY17A). (Arrows point to sensilla in Figs 181, 182.)

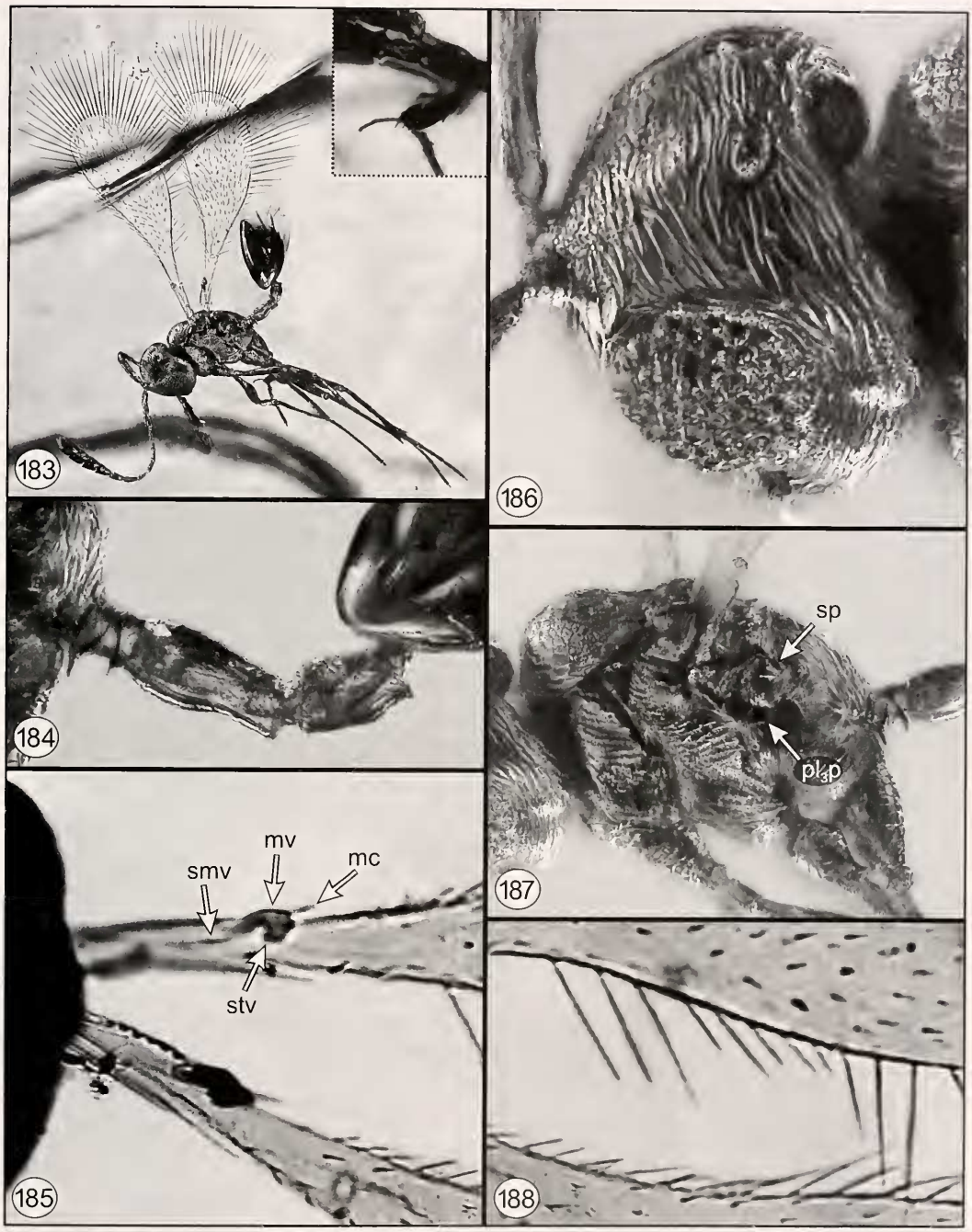

Figs 183–188. **183–188**, *Gallorommа agapa* (holotype ♀): **183**, habitus (insert: calcar); **184**, petiolar segments; **185**, proximal part of forewings; **186**, head, dorsolateral; **187**, mesosoma, lateral; **188**, forewing posterobasal marginal setae.

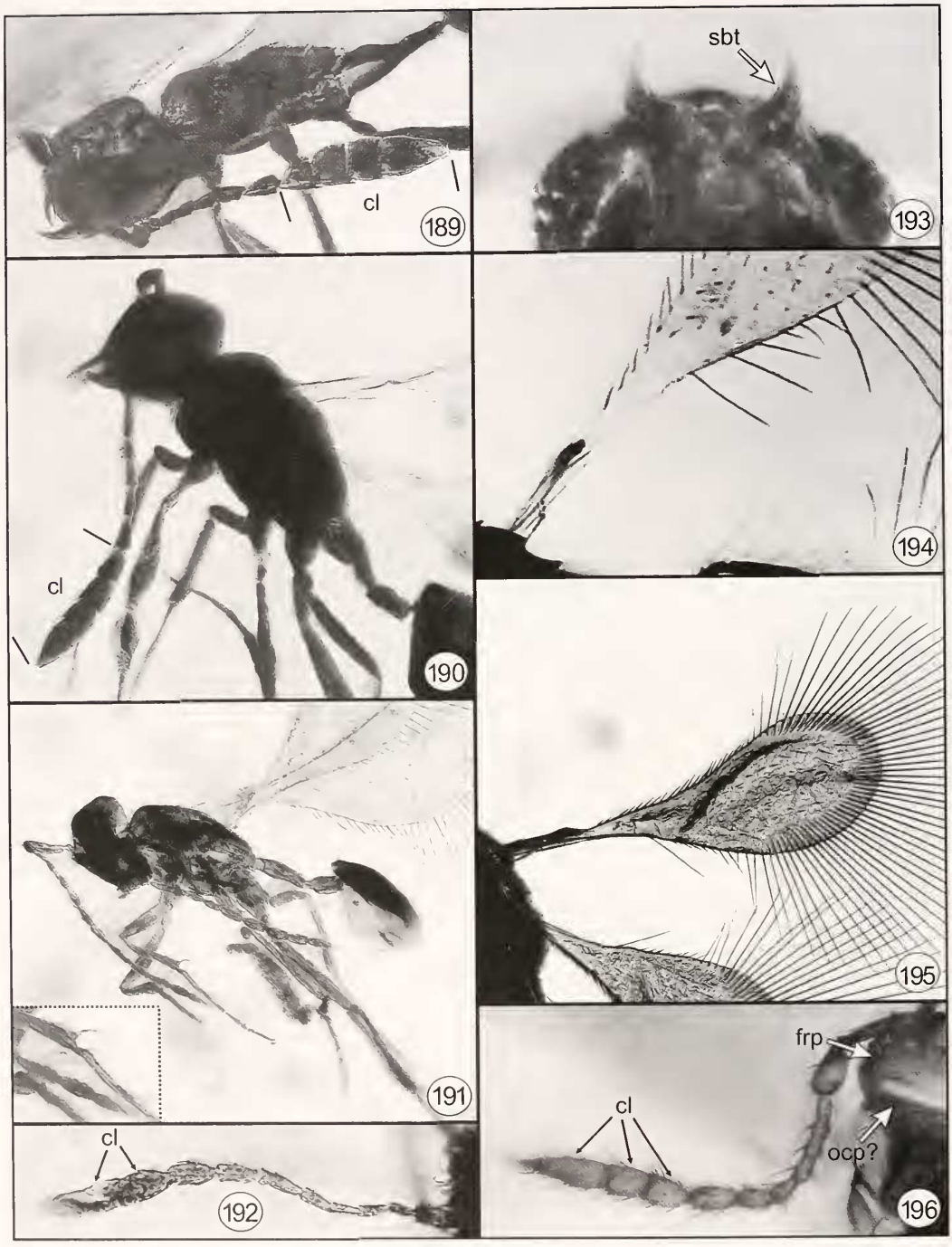

Figs 189–196. **189–191**, *Galloromma* sp. (AMNH: B-0107): **189**, ♀ head and antenna, dorsal; **190**, ♀ body except gaster, lateral; **191**, ♂ habitus (insert: calcar). **192**, *Archaeromma minutissimum*, antenna (holotype ♀). **193**, *Galloromma* sp. ♀, mandibles, ventral (GPPC: HY17A). **194**, *Archaeromma nearcticum* ♀, forewing posterobasal marginal setae (CNC: CAS-598). **195**, *Archaeromma* sp. ♂, forewing (AMNH: NJ-179). **196**, *Archaeromma masneri*, head (dorsal) and antenna (holotype ♀).

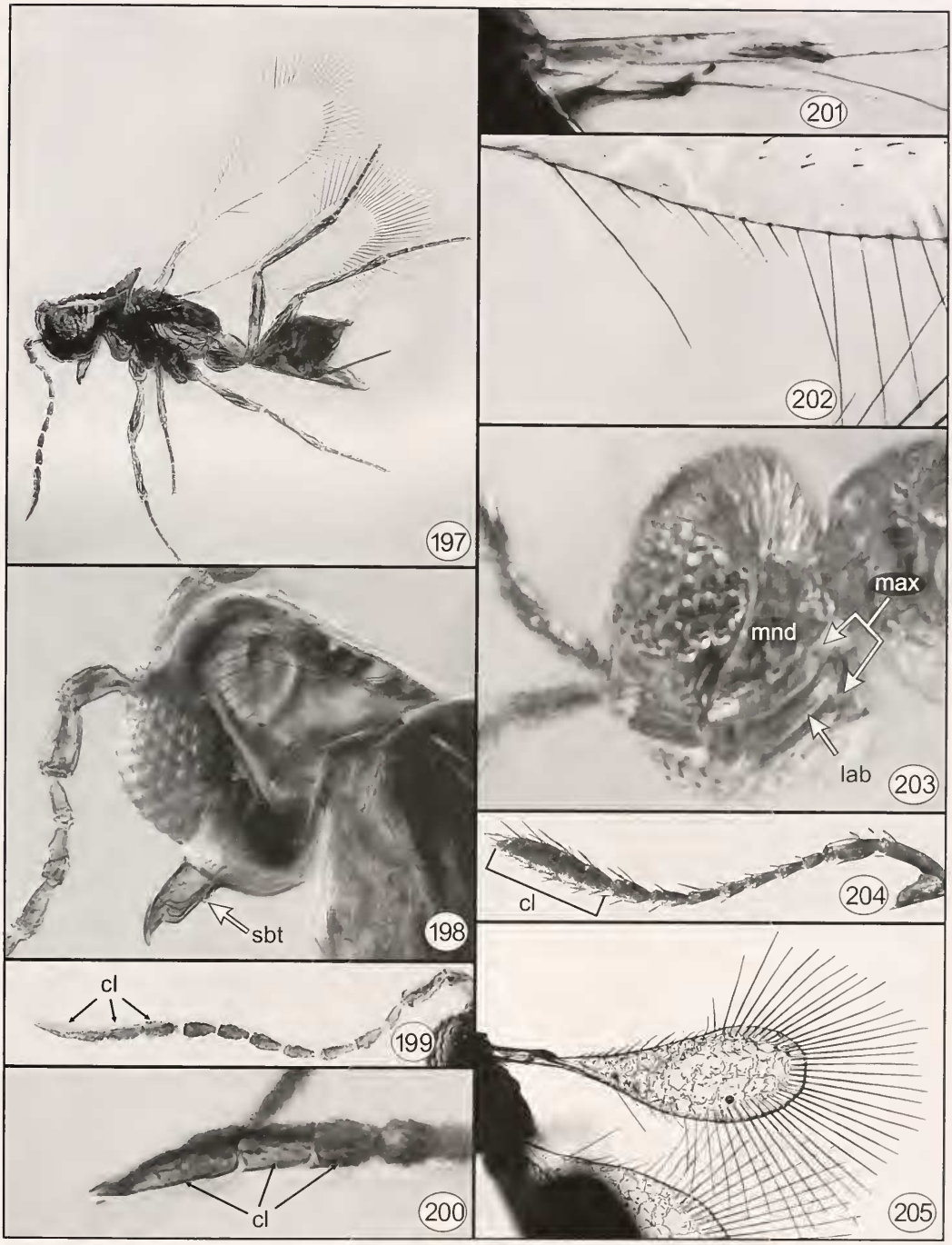

Figs 197–205. **197–202**, *Archaeromma mandibulatum* (holotype ♀): **197**, habitus; **198**, head, dorsolateral; **199**, antenna; **200**, clava; **201**, proximal part of forewing stalk; **202**, forewing posterobasal marginal setae. **203–205**, *Archaeromma senonicum* (paratype ♀): **203**, head, ventrolateral; **204**, antenna; **205**, forewing.

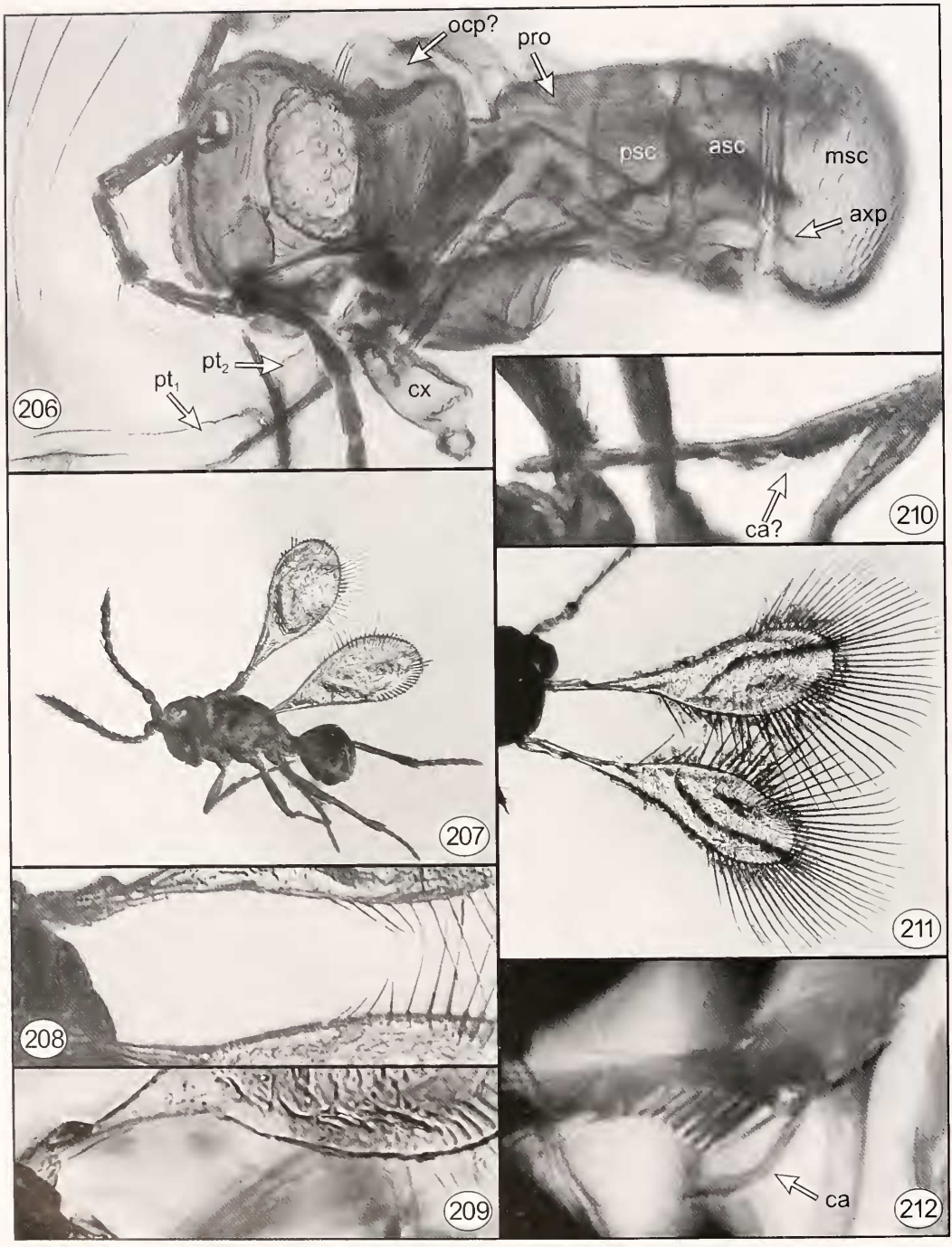

Figs 206–212. **206**, *Archaeromma masneri* (holotype ♀). **207–210**, *Palaeomymar succini*: **207**, habitus (neotype ♂); **208**, forewing posterobasal marginal setae (neotype ♂); **209**, ♀ forewing posterobasal marginal setae (ZMUC: 16-1/1961); **210**, foreleg (neotype ♂). **211 and 212**, ? *Mymaromella* sp. ♀ (ZMUC: 17-5/1963): **211**, forewings; **212**, calcar.

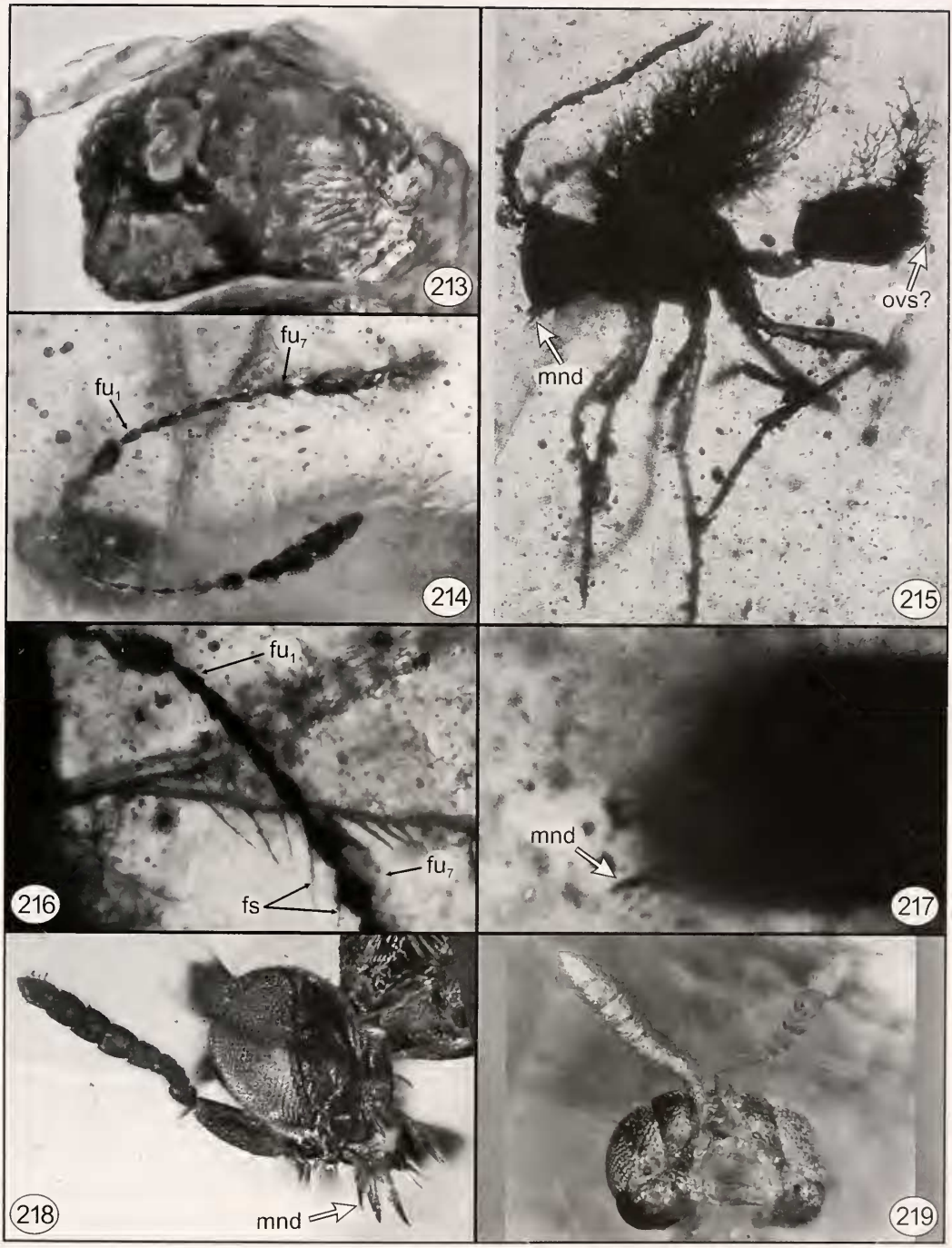

Figs 213–219. **213**, *Galloromma* sp. ♀, head, dorsal (GPPC: HY17A). **214–217**, *Galloromma bezommaisensis* (holotype): **214**, antenna, dorsal; **215**, lateral habitus reproduced from Schlüter (1978); **216**, forewing posterobasal marginal setae and antennal funicle; **217**, head, dorsal. **218 and 219**, head and antennae of *Serphites* sp.: **218**, lateral (MCZ: 5330); **219**, frontal (PIN: 3730/28-30).

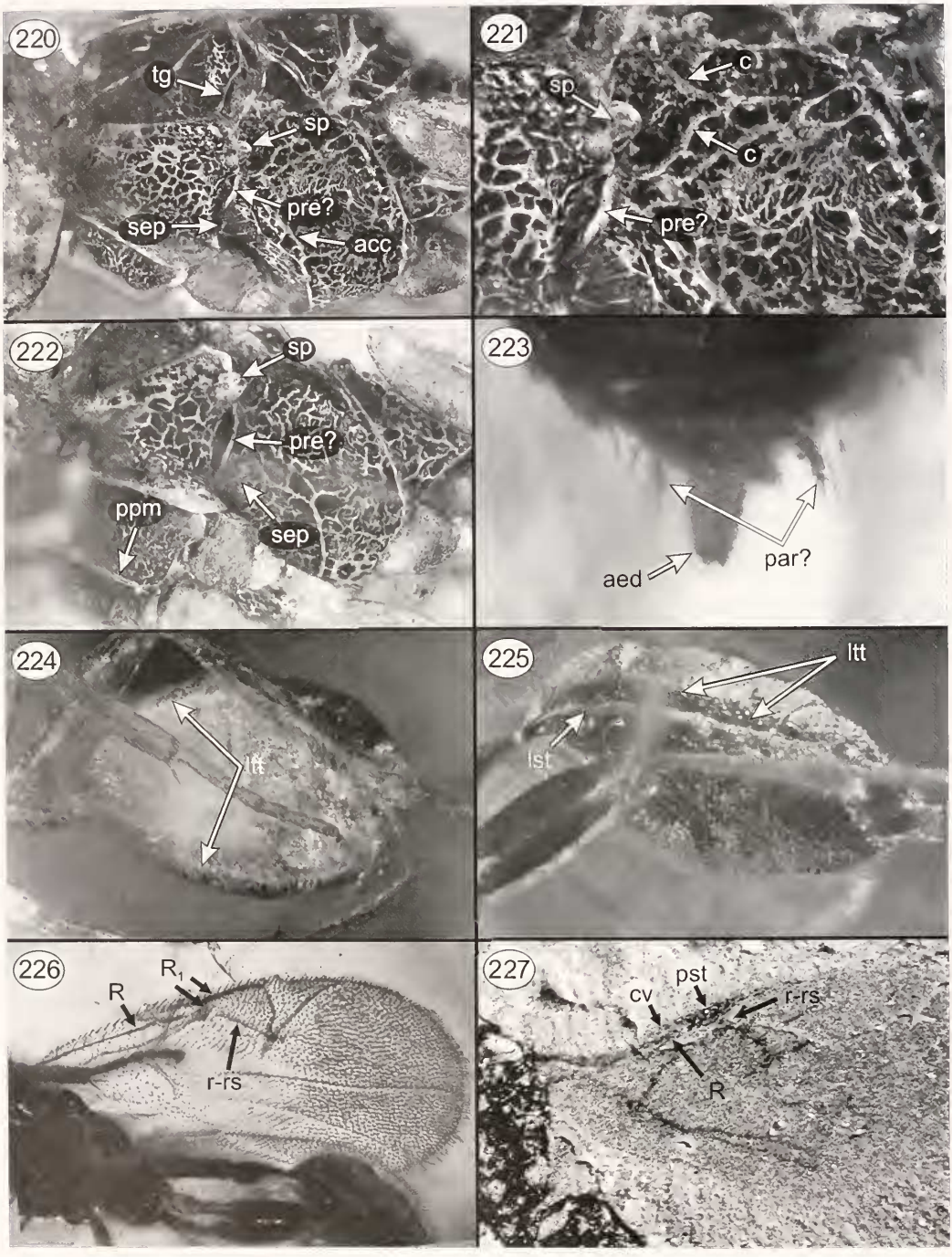

Figs 220–227. **220–222**, *Serphites* sp. (PIN: 3730/31): **220**, mesosoma, lateral; **221**, pronotum-mesopectus; **222**, mesosoma, ventrolateral. **223**, *Serphites* sp. ♂ (MCZ: 5343), apex of gaster. **224 and 225**, *Serphites* sp., gaster: **224**, ventrolateral (PIN: 3730/28-30); **225**, lateral (MCZ: 5330). **226**, *Serphites* sp., forewing venation (MCZ: 5530). **227**, forewing of undescribed representative of Scelionidae (PIN: 4703/10).